GSC OPEN FILE 2424

Clay sized mineralogy of core 87-008-003 from the J-Anomaly Ridge and from comparison cores along the eastern Canadian continental margin.

K.I. Skene, D.J.W. Piper & R.A. Armstrong.
Atlantic Geoscience Centre

October 1991

CLAY SIZED MINERALOGY OF CORE 87008-003 FROM THE J-ANOMALY RIDGE AND FROM COMPARISON CORES ALONG THE EASTERN CANADIAN CONTINENTAL MARGIN: DOWN-CORE VARIATION AND SOURCE AREA INTERPRETATION

Kenneth I. Skene, David J.W. Piper and R. A. Armstrong

Atlantic Geoscience Centre, Geological Survey of Canada, Bedford Institute of Oceanography, P.O. Box 1006, Dartmouth, N.S., Canada B2Y 4A2

Geological Survey of Canada Open File **** September 1991

ABSTRACT

This Open File reports analytical results and preliminary interpretation of the variation in clay mineralogy down a 20 m-long piston core from the J-Anomlay ridge, south of the Grand Banks of Newfoundland, sampling the last 650 000 years of Quaternary sedimentation. In addition, results are presented for clay mineral analysis of a further 50 samples from elsewhere on the Canadian margin. Data has been analysed by normalising to illite, standardising to a common scale, and subtraction of the inverse of the standardised raw illite value to yield a residual value. Principal components analysis using a correlation matrix was performed on the data set of residual values. Clay mineral variability reflects changes in the relative importance of supply from (1) northern sources, principally by ice-rafting, indicated by high dolomite and plagioclase; (2) sources in the island of Newfoundland, derived through glacial erosion and dispersion in outwash plumes, indicated by high chlorite; and (3) sources on the Grand Banks, derived either by glacial or fluvial erosion, indicated by high kaolinite and/or smectite. Although source interpretation is not possible at all levels in the core, clay-sized minerals in isotopic stages 1-3 were predominantly derived from southern sources (Newfoundland, Grand Banks); northern sources predominate in stages 4-11; and stages 16-24 have a strong indication of southern sources.

CONTENTS

TABLES

FIGURES

Figure 4.1. Residual peak areas for groups of comparison samples. v = highly variable data:

a) Holocene from Tantallon, Narwhal and St Pierre Slope
b) Holocene from Tail of the Banks
c) Holocene from eastern Flemish Pass
d) Late Wisconsinan from Tantallon
e) Late Wisconsinan from St Pierre Slope
f) Late Wisconsinan from Narwhal
g) Fogo Seamounts: red muds
h) Fogo Seamounts: brown muds
i) Fogo Seamounts: grey muds
j) Late Wisconsinan from Tail of the Banks
k) Labrador Shelf: Makkaq Clay
l) Labrador Shelf: Qeovik Silt
m) Labrador Shelf: Till
n) Labrador Sea
o) Davis Strait
p) Baffin Bay Basin

Figure 4.2. Type mineral horizons in core 87008-003 and their correlation with oxygen isotope stratigraphy.

1.0 INTRODUCTION

Deep-water areas adjacent to Eastern Canada contain a detrital record of glaciation on the eastern Canadian margin. Alam and Piper (1977) showed that the mid to late Pleistocene sediment record in cores from the Fogo Seamounts could be used to infer the denudational history of the adjacent continent. In 1987, D.J.W. Piper, P.J. Mudie and A.E. Aksu obtained a 20-m long core (87-008-003) of pelagic sediments from the J-Anomaly ridge south of the Grand Banks of Newfoundland (Fig. 1.1), in order to investigate Quaternary paleo-oceanography and denudation history. Mudie and Aksu (1990) and Aksu and Mudie (in prep.) have shown that this core has an almost 1 Ma stratigraphic record, back to isotopic stage 28, and have outlined the paleo-environmental history of the site. Core 87-008-003 is located in 3877 m water depth at 40° 22.6'N 51° 29.2'W. It is about 10 km from DSDP site 384 (Tucholke, Vogt et al., 1979).

The purpose of this study was to determine variations in clay mineralogy in this long stratigraphic core, in order to better understand Pleistocene changes in sediment dispersion and glacially-determined sediment sources, as part of the overall investigation of the Quaternary history of the J-Anomaly ridge. In this study, we have also made determinations of clay mineralogy in other cores from the eastern Canadian margin (Fig. 1.1) that might provide more proximal samples in the glacial - marine dispersion system.

Previous studies of clay mineralogy on the continental margin off Newfoundland include examination of a core on the SE Newfoundland Ridge by Pastouret et al. (1975); cores from the Fogo Seamounts by Alam and Piper (1977); and a more regional study by Alam and Piper (1981). All these previous studies found variations in relative abundance of clay minerals with glacial stages (although except for the Fogo Seamount cores, only the late Wisconsinan was sampled). These studies show that at times of high sea level stand, smectites predominate; at low sea level stands, generally corresponding to glacial advances, clay mineral assemblages are regionally much more variable, probably reflecting various glacially-influenced sources.

Terrestrial sources of clay minerals were reviewed by Piper and Slatt (1987). Volumetrically, shales are the principal source of clay minerals. Kaolinite is present in both Carboniferous and Triassic red beds; montmorillonite is restricted to the Triassic (Brydon, 1958; Allen and Johns, 1960; Barnett and Abbott, 1966). Kaolinite is predominant in outliers of

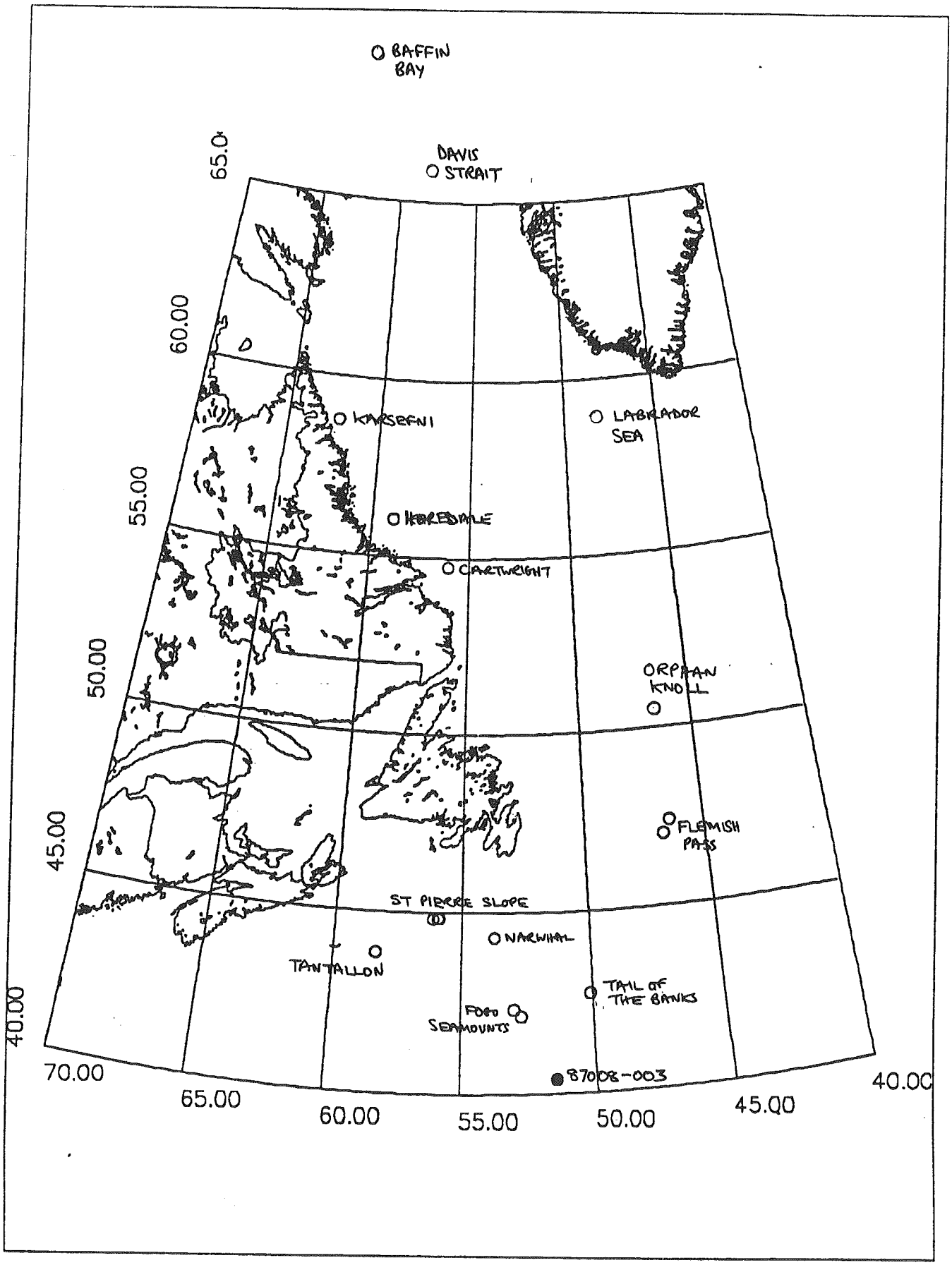

Figure 1.1. Regional map showing locations of core 87-008-003 and comparison samples.

Cretaceous clays in Nova Scotia and is abundant in offshore Cretaceous strata, and occurs in some younger Tertiary offshore strata. However, the principal clay in Tertiary offshore strata is smectite (Segall et al., 1987; L.F. Jansa, pers. comm., 1991). Well crystallised chlorite is likely exclusively derived from crystalline bedrock; it occurs at substantial depths in offshore wells (Jansa and Noguera, 1990). On the Labrador Shelf, Tertiary strata contain subequal amounts of smectite, kaolinite and illite (Umpleby et al., 1978). Upper Cretaceous strata contain predominant smectite, lower Cretaceous strata mainly kaolinite (Hiscott, 1984).

Other studies of the distribution of clay minerals in marine cores adjacent to eastern Canada provide additional constraints on our interpretations. Clay minerals in sediments from Baffin Bay are described by Boyd and Piper (1976), Aksu and Piper (1987), Hiscott et al. (1989) and Thiébault et al. (1989). Clay minerals in sediments in the Labrador Sea are described by Latouche and Parra (1979) and Cremer et al. (1989); and on the Labrador Shelf by Slatt and Lew (1973) and . Clay minerals at the Hibernia field, including modifications resulting from weathering, are described by Segall et al. (1985, 1987). Clay minerals on the Scotian Margin are described by Stow (1977, 1978) and Hill (1981).

Throughout this report, the term "illite" is used for minerals with a 10Å peak that are more correctly termed mica (Martin et al., 1991).

2.0 METHODS

2.1 Introduction

Core 87-008-003 was collected using the University of Rhode Island prototype long coring facility. Comparison of the trigger weight and piston core showed that there was no significant sediment loss at the top of the core. The core was split on board ship and initially sampled at 5-10 cm intervals for oxygen isotopes and palynomorphs and at 20 cm intervals for mineralogy. The $<2\mu m$ fraction of this initial set of samples was analysed using X-ray diffraction by Armstrong (1988). Because some high-sedimentation rate intervals were poorly represented by this sampling strategy, additional samples were taken at 10 or 5 cm intervals and analysed by Skene. In addition, all the 87008-003 diffractometer data were re-analysed for peak identification and area using the same diffractometer software.

A suite of 87 terrigenous samples from the eastern Canadian margin (Fig. 1.1) between the Scotian Slope and Baffin Bay were also analysed, in order to characterise possible source area mineralogy. These are referred to as the comparison samples. This report also documents analyses of 30 samples from Flemish Pass briefly reported by Piper and Pereira (in press).

2.2 Sample preparation and mounting

The <2 μm fraction required for X-ray diffraction analysis was prepared according to the following procedure for the comparison samples:

1) Sufficient sample was selected to contain 30-50 mg of <2μm sediment fraction. Add 10 ml of 10% sodium hexametaphosphate to the raw sample. Leave overnight.

2) Mechanically disaggregate (using automatic shaker) for two hours then place in sonic bath for approximately three minutes.

3) Sieve through 63 μm sieve, saving sand fraction.

4) Transfer the <63 μm washings into a sidearm cylinder. Top up with distilled water to the 1000 ml mark.

5) Shake for 1 minute. Let cylinder stand undisturbed for 16 hours, then tap off the upper 20 cm of the cylinder. Since the spigot is mounted 20 cm below the 1000 ml mark, according to Stokes' Law, after 16 hours the upper 20 cm should contain only the <2 μm fraction.

6) Flocculate sample with approximately 1 ml saturated magnesium chloride and stir.

7) After 12-16 hours, decant excess liquid, save clay fraction, and store wet.

The J-Anomaly Ridge samples were prepared in the same manner except that they were disaggregated using 20 ml of 10% sodium hexametaphosphate and flocculated using 10 ml saturated magnesium chloride. This technique led to the formation of magnesium phospate precipitates over time. Such contamination was observed in some of the J-anomaly Ridge samples and affected the peak areas of kaolinite and chlorite. In those samples where there was such interference, these clay peaks were removed from the data set. A more comprehensive discussion of the contamination problem is included in Appendix 1. In addition, the J-anomaly Ridge samples were decalcified by the addition of 10 ml of 10% acetic acid. This decalcification is inferred to have been total in some samples and only partial in others. Because of this inconsistent decalcification, and the fact that calcite is both of biogenic and detrital

origin, measured calcite abundances are of almost no interpretative value. Experimentation suggests that the acid has little or not effect on the dolomite. The use of an internal standard for the Flemish Pass samples is documented in Appendix 3.

Oriented sample mounts were obtained by vacuum-filtering the <2 μm fraction onto 0.4 μm pore size filter membrane (25 mm diameter). Transfer of the sample to a glass slide employed the "peel-on" technique outlined by Drever (1973). After drying for 10-15 minutes, the mounted samples were ready for X-ray diffraction analysis.

2.3 X-ray Diffraction Analysis

Clay-sized mineralogy was investigated using a Siemens Kristaloflex diffractometer using three scans of each sample. The long scan (2-52° 2θ) covered the range over which all minerals present could be identified. The short scan (24-26° 2θ) examined, at a higher resolution, slower scan rate, the range containing the kaolinite (3.54 Å)/chlorite (3.58 Å) doublet. After saturating the sample with ethylene glycol in an evacuated chamber for 16 hours, the glycol scan re-examines the 2-15° 2θ range in order to identify the expandable clay minerals present (referred to here as smectite). Table 1 summarizes the parameters used in each scan.

2.4 Peak Identification

Peak identification and peak area calculation was done automatically during each scan, employing the Peak Finding routine (Specplot 2nd derivative option) of Siemems Diffrac 500 Powder Diffraction Software. Visual inspection of each diffractogram verified the peak finding ouput. Peaks of interest that were not recognised by the program, but upon visual inspection thought to be realistic, were manually entered. All the smectite peaks were manually entered. The program did not adequately calculate the smectite peak area because of the steep background over the 2-15° 2θ range and the wide width at half maximum of the peak. The Profile Fitting option deconvoluted the kaolinite/chlorite doublet by fitting the data to a pseudo-Voigt distribution function. These peak areas were then used to ratio the 7Å peak area between the two minerals.

Table 2 summaries the characteristic 2θ values used to identify the major peaks for the mineral of interest in this study. Excluding amorphous material,

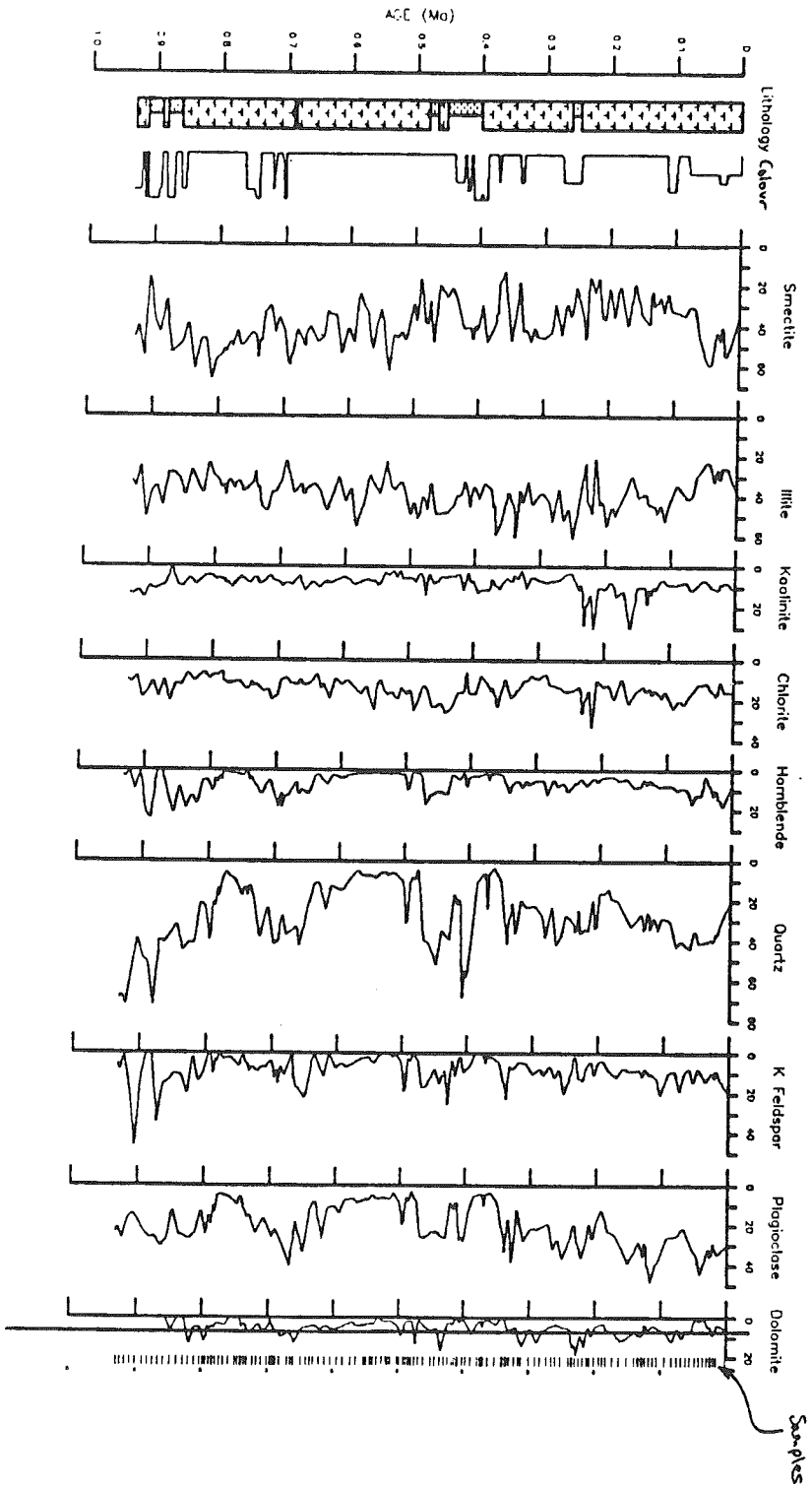

Figure 3.1. Plot of raw peak areas (arbitary scale) against age for clay size minerals from core 87008-003. Ticks on right side of figure indicate sample locations. (courtesy A.E. Aksu and P.J. Mudie who provided age control).

these minerals account for all detected phases.

3.0 DATA PREPARATION AND ANALYSIS

3.1 Introduction

The data set (Fig. 3.1) was prepared for analysis by first normalizing it to illite and then standardizing each mineral as a percentage of its respective maxima. Normalization removes variations caused by matrix effects; standardization removes variations caused by normal regional abundances, setting all the data to a comparable scale of measurement.

3.2 Data Normalization

Illite was chosen as the basis for normalization for several reasons. No internal standard was added to the samples; therefore, illite, an abundant easily measured clay-sized mineral, was used instead. Though variations in the peak area of illite will to some extent drive variations seen in the other minerals, illite tends to mimic the intensity of the overall diffractogram. Plots of mineral abundance normalised to illite are shown in Fig. 3.2.

3.3 Data Standardization

With the data normalized to illite = 100, downcore variations in relative abundance of minerals can be observed. Normalization allows for intra-mineral relational observations; however, comparisons between minerals (inter-mineral relationships) are hampered because they lack a common scale of measurement. The range over which the peak areas of a mineral may vary tend to be specific to that mineral, making comparisons of absolute magnitudes meaningless. However, peak area is related to mineral concentration in a sample; thus, the differing magnitudes of the observed peak areas after normalization must, in part, reflect regional abundances.

Given this assumption, the data set was standardized removing differences in peak area due to regional abundance. The algorithm for standardization was developed using a finite series approximation to scale the data for each mineral as a percentage of its respective maxima. Development of the algorithm and its parameters is included in Appendix 2.

The standardized data set (Fig. 3.3) is now in a more interpretable form, allowing inter-mineral relationships to be examined. The values produced by

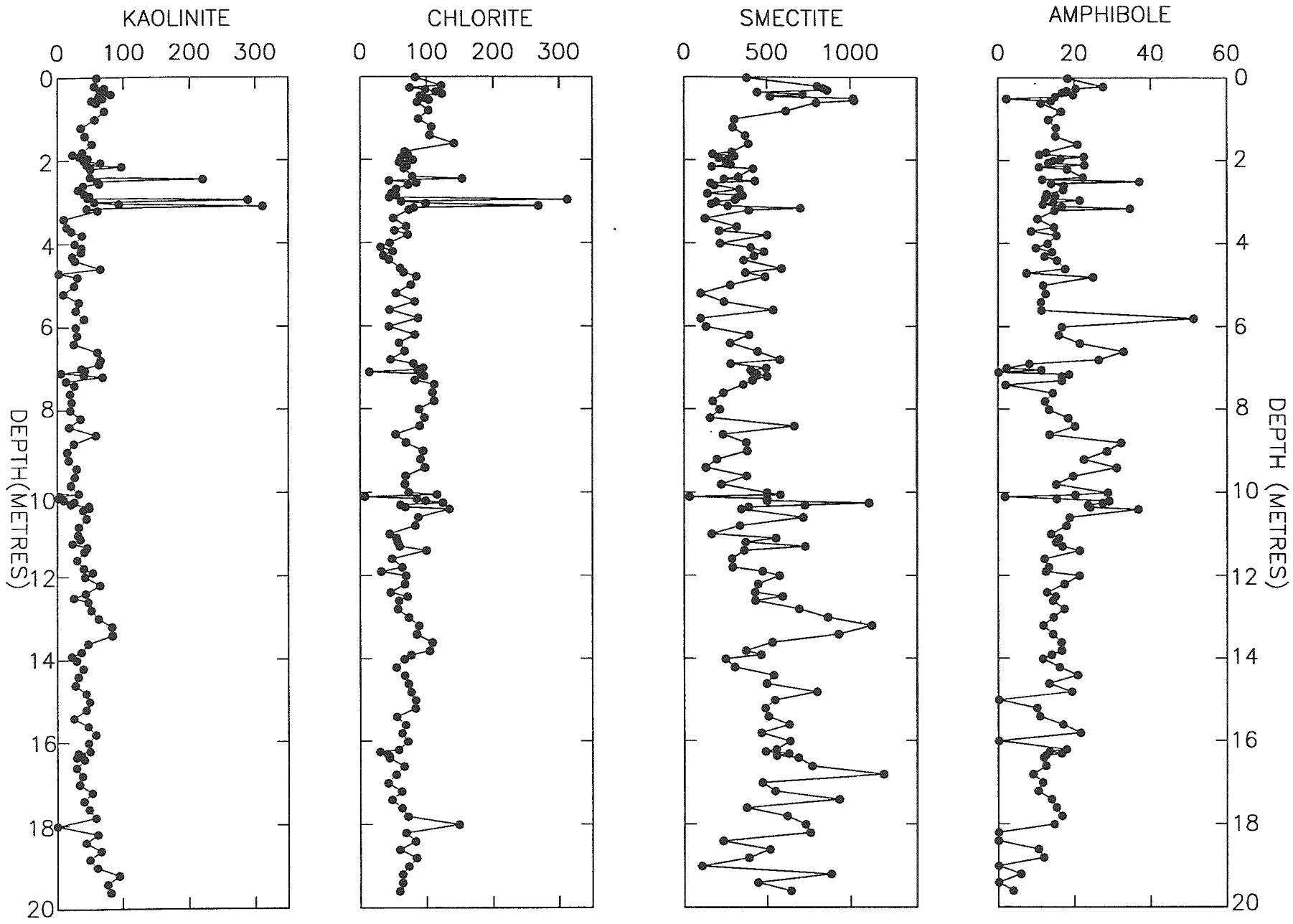

Figure 3.2a. Plot of peak areas normalised to illite against depth for clay-sized minerals from core 87-008-003.

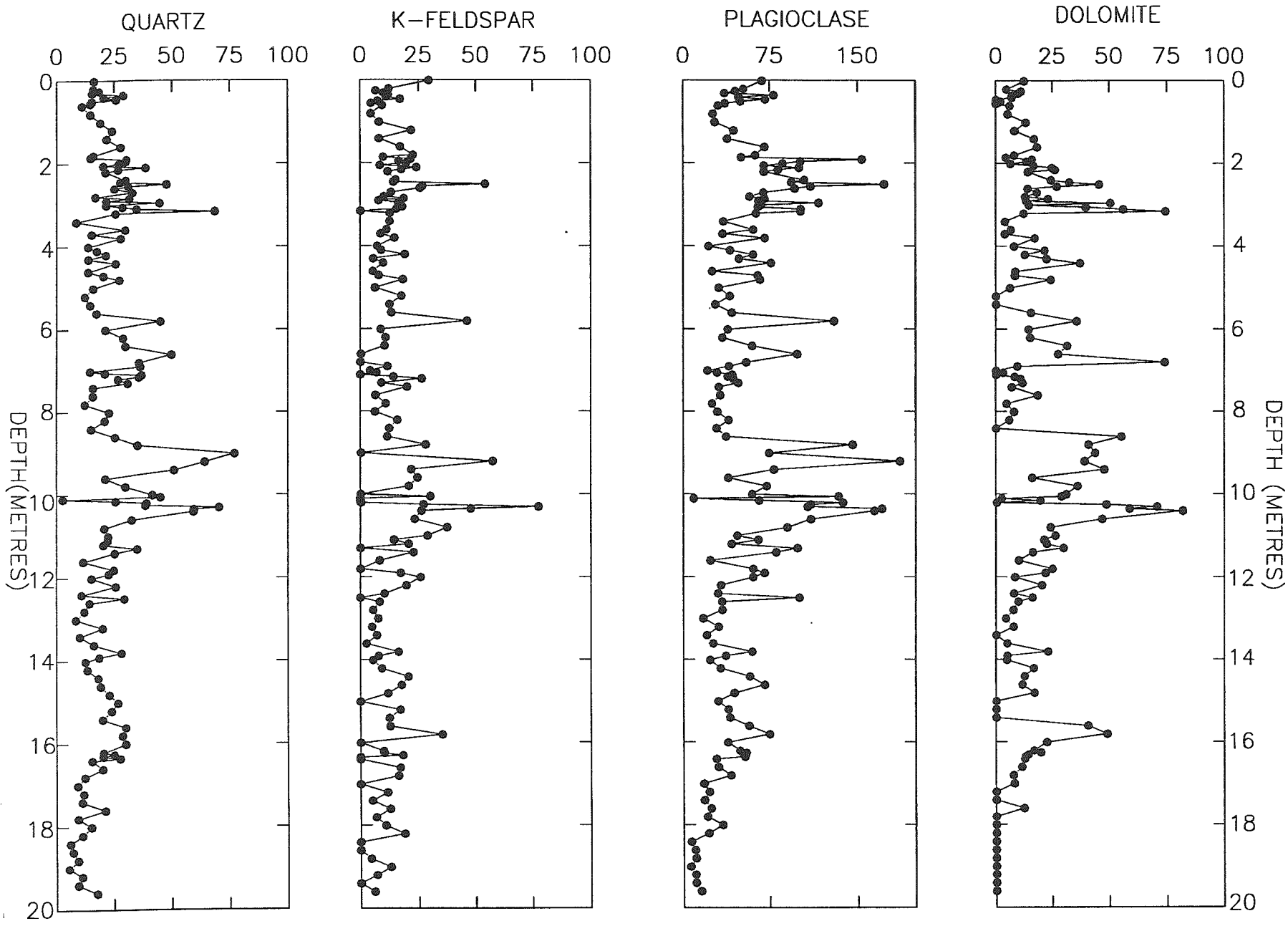

Figure 3.2b. Plot of peak areas normalised to illite against depth for clay–sized minerals from core 87–008–003.

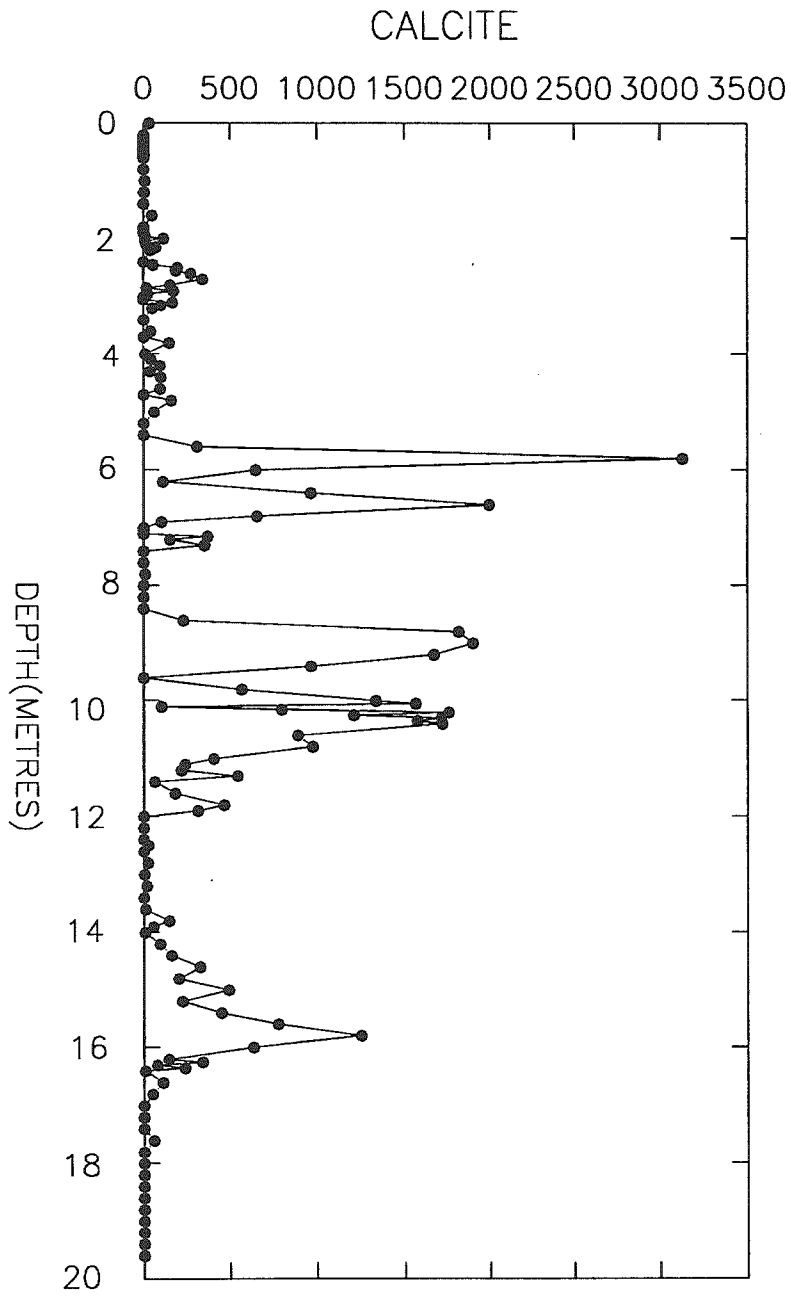

Figure 3.2c. Plot of calcite peak areas normalised to illite against depth for clay–sized minerals from core 87–008–003.

standardization represent a percentage of the highest peak area seen for that mineral in a specified region and sample set. The underlying assumption linking standardization to the geologic setting is that the percentiles calculated represent relative abundances. For example, chlorite=smectite=50 would mean that the input of these minerals into the sedimentation are both half of what they could be. Therefore the conclusion is that chlorite and smectite as contributors to the overall mineralogy of the sample are of equal importance. Of course, in marine sediments studied these minerals are invariably present. The greatest impact of standardization is in allowing a more detailed analysis of the trace minerals which tend to be more diagnostic of sediment source.

3.4 Removal of illite-induced noise

Though illite was chosen as the basis for normalization, its variations still have to be accounted for when analysing the data. To resolve this issue the inverses of the raw illite values were standardized in the same fashion as the normalized minerals. These values were subtracted from the standardized mineral values obtaining residuals. The residuals were then plotted downcore (Fig. 3.4). Positive values represent mineral highs above those induced by low raw illite values. Zero values or values close to zero represent intervals where a respective mineral is varying directly with illite (i.e. illite masking of mineral variations, a strong correlation between raw illite and the normalized mineral). Negative values correspond to intervals of mineral lows below those induced by elevated raw illite values.

3.5 Principal components analysis

In an attempt to duplicate the data analysis performed by Krissek (1989), a principal component analysis (PCA) of the data from core 87-008-003 was performed. In contrast to Krissek (1989), a correlation matrix was used for the PCA. This matrix was chosen over a variance-covariance matrix, since correlation coefficents rely solely on relative rather than absolute magnitudes in their calculation. Since the original data had varying magnitude ranges between minerals and since the standardization procedure retains relative magnitudes during the transformation, a correlation PCA retains the closest relationship to the original data. The data was further refined before principal component analysis by subtracting illite induced variations and using

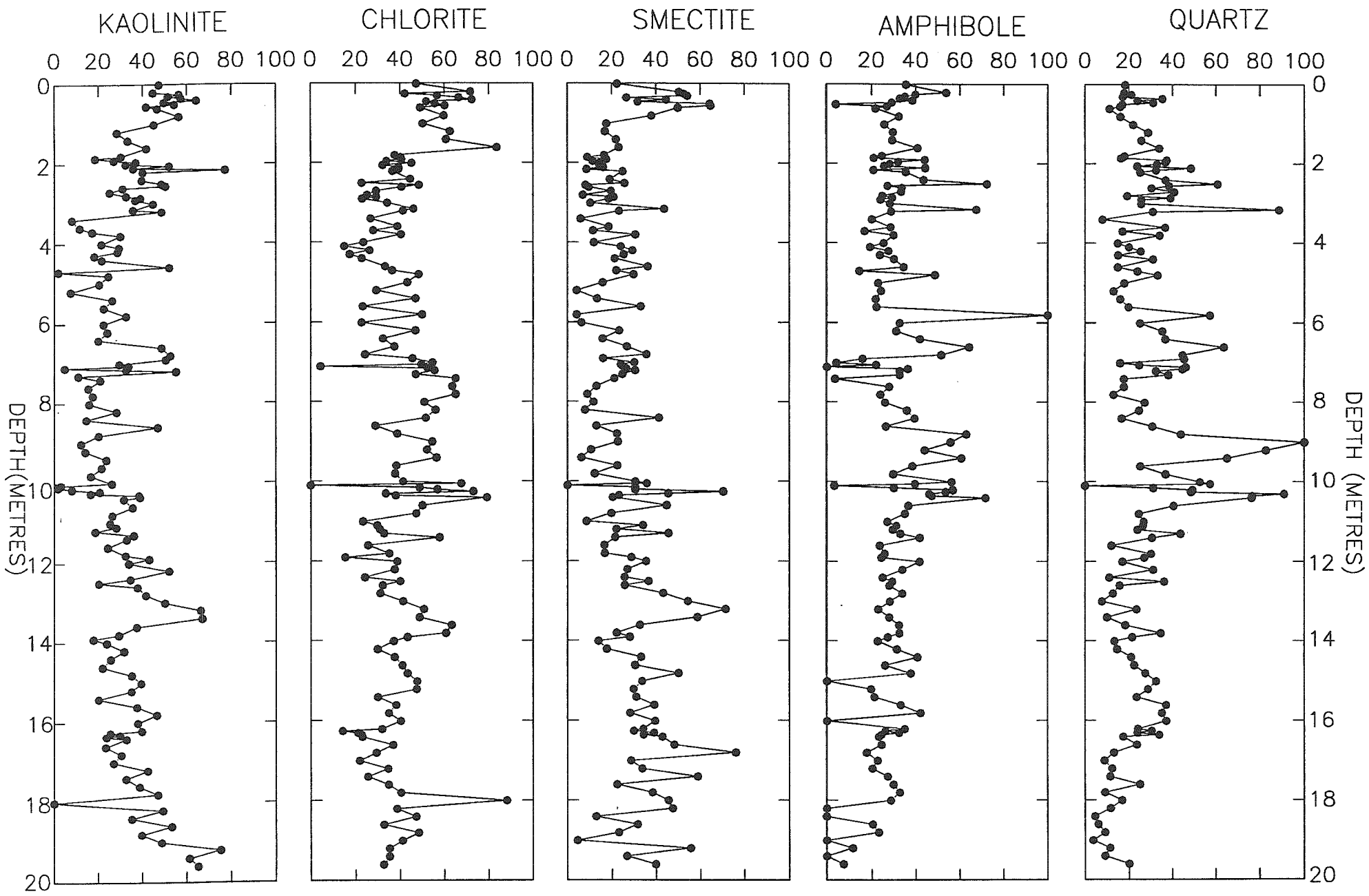

Figure 3.3a. Peak areas normalised to illite and standardised for regional range plotted against depth for clay–sized minerals from core 87–008–003.

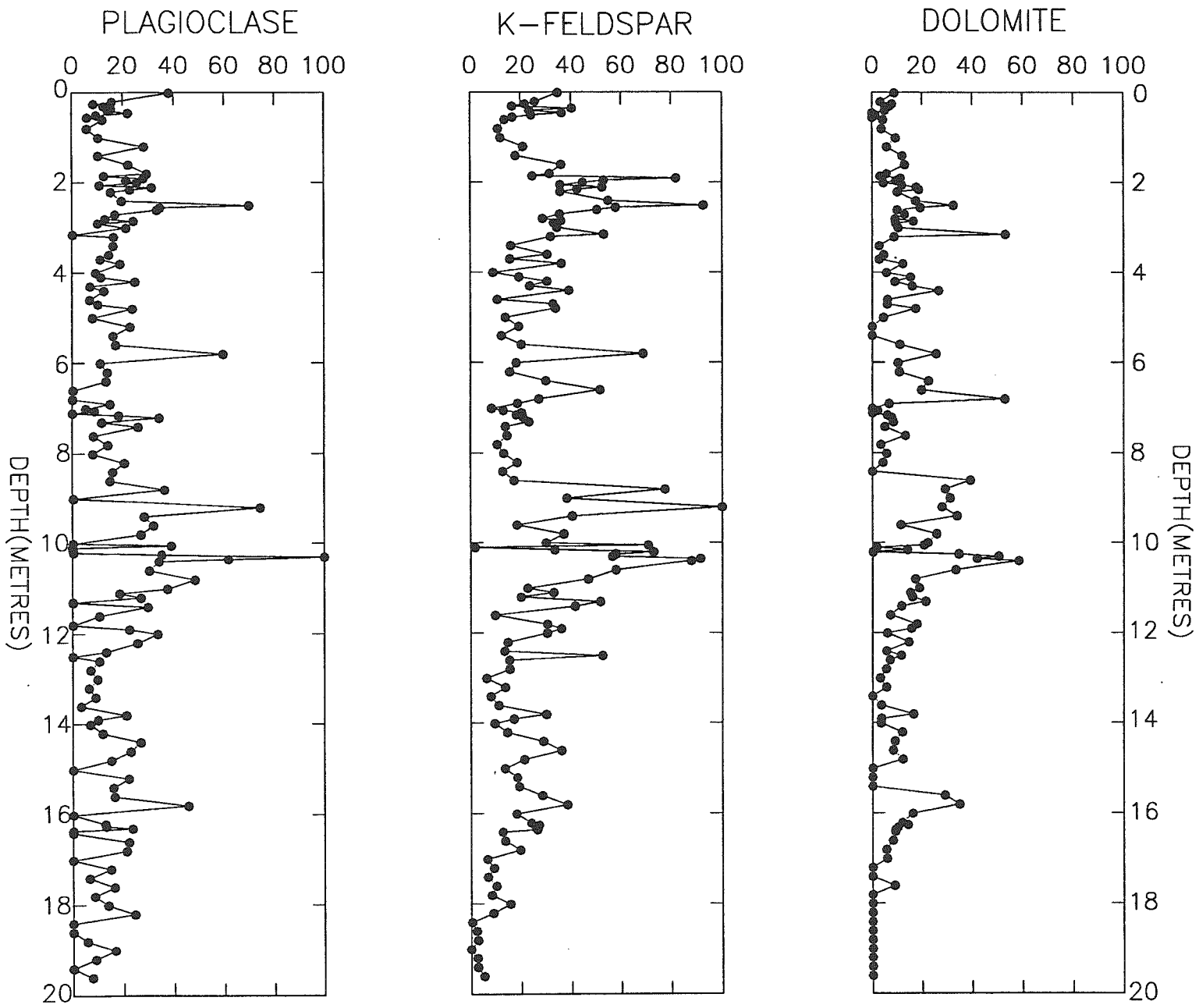

Figure 3.3b. Peak areas normalised to illite and standardised for regional ranges plotted against depth for clay–sized minerals from core 87–008–003.

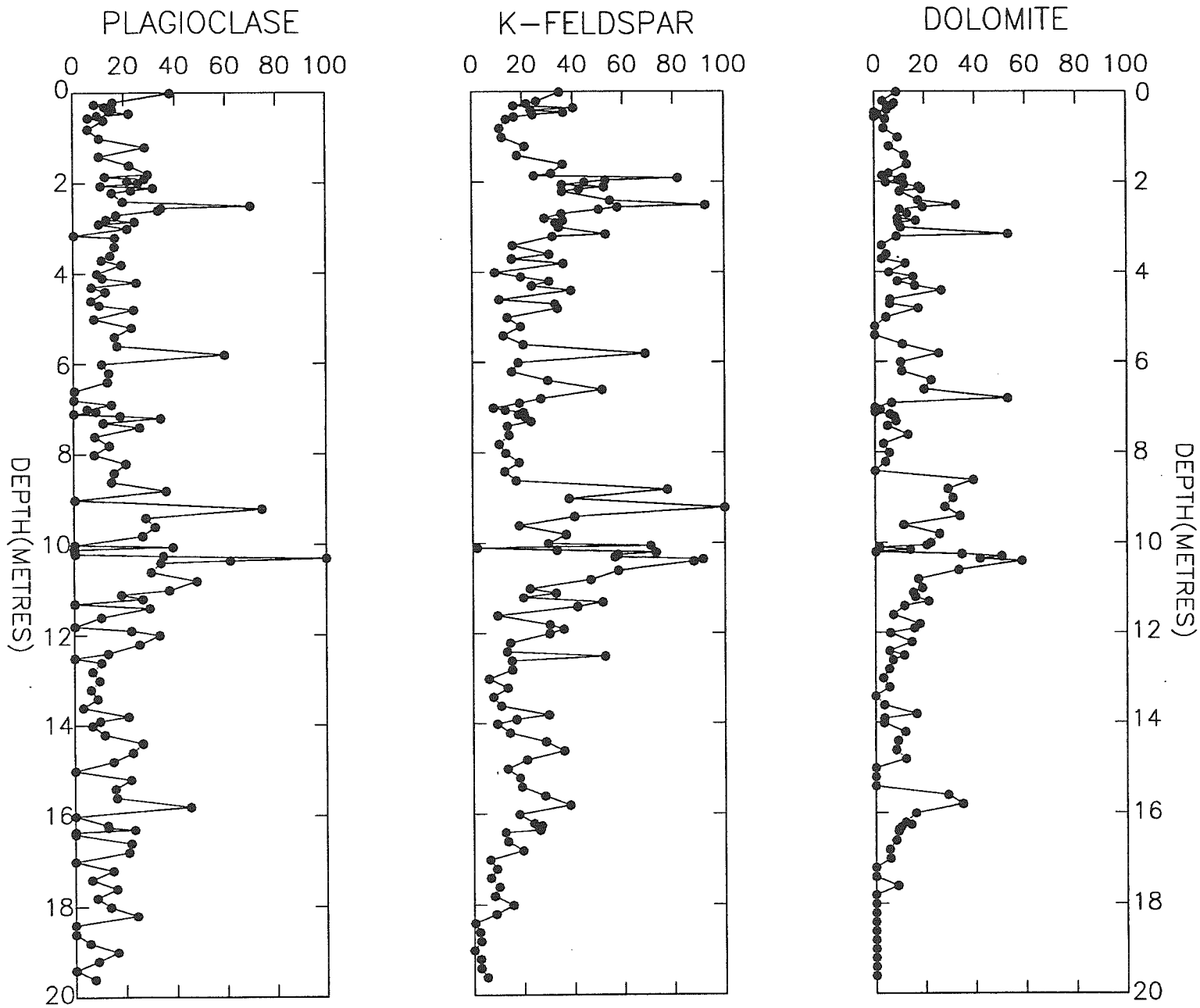

Figure 3.3b. Peak areas normalised to illite and standardised for regional ranges plotted against depth for clay–sized minerals from core 87–008–003.

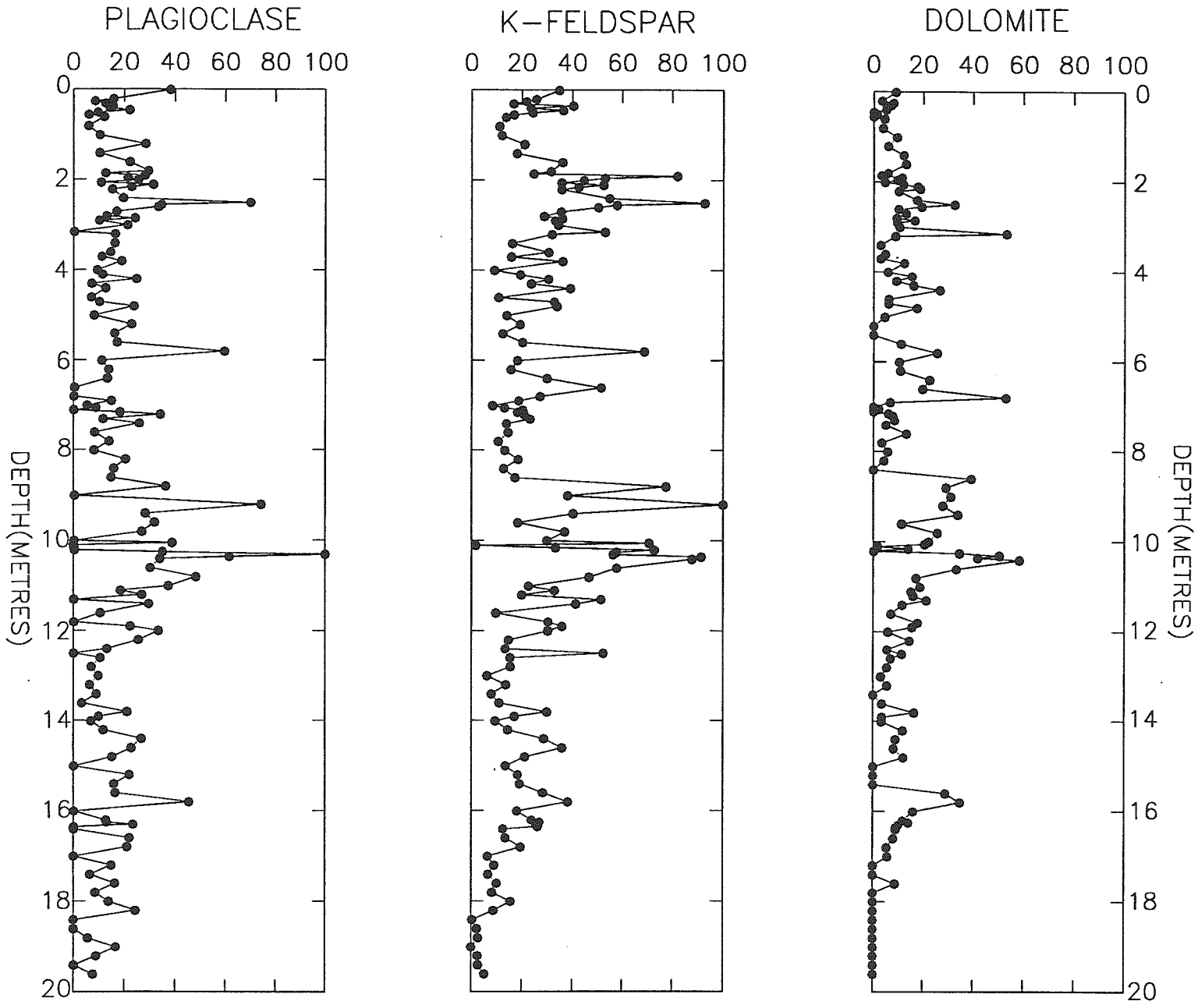

Figure 3.3b. Peak areas normalised to illite and standardised for regional ranges plotted against depth for clay-sized minerals from core 87-008-003.

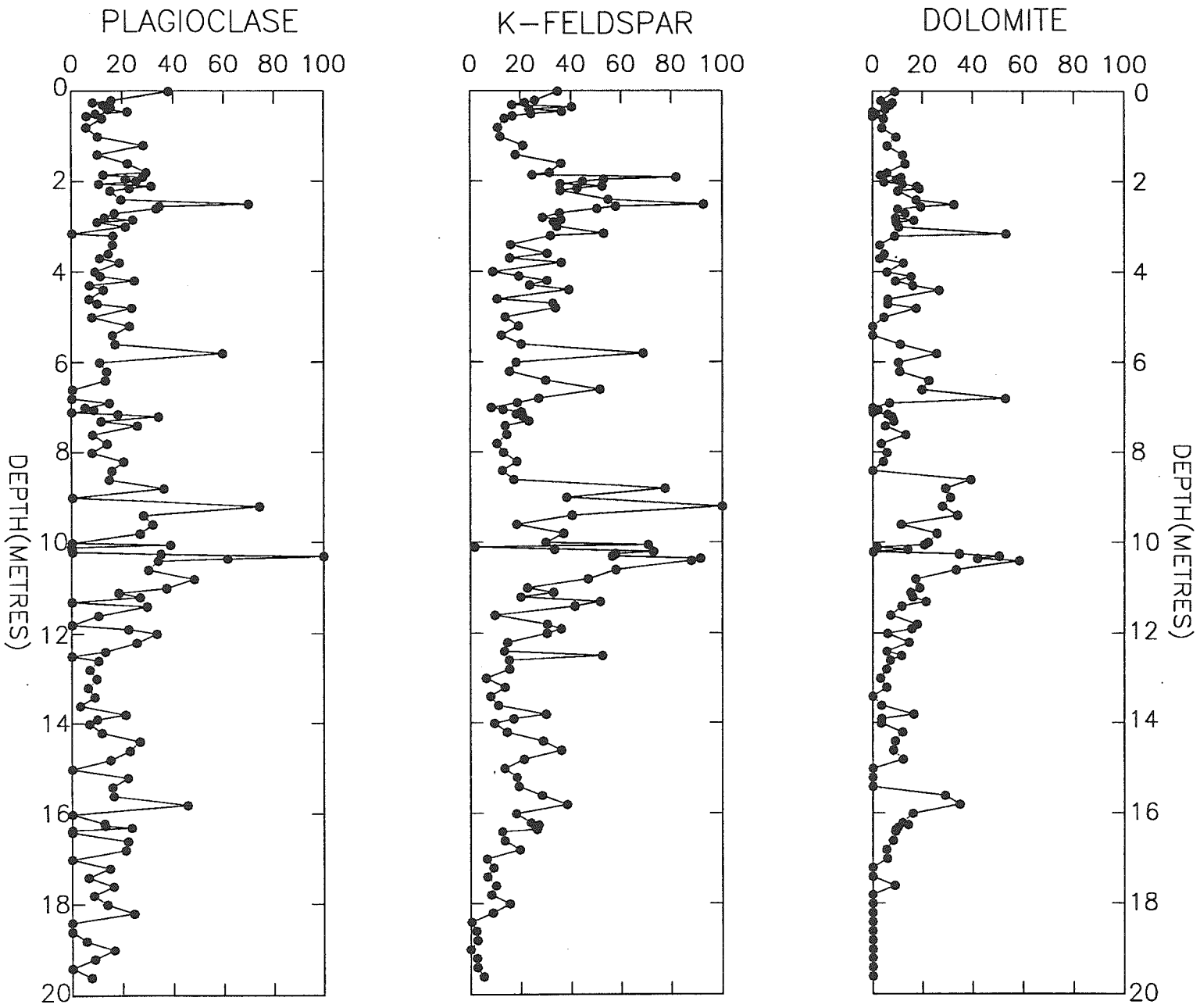

Figure 3.3b. Peak areas normalised to illite and standardised for regional ranges plotted against depth for clay-sized minerals from core 87-008-003.

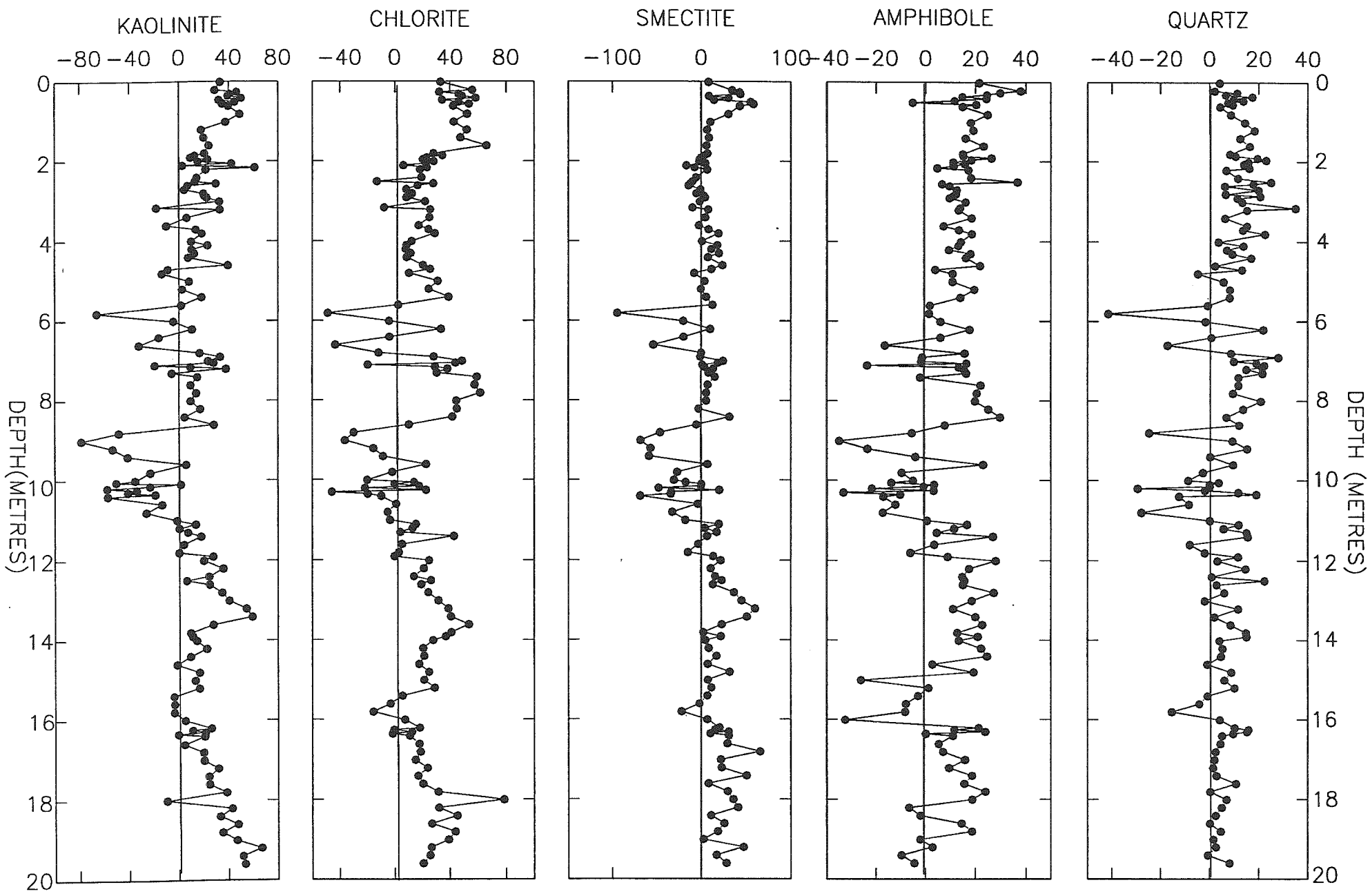

Figure 3.4a. Residual peak areas using standardised peak area minus standardised illite peak area plotted against depth for clay−sized minerals from core 87−088−003.

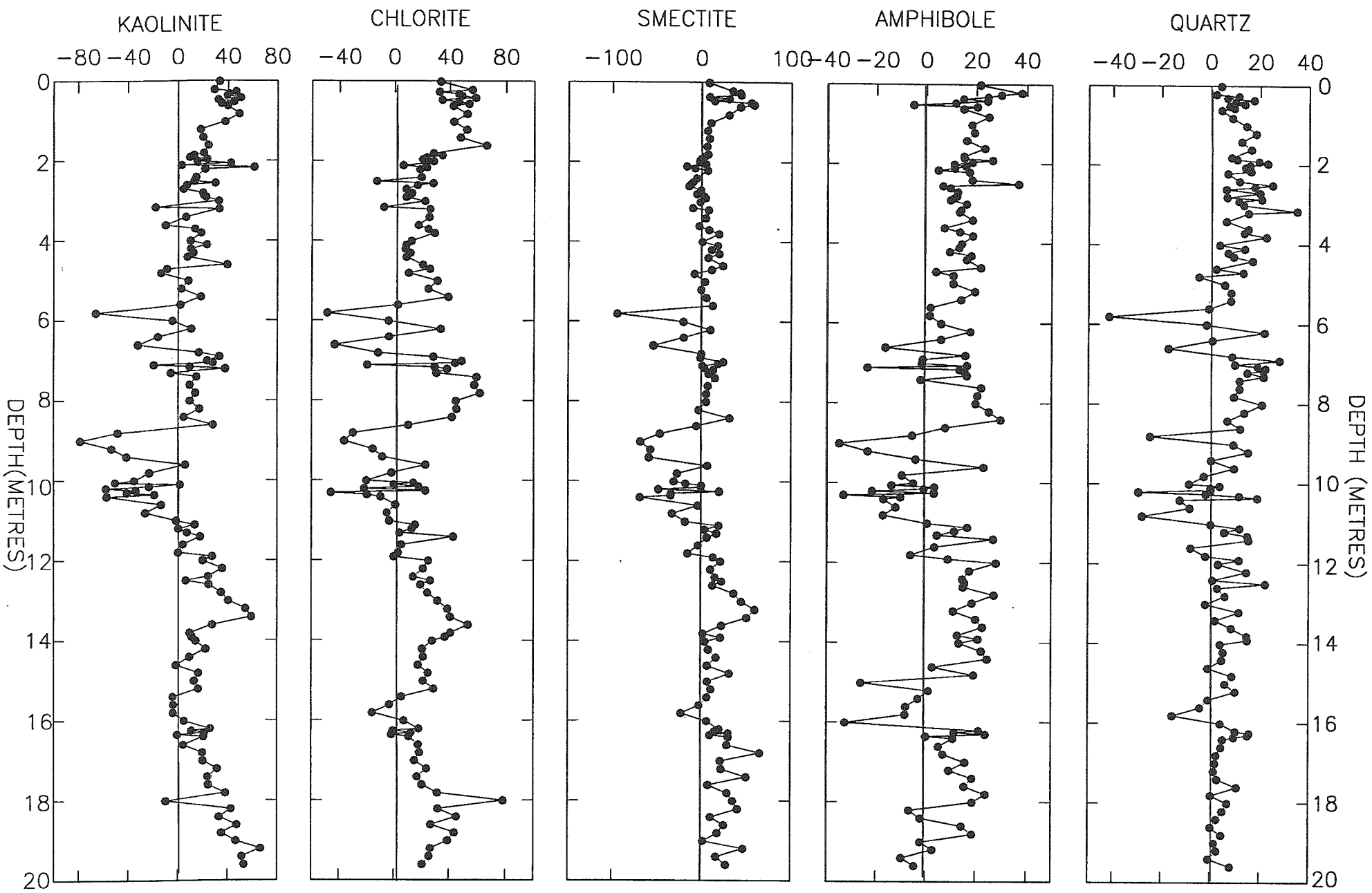

Figure 3.4a. Residual peak areas using standardised peak area minus standardised illite peak area plotted against depth for clay−sized minerals from core 87−088−003.

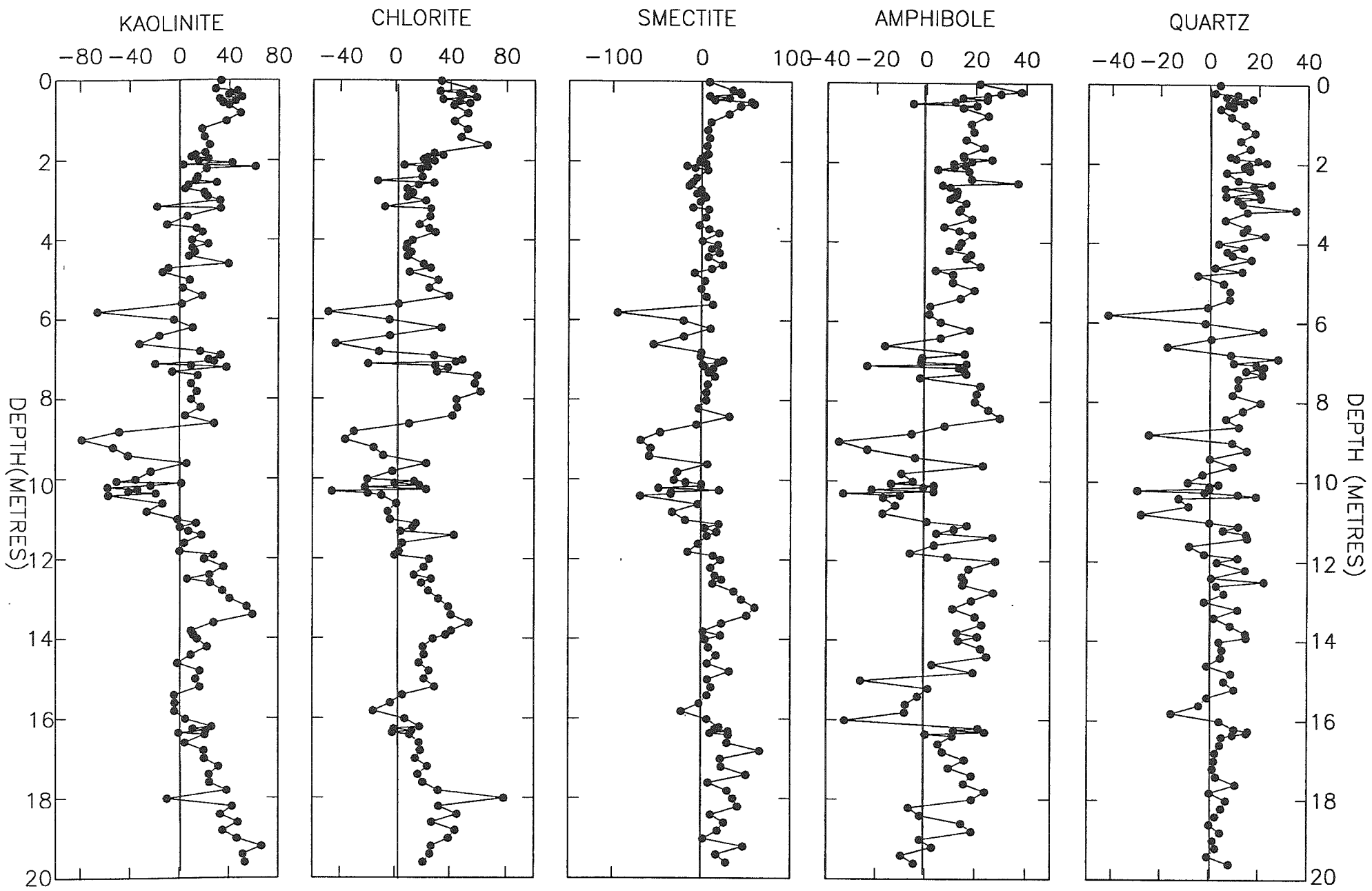

Figure 3.4a. Residual peak areas using standardised peak area minus standardised illite peak area plotted against depth for clay−sized minerals from core 87−088−003.

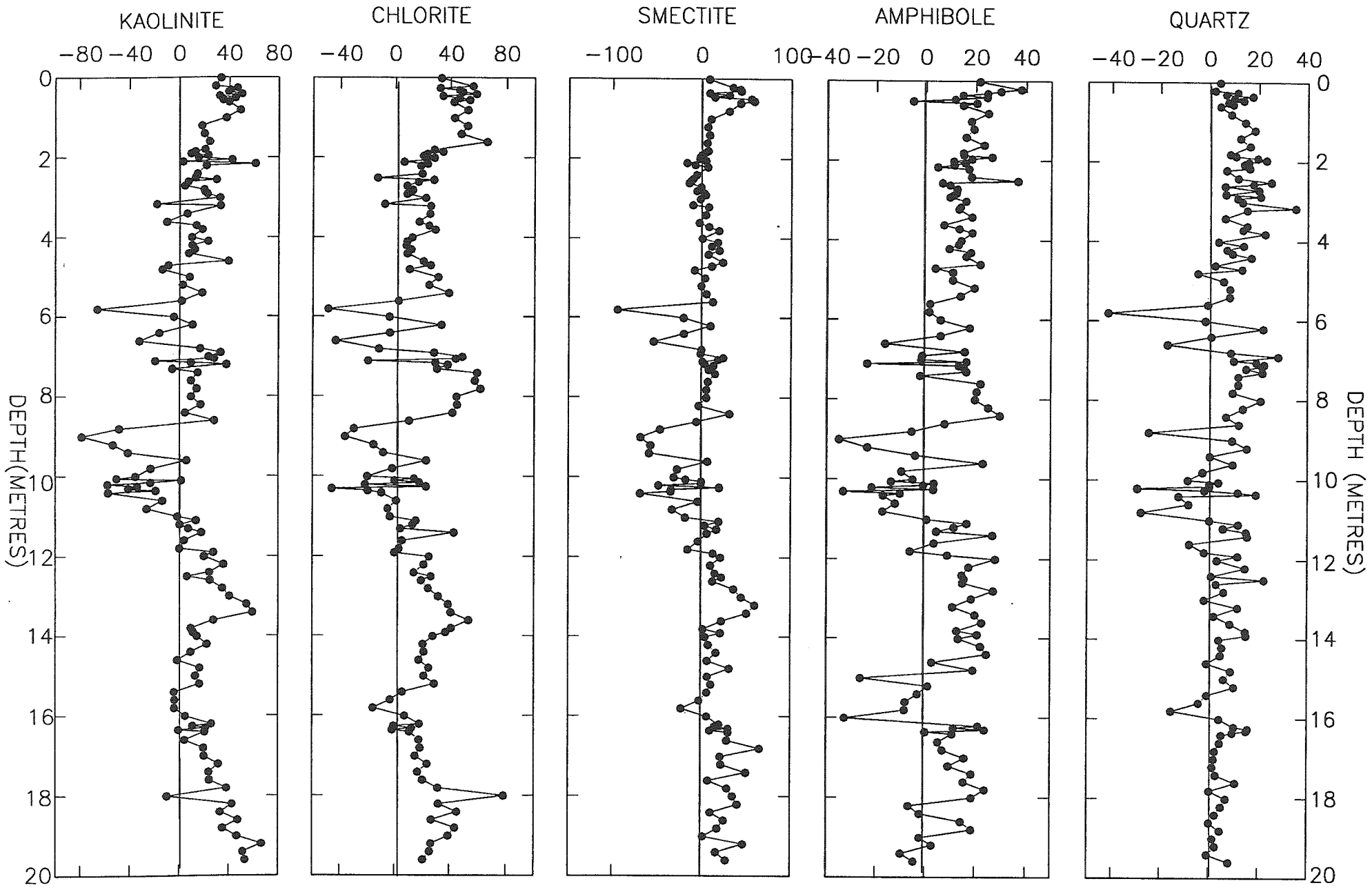

Figure 3.4a. Residual peak areas using standardised peak area minus standardised illite peak area plotted against depth for clay–sized minerals from core 87–088–003.

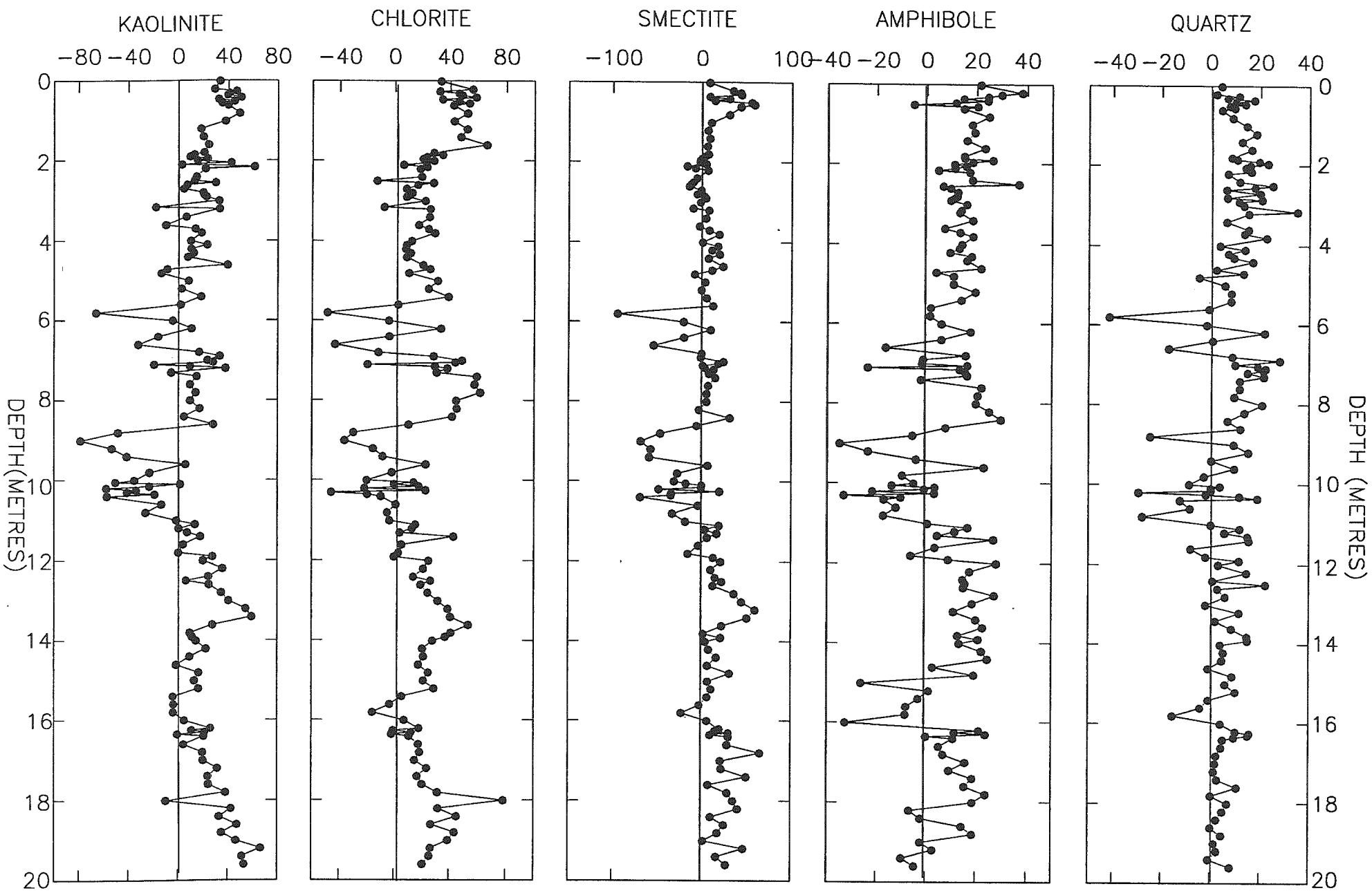

Figure 3.4a. Residual peak areas using standardised peak area minus standardised illite peak area plotted against depth for clay-sized minerals from core 87-088-003.

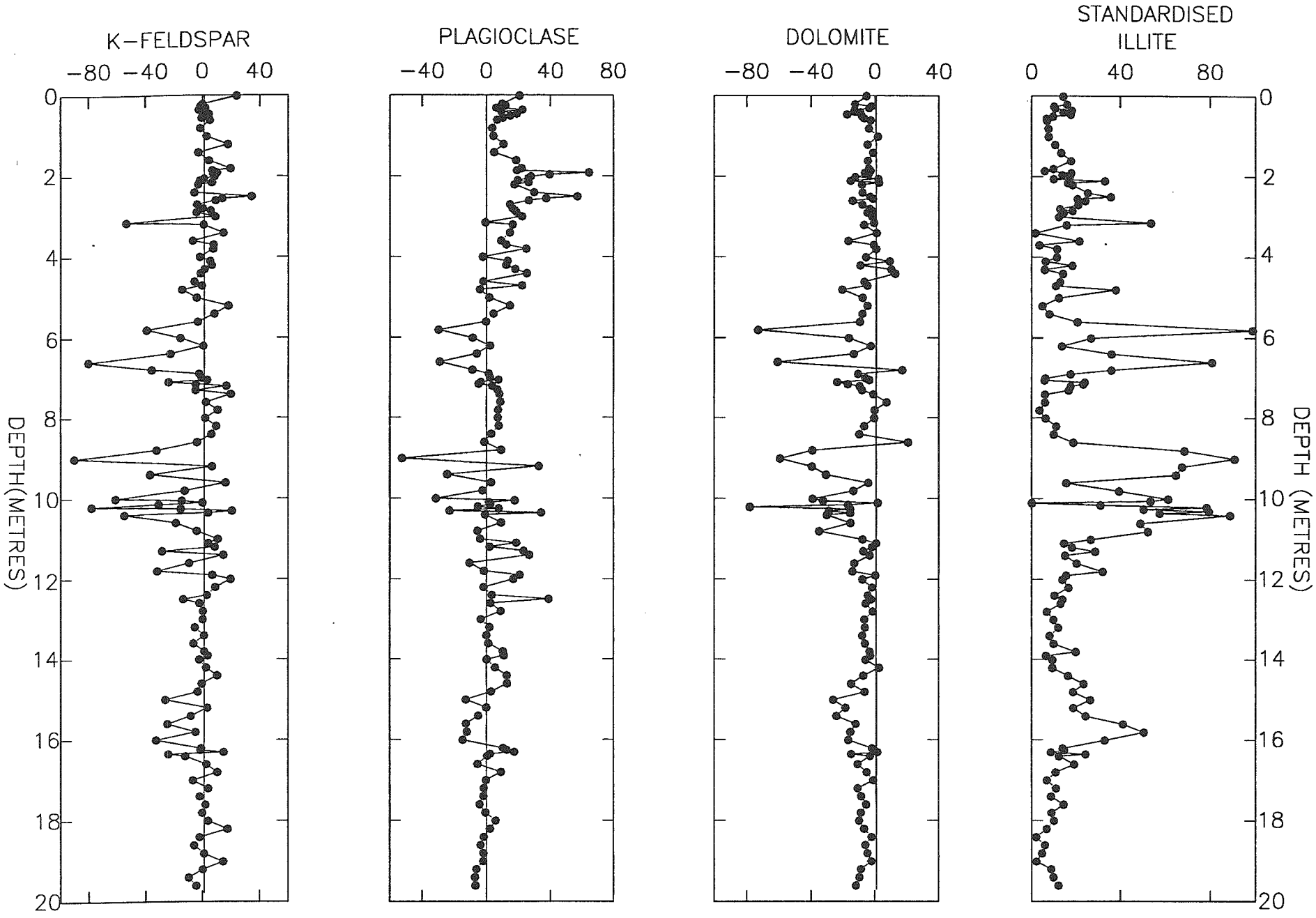

Figure 3.4b. Residual peak areas using standardised peak area minus standardised illite peak area plotted against depth for clay–sized mineral from core 87–008–003. Standardised illite is also included..

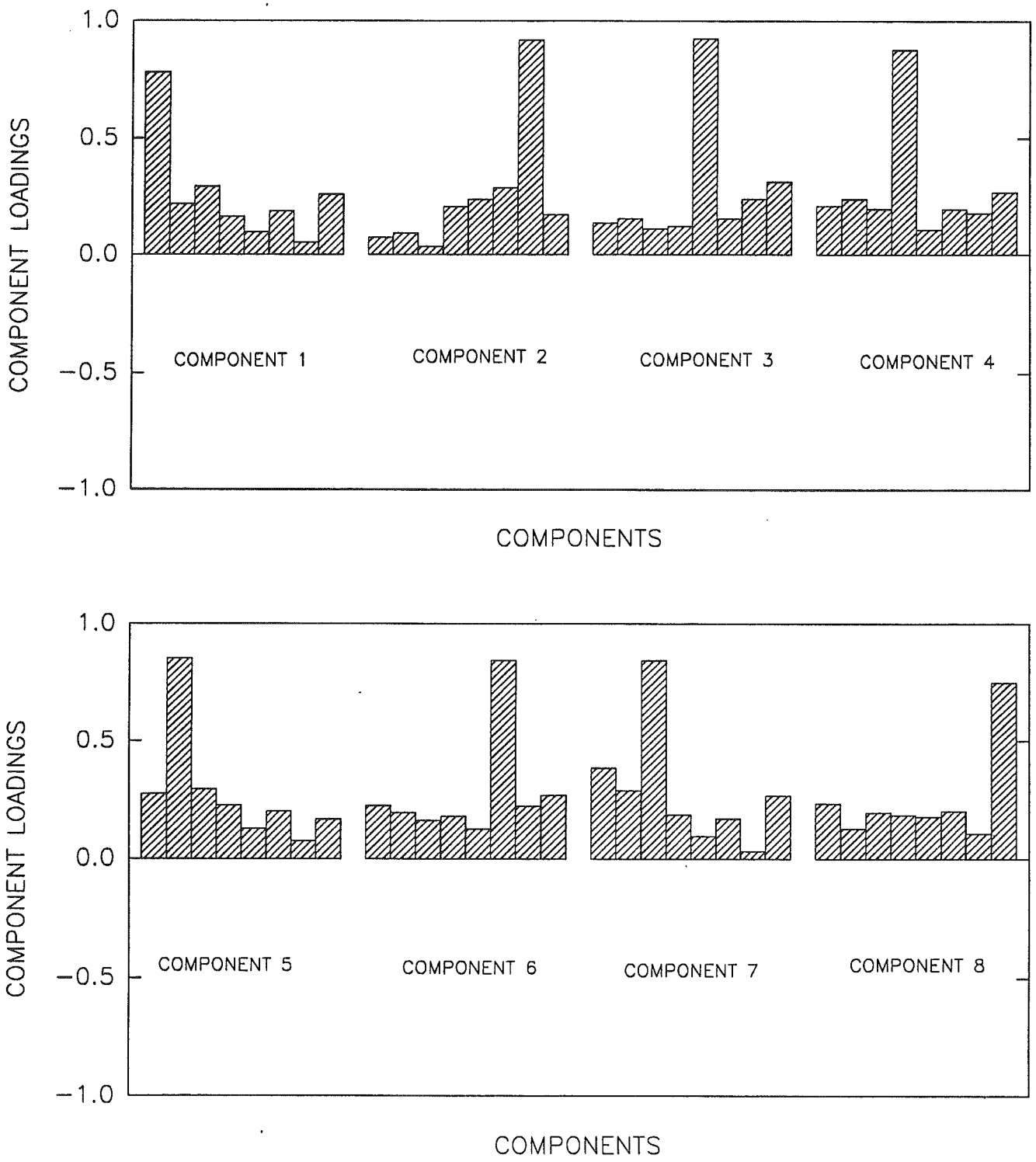

Figure 3.5a. Component loadings for core 87–008–003 using residual values. From left to right each bar graph shows the component loadings for the following minerals: kaolinite, chlorite, smectite, amphibole, quartz, K–feldspar, plagioclase, and dolomite.

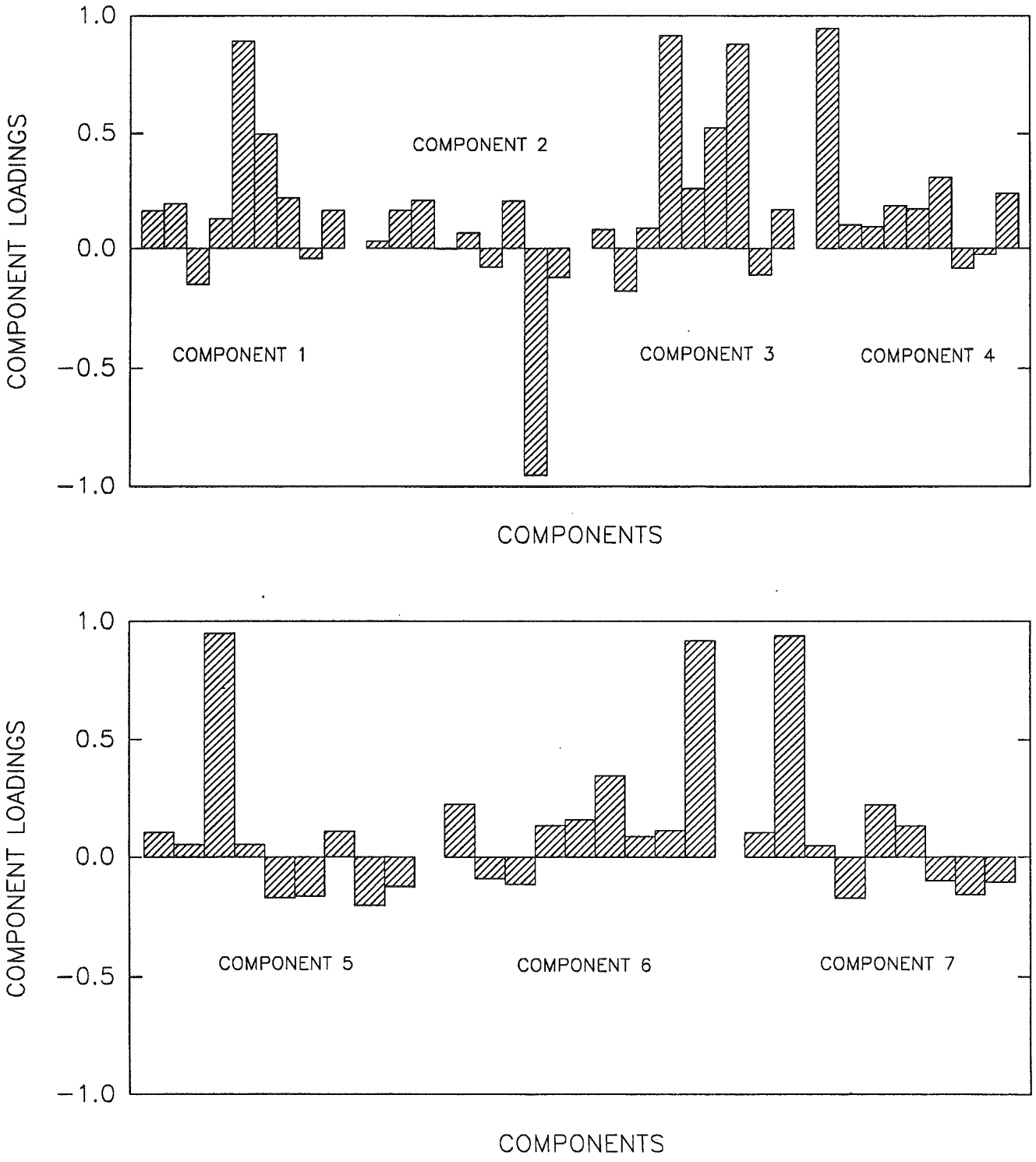

Figure 3.5b. Component loadings for comparison samples using residual values. From left to right each bar graphs shows the component loadings for the following minerals: kaolinite, chlorite, smectite, amphibole, quartz, K−feldspar, plagioclase, calcite, and dolomite.

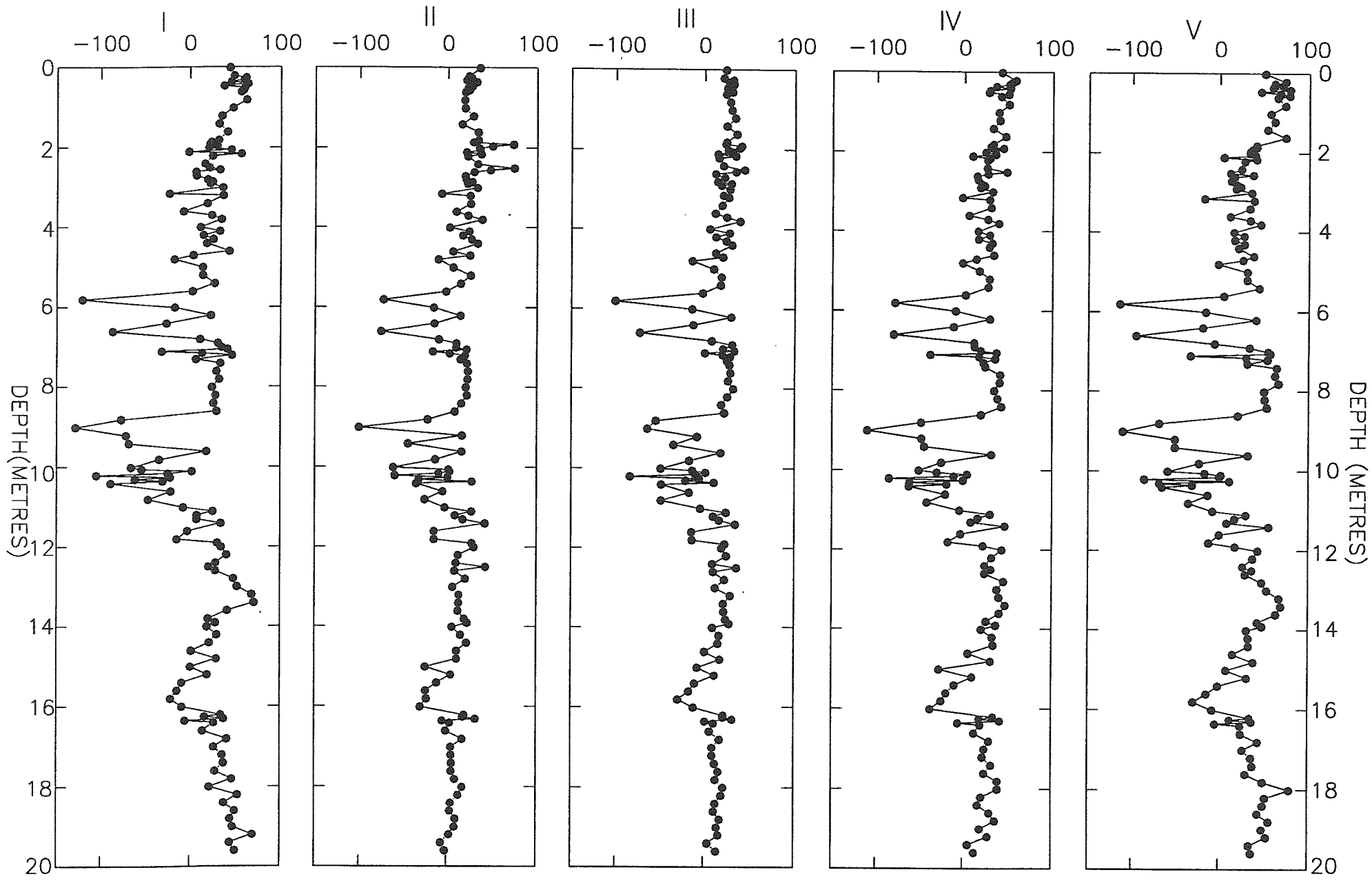

Figure 3.6a. Downcore variations in component loadings (components 1–5) in core 87–008–003.

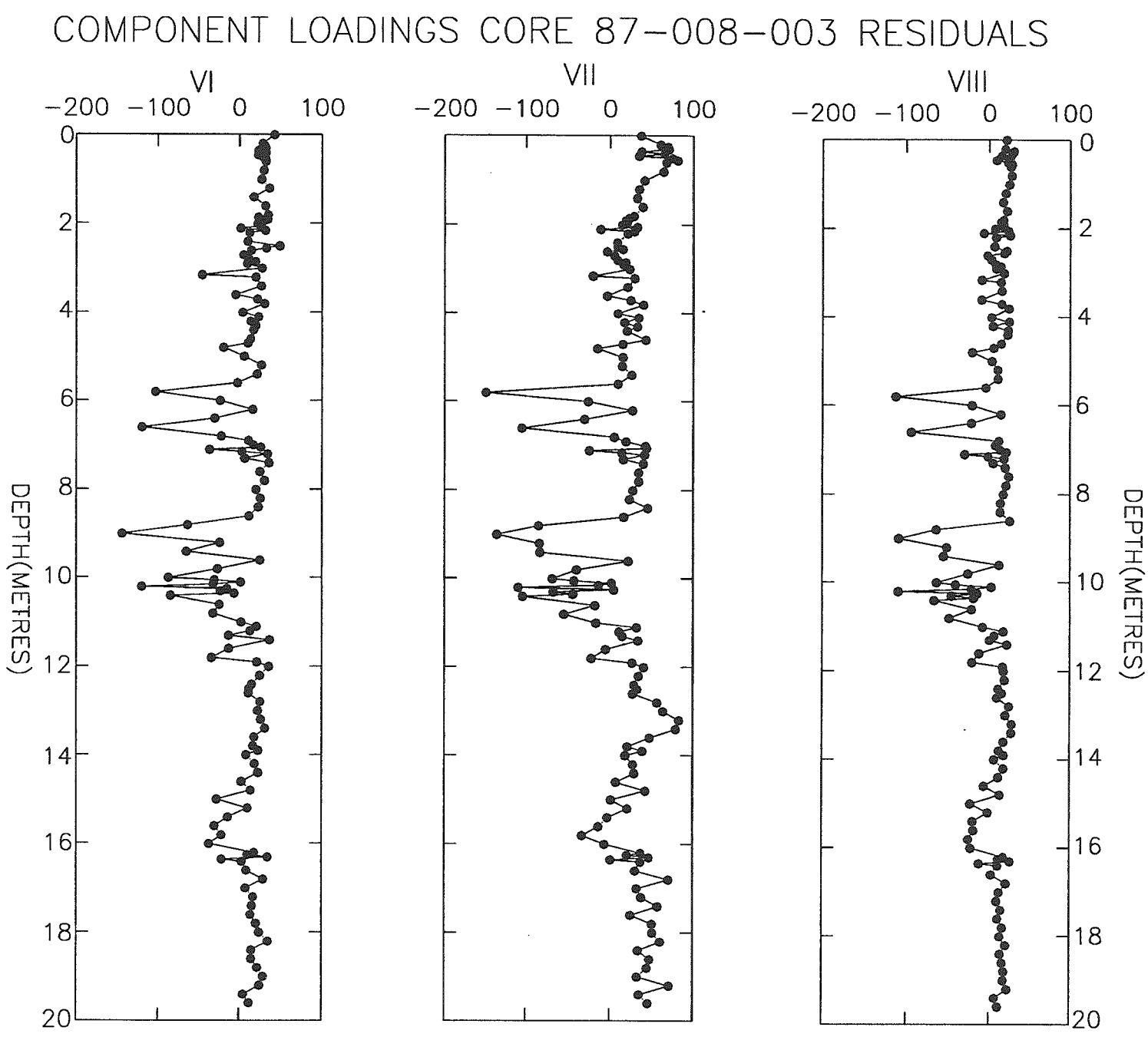

Figure 3.6b. Downcore variations in component loadints (components (6-8) in core 87-008-003

the residual values.

A strong degree of inter-mineral relationships is seen in the component loadings calculated from the residual values (Fig. 3.5). Individual components are characterized by a strong weighting of one mineral and moderate weights for two to four others. In addition, the variance of the VARIMAX rotated loadings is spread approximately evenly across the eight factors. Downcore variations of the component loadings (Fig. 3.6) supports the intermineral relationships conclusion. For the most part, each graph shows the same major trends with only marginal deviations. Interpretation of the PCA results suggests that the J-anomaly ridge represents a complex mixing of sources in which no one mineral assemblage explains a significant amount of the variance.

4.0 DATA INTERPRETATION AND DISCUSSION

4.1 Introduction and approach

Data interpretation involves three inter-related steps: i) interpreting source areas of comparison samples; ii) characterizing mineralogic trends of the comparison samples with an attempt at determining mineralogic source areas; and, iii) defining and discussing down-core variations in mineralogy at the J-anomaly ridge with qualitative comparison to source area characteristics.

4.2 Geologic setting and sources of comparison samples

Comparison samples were chosen to represent a stratigraphic and geographic range of potential source areas. Most samples are late Wisconsinan to Holocene in age and represent sites closer to potential glacial sources than the J-anomaly ridge.

The Holocene sources of sediment on the outer continental shelf are uncertain: north of the Tail of the Banks (samples 40, 46, 47, 49: see tables 6 and 7) reworking of sediments by iceberg scour and storms, followed by advection by surface currents, probably predominate, but off Nova Scotia and southern Newfoundland (1, 2, 6, 9, 12), cross-shelf transport of sediment from the coastal zone and rivers may also be important (Piper, 1991).

Late Wisconsinan samples from the Tantallon well-site (3-5) are from an area interpreted by Stow (1978) as showing sand and gravel mineralogy reflecting sources in Cape Breton Island, the adjacent continental shelf and the Gulf of St

Lawrence. On similar grounds, Bonifay and Piper (1988) interpreted Late Wisconsinan samples from St Pierre Slope (7, 8, 10, 11) as reflecting a source on the Avalon Peninsula and adjacent continental shelf.

The source of Late Wisconsinan sediments at the Narwhal well site (13-15) and the Tail of the Banks (41-45) is less certain. In part they represent sediment advected by the Labrador Current or Western Boundary Undercurrent. They may also be influenced by ice-margin discharge from ice crossing the Avalon Channel or even fluvial erosion on the outer Grand Banks (Slatt, 1977). Samples from Narwhal are from a turbidite dominated sequence. At the Tail of the Banks, two samples (41, 42) are from a distinctive light-grey marker horizon, thought to be carbonate-rich; others are from olive grey muds with ice-rafted detritus.

Samples from the northern Fogo Seamounts (16-35) represent a range of lithologies and ages. As with the J-anomaly ridge, it is likely that most horizons represent a mixture of sediment from various sources. Alam (1987) showed that the Fogo Seamounts experienced at times high rates of sedimentation from nepheloid layers or surface plumes originating from glacial discharge on the northwestern Grand Banks and the Gulf of St Lawrence. Alam and Piper (1977), using the sand content of muds, inferred that red muds (16, 25, 26, 33) had a predominant source from the Gulf of St Lawrence, whereas grey muds (21, 22, 28) had a source with more first cycle quartz grains, probably from insular Newfoundland crossing the Avalon Channel. The source of brown muds (?17, 24, 34) is less certain, although they may probably include a component similar to that on St Pierre Slope. Foram oozes represent times of lower sedimentation rate when sediment sources were probably more diverse, and may have included transport of montmorillonite by the Gulf Stream (Alam, 1979). The samples from the northern Fogo Seamounts span isotopic stages 1-6, with a few samples (28-31) from stages 10-12.

Only three samples from Flemish Pass have been analysed in a manner consistent with the J-anomaly ridge data, although some 20 additional samples have been analysed with an internal standard. Two samples (46, 47) are from a winnowed early Holocene horizon that in places includes significant ice-rafted carbonate detritus. Sample 48 may represent a debris flow from the eastern margin of the Grand Banks or may be ice rafted. Sample 49 is a surface sample of winnowed Quaternary sediment overlying a shallow Tertiary unconformity from the

western edge of Flemish Cap.

Three suites of samples have been analysed from the Labrador Shelf. In each case, they include a sample from till with a Labrador provencance (63, 66, 70). Overlying the till, the Qeovik Silt consists of ice-rafted and outwash plume sediments derived from deglaciation around Baffin Bay (probably a minor component), deglaciation of Hudson Bay and Strait (characteristically rich in carbonate), and deglaciation of the inner Labrador Shelf, the latter increasing in importance southwards (68, 69 from northern, 64, 65 from central, 61, 62 from southern Labrador Shelf). The overlying Makkak Clay (60, 67) probably reflects a post-glacial regime dominated by reworking of shelf sediments by iceberg scour and lesser advection of sediment from the north.

Samples from the northeast Labrador Sea (71-75), Davis Strait (76-80) and Baffin Bay Basin (81-87) provide stratigraphic control probably through stages 1-4. Samples from the northeast Labrador Sea probably reflect mostly sediment supply from the Norwegian-Greenland Sea, with a contribution from southern Greenland; those from Baffin Bay probably reflect nearby sources (Aksu and Piper, 1987); and those from Davis Strait a mixture of the two. In particular, samples 82 and 87 are from carbonate-rich ice-rafted sediment probably derived from break up of ice sheets off Ellesmere Island, whereas sample 84 is from a reddish sediment with a provenance in Proterozoic sediments of Lancaster Sound area or northern Greenland (Aksu and Piper, 1987). Both sediment types probably contain admixtures of sediment derived from older shield rocks of Baffin Island and Greenland and from Cretaceous-Tertiary shelf sediments.

Samples from Orphan Knoll (50-59) are hemipelagic and ice-rafted sediments. They are the only Early Pleistocene to Late Pliocene sediments analysed in this study and are therefore not directly comparable with either the other comparison samples or the J-anomaly ridge samples.

4.3 Identification and definition of mineralogic characteristics of comparison samples

The Holocene samples from Tail of the Banks (40-42) are characterized by the absence of kaolinite and relatively high values for quartz, amphibole, plagioclase, and chlorite (Fig. 4.1b). In contrast, samples from Tantallon, St Pierre Slope and Narwhal (1, 2, 6, 9, 12) have high chlorite and moderate quartz

(Fig. 4.1a), and smectite abundance is high at Narwhal. It should be noted that such generalizations are made based on an extremely limited sample suite.

Samples from Tantallon (3-5), St. Pierre Slope (7, 8, 10, 11), Narwhal (13-15), and the Tail of the Banks (43-45) are late Wisconsinan in age. Tantallon samples have high kaolinite and chlorite (Fig. 4.1d). Samples from St. Pierre Slope have high chlorite as well, but moderate kaolinite (Fig. 4.1o). Quartz is also moderate in these samples. Narwhal is characterized by high values for chlorite, kaolinite, and smectite (Fig. 4.1f). Moderate quartz and low calcite are also notable. The Tail of the Banks has moderate values for a suite of minerals including plagioclase, kaolinite, chlorite, and amphibole (Fig. 4.1j).

Clayey samples from the Fogo Seamounts have been divided on the basis of colour. Red muds (16, 25, 26, 33) have high chlorite and moderate kaolinite (Fig. 4.1g). The brown muds (17, 24, 28) appear to be more variable. However, they have high chlorite values but lower kaolinite values than the red muds (Fig. 4.1h). The grey muds (21, 22, 28) have high amphibole with low to moderate amounts of plagioclase, chlorite, kaolinite (Fig. 4.1i). Remaining Fogo Seamount samples have rather variable mineralogical characteristics.

Holocene samples from Flemish Pass (46, 47) are distinguished by their high chlorite, elevated quartz, and slightly elevated plagioclase (Fig. 4.1c). Though taken from a unit rich in ice-rafted carbonate detritus, the clay-sized mineralogy suggests the ambient sedimentation to be more closely related to the Holocene samples from Tantallon, St. Pierre Slope, and Narwhal (Fig. 4.1a). However, plagioclase is more variable at these locations than at Flemish Pass.

Amphibole and plagioclase appear high within the Labrador Shelf till (63, 66, 70; Fig. 4.1m). These minerals are more variable but still elevated in the Qeovik silt (61, 62, 64, 65, 68, 69; Fig. 4.1l). The Makkaq clay samples (60, 67) shows more consistent, though lower, values for plagioclase with amphibole also lower but still variable (Fig. 4.1k).

Samples from Davis Strait (76-80) are characterized by high kaolinite and amphibole (Fig. 4.1o). Plagioclase and K-feldspar make up a lesser and more variable contribution to the assemblage. Baffin Bay Basin (81-87) is strikingly different from Davis Strait due to its lower and more variable kaolinite (Fig. 4.1p). Amphibole values are also noticably lower. The Labrador Sea samples (71-75) have highly variable values for most minerals; of note is the high and

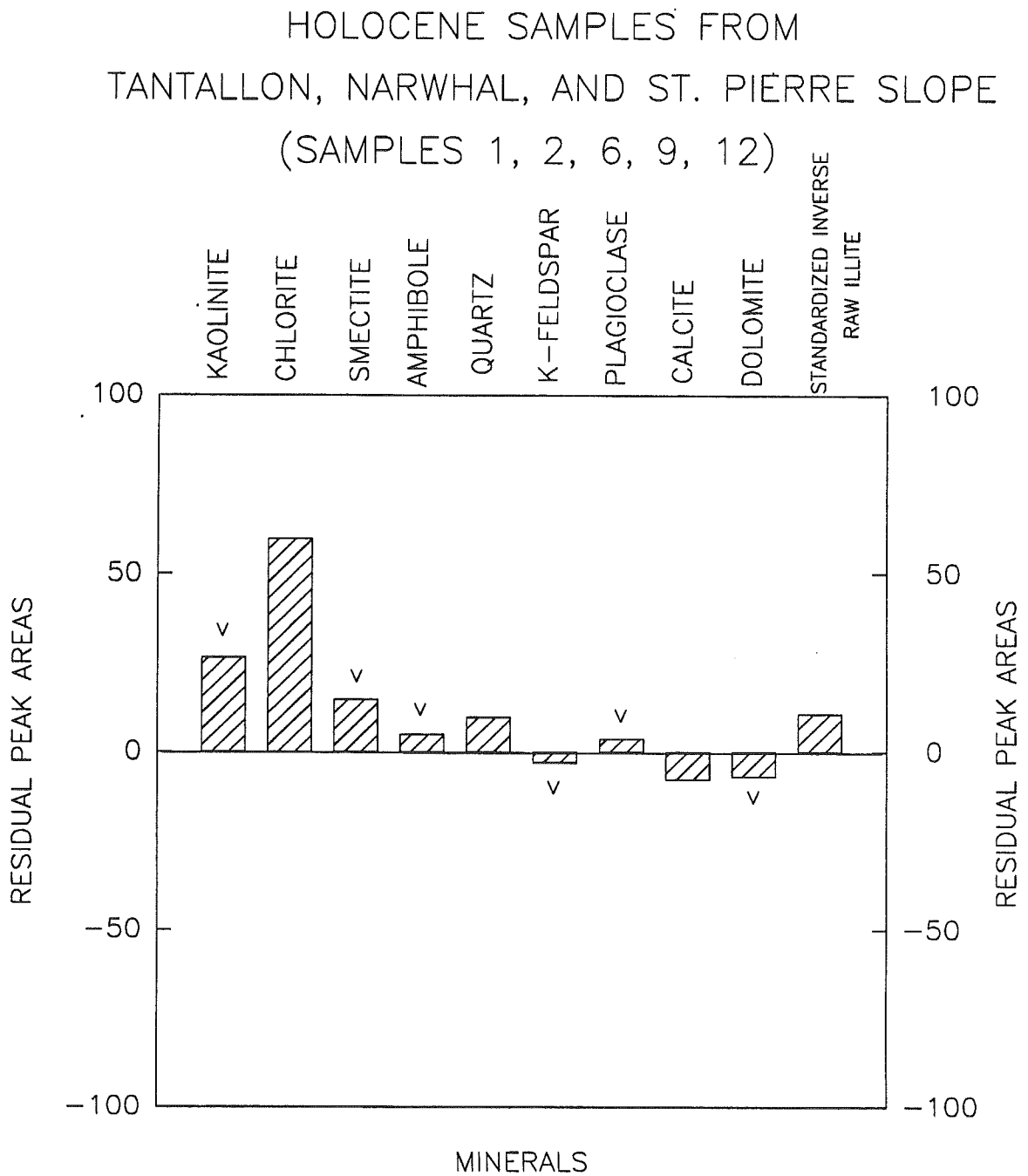

Figure 4.1a. Residual peak areas for groups of comparison samples. V = highly variable.

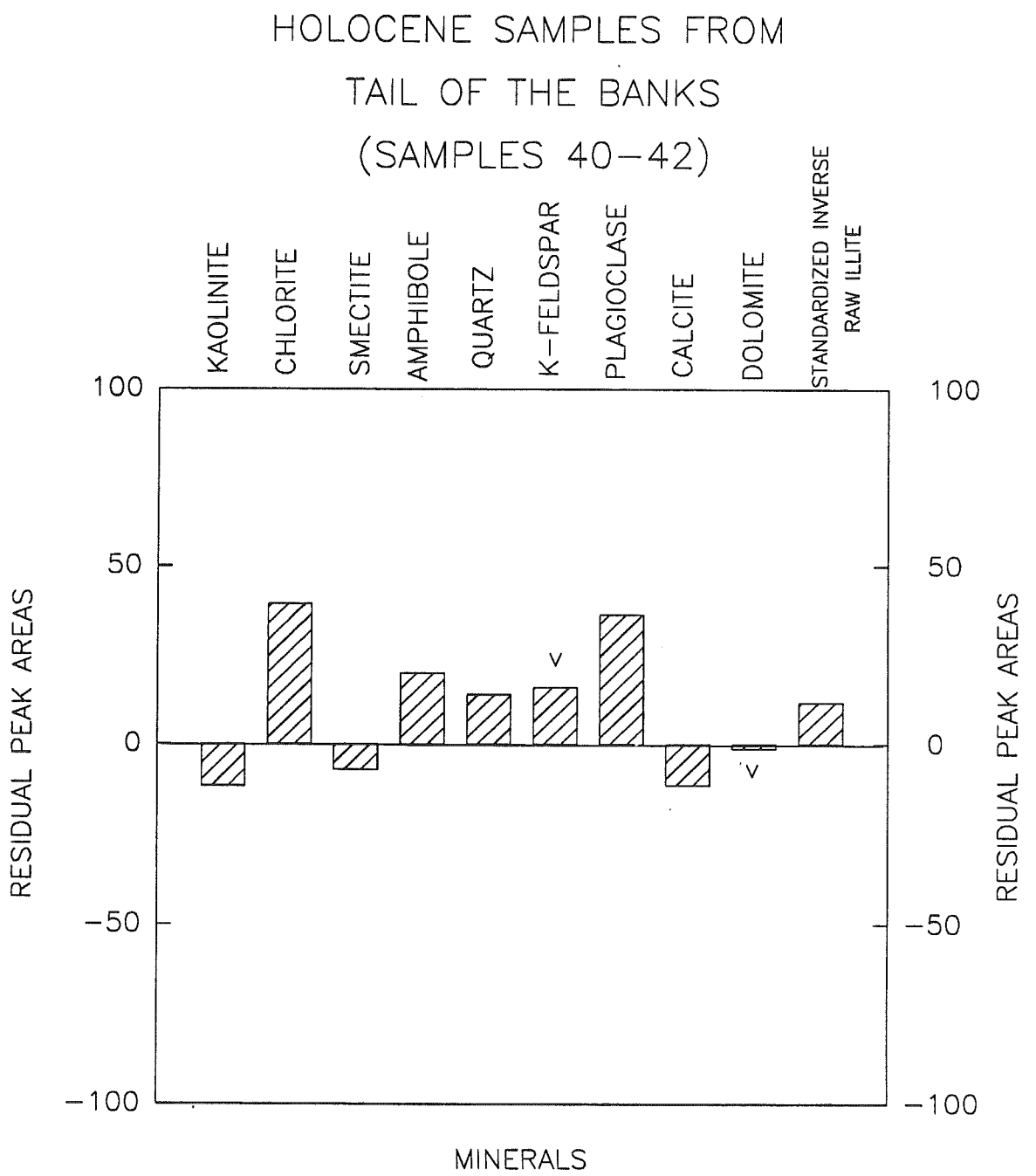

Figure 4.1b. Residual peak areas for groups of comparison samples. V = highly variable.

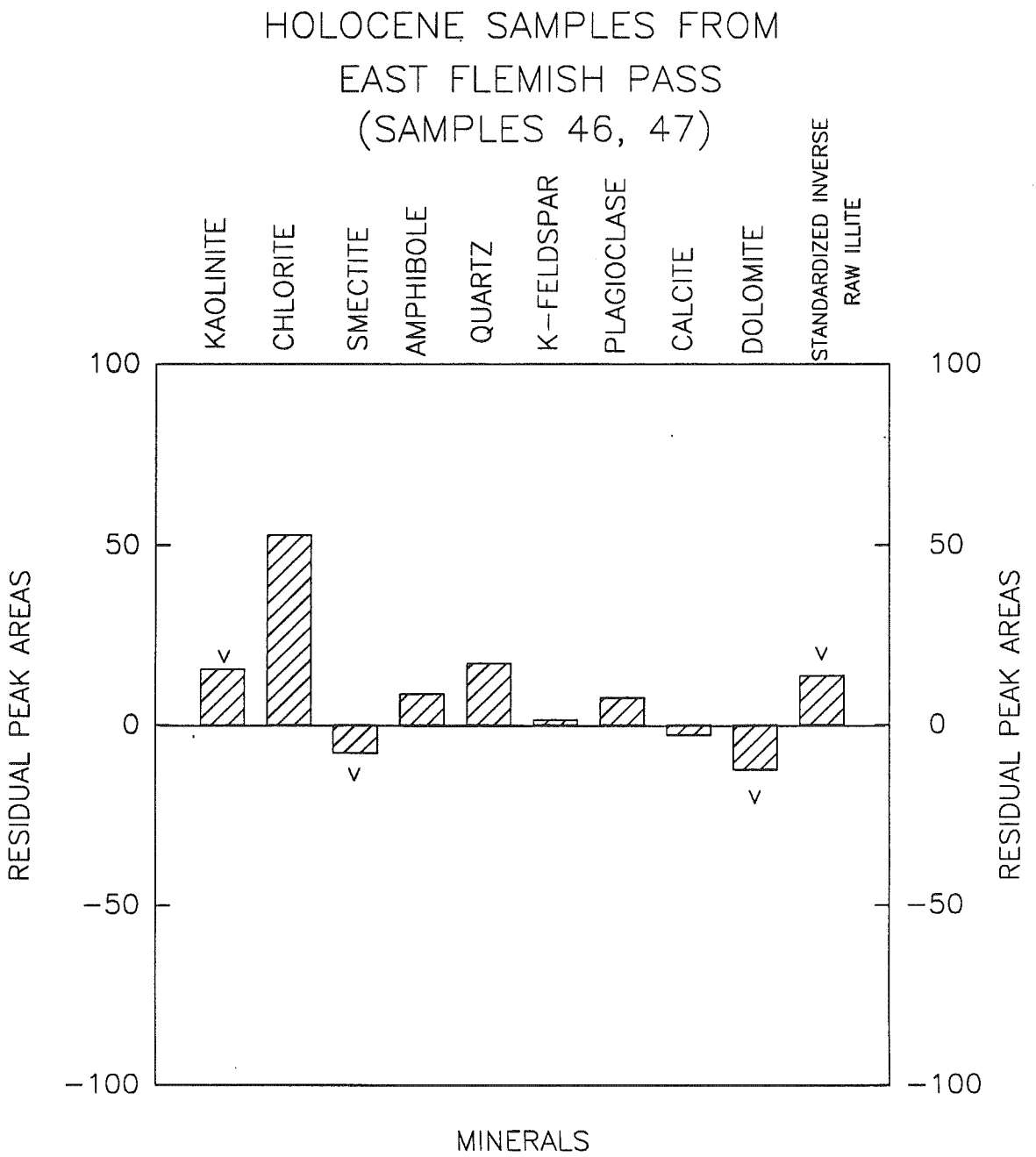

Figure 4.1c. Residual peak areas for groups of comparison samples. V = highly variable.

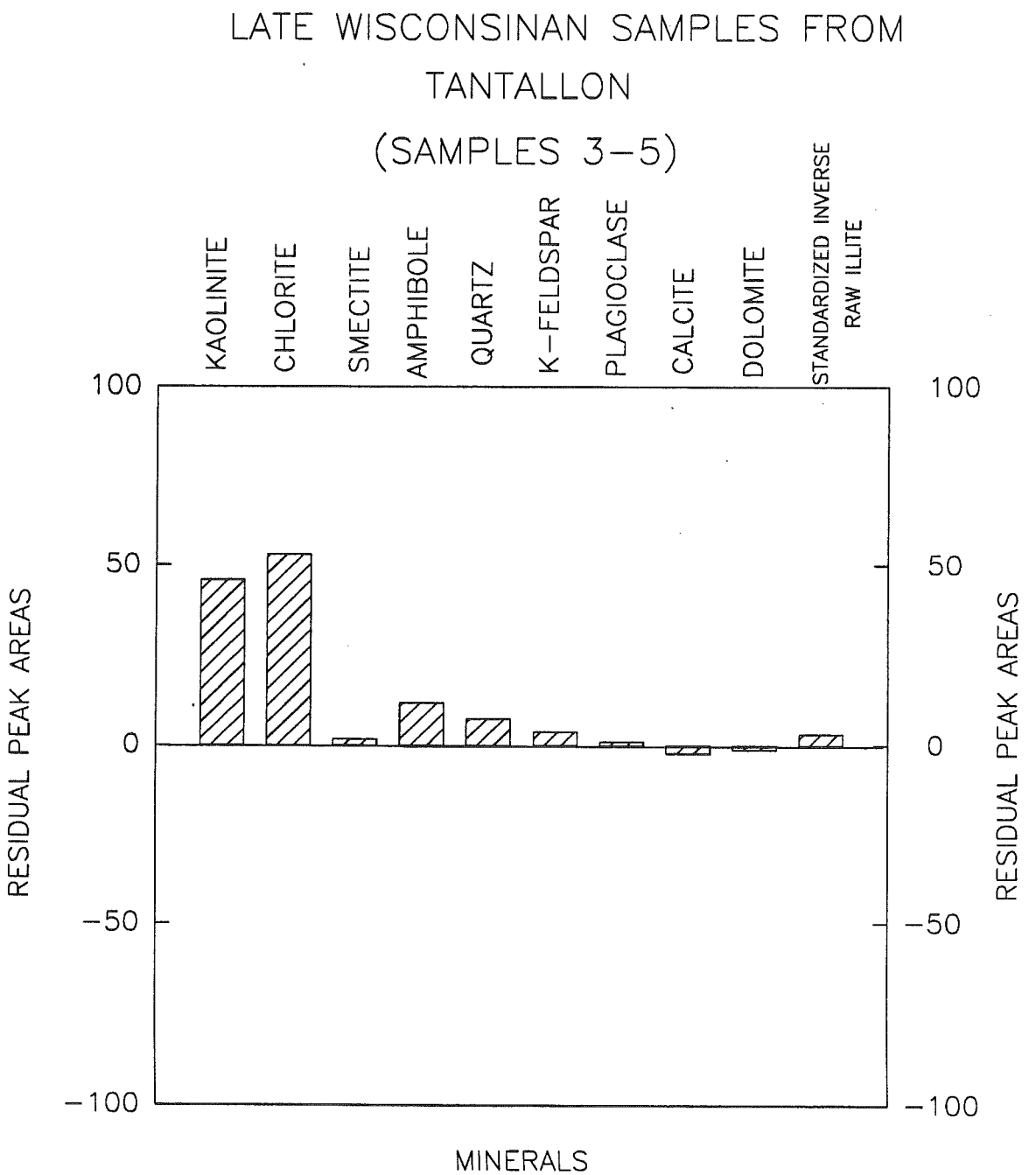

Figure 4.1d. Residual peak areas for groups of comparison samples. V = highly variable.

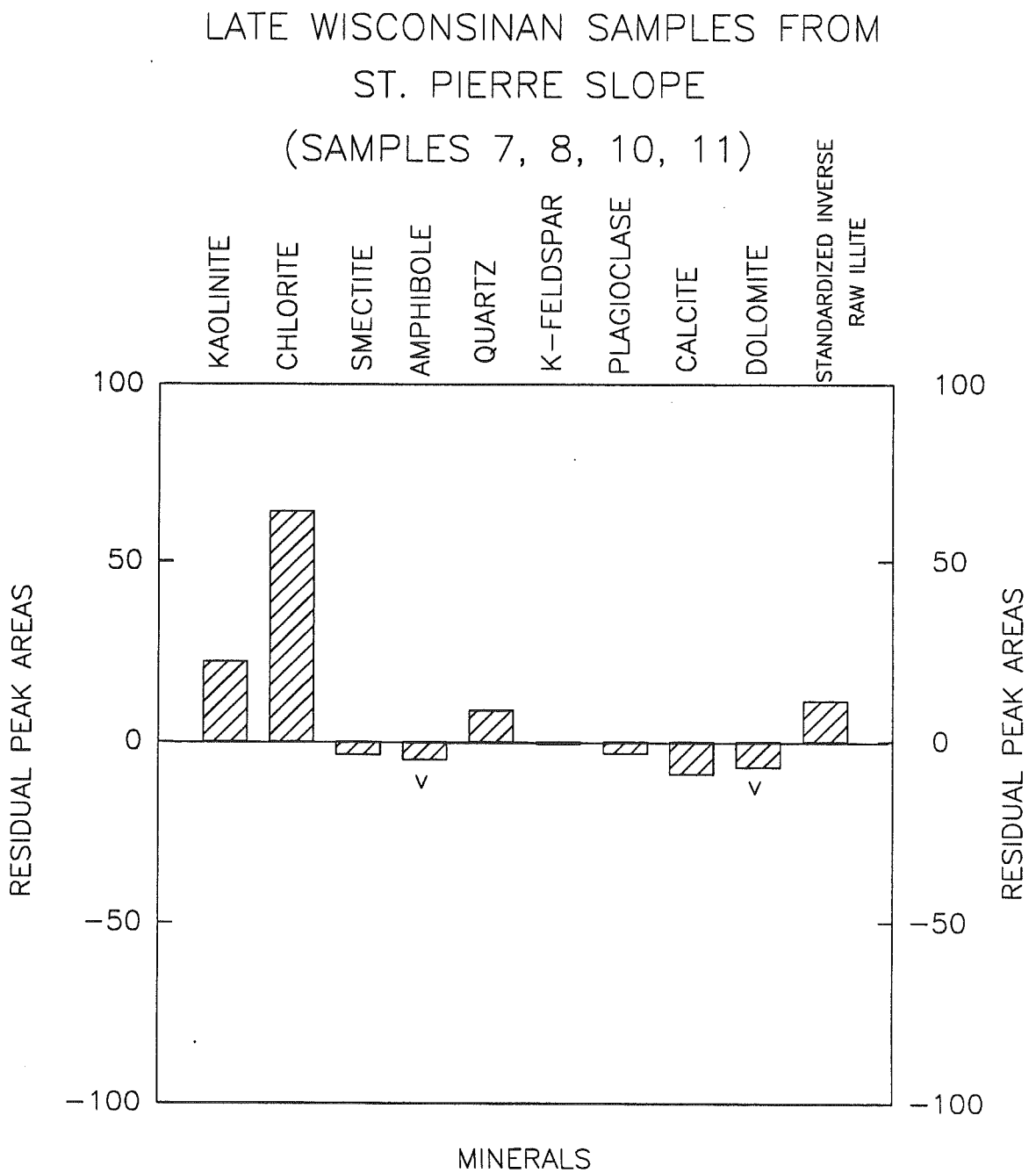

Figure 4.1e. Residual peak areas for groups of comparison samples. V = highly variable.

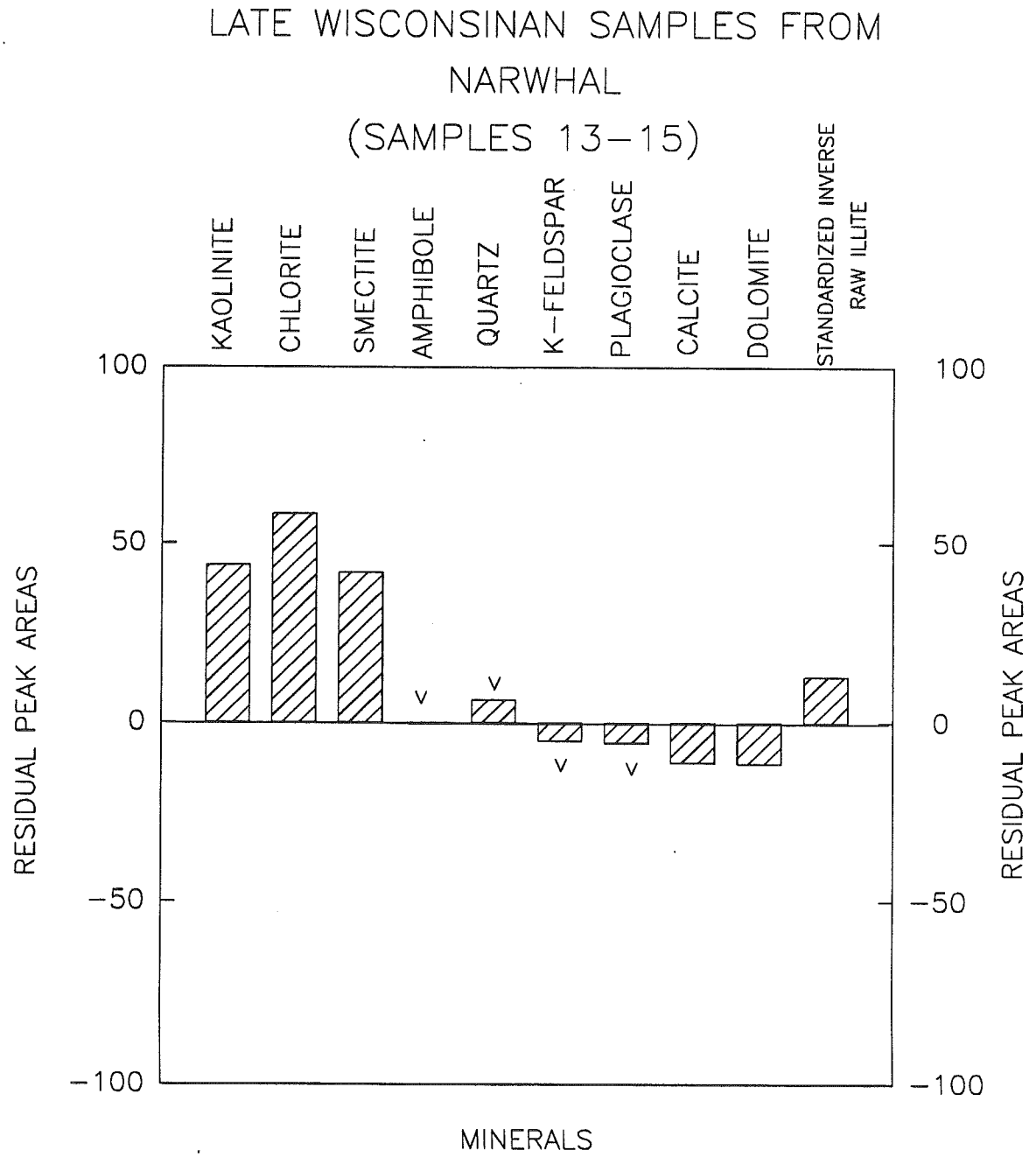

Figure 4.1f. Residual peak areas for groups of comparison samples. V = highly variable.

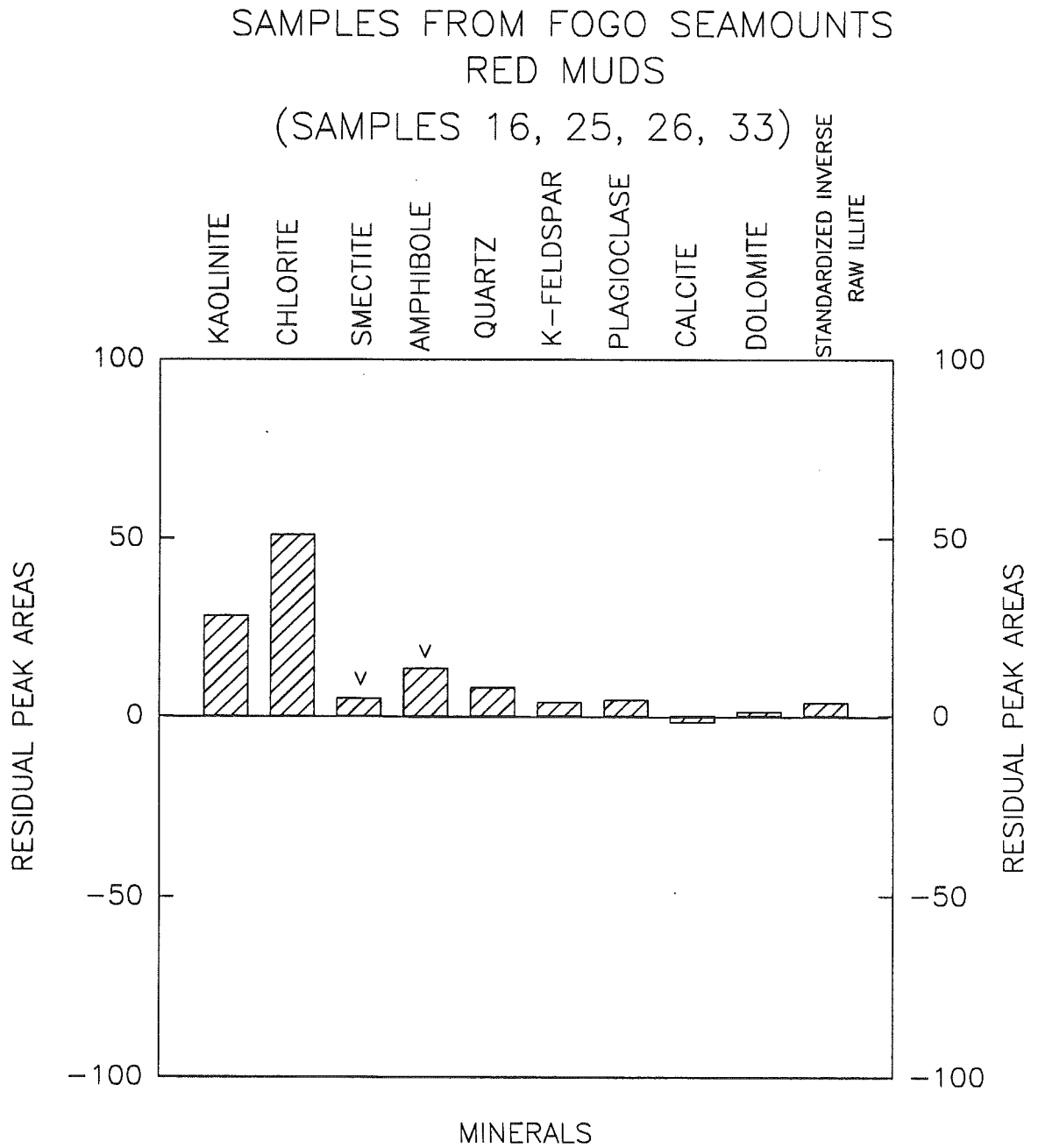

Figure 4.1g. Residual peak areas for groups of comparison samples. V = highly variable.

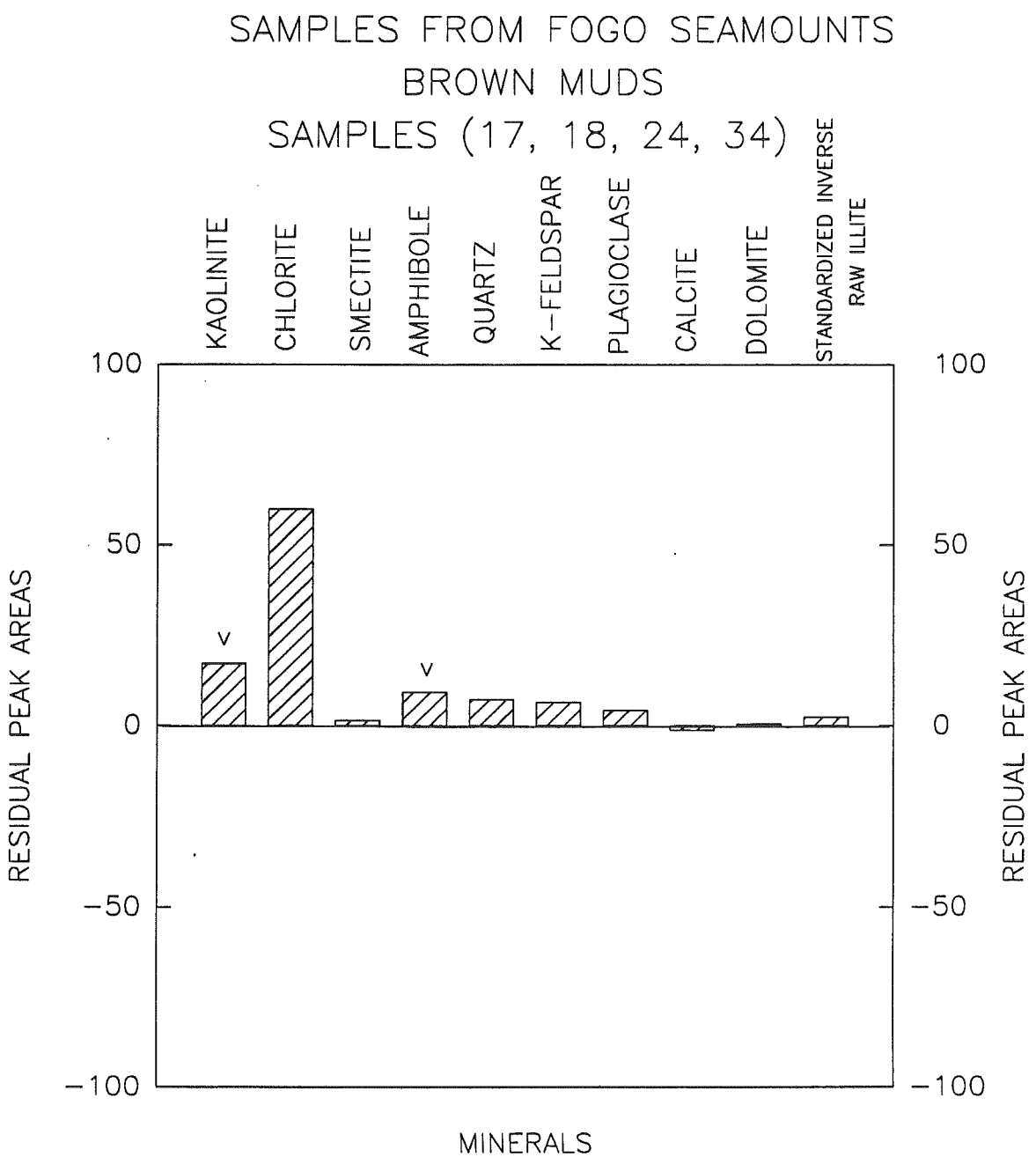

Figure 4.1h. Residual peak areas for groups of comparison samples. V = highly variable.

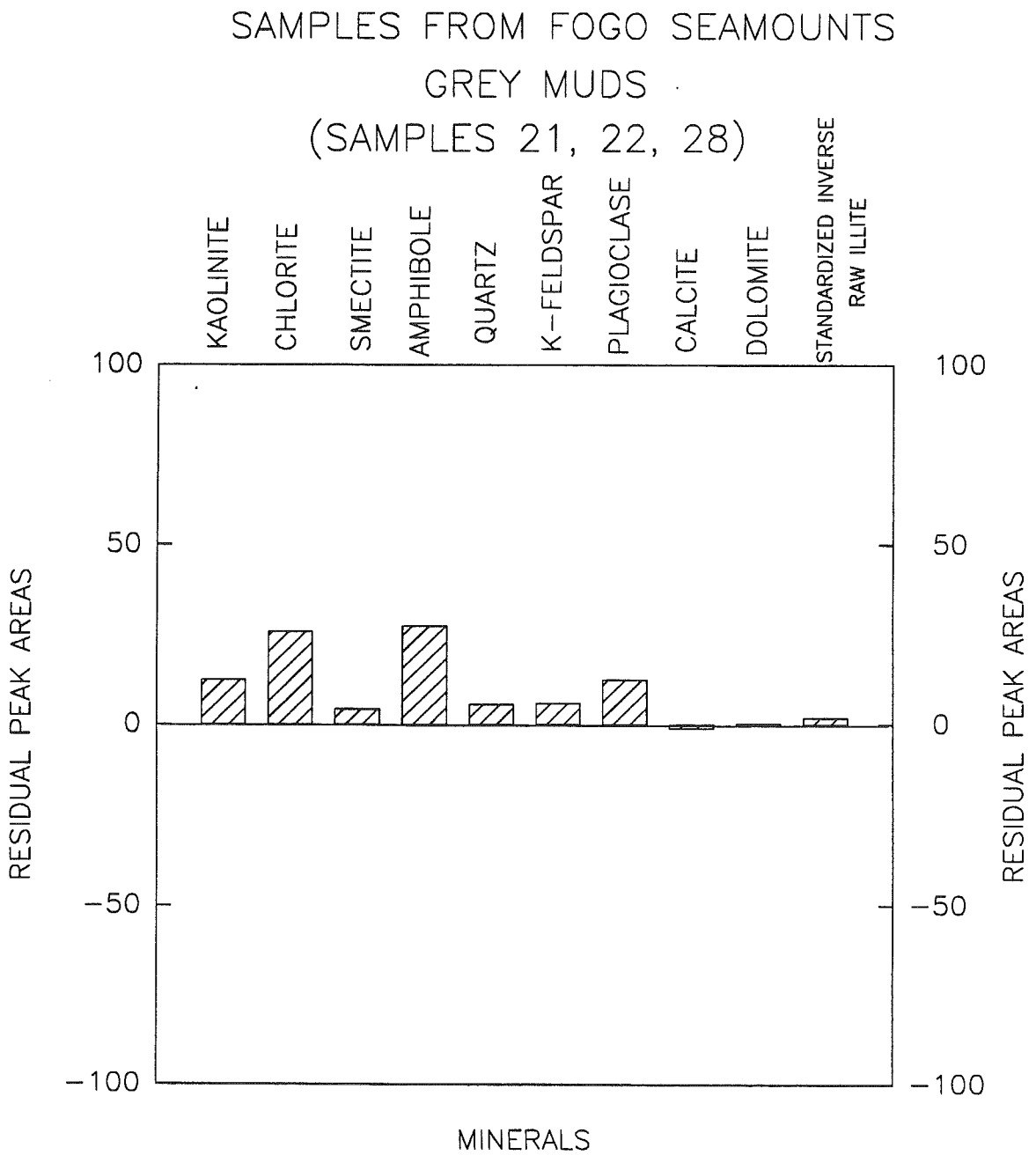

Figure 4.1i. Residual peak areas for groups of comparison samples. V = highly variable.

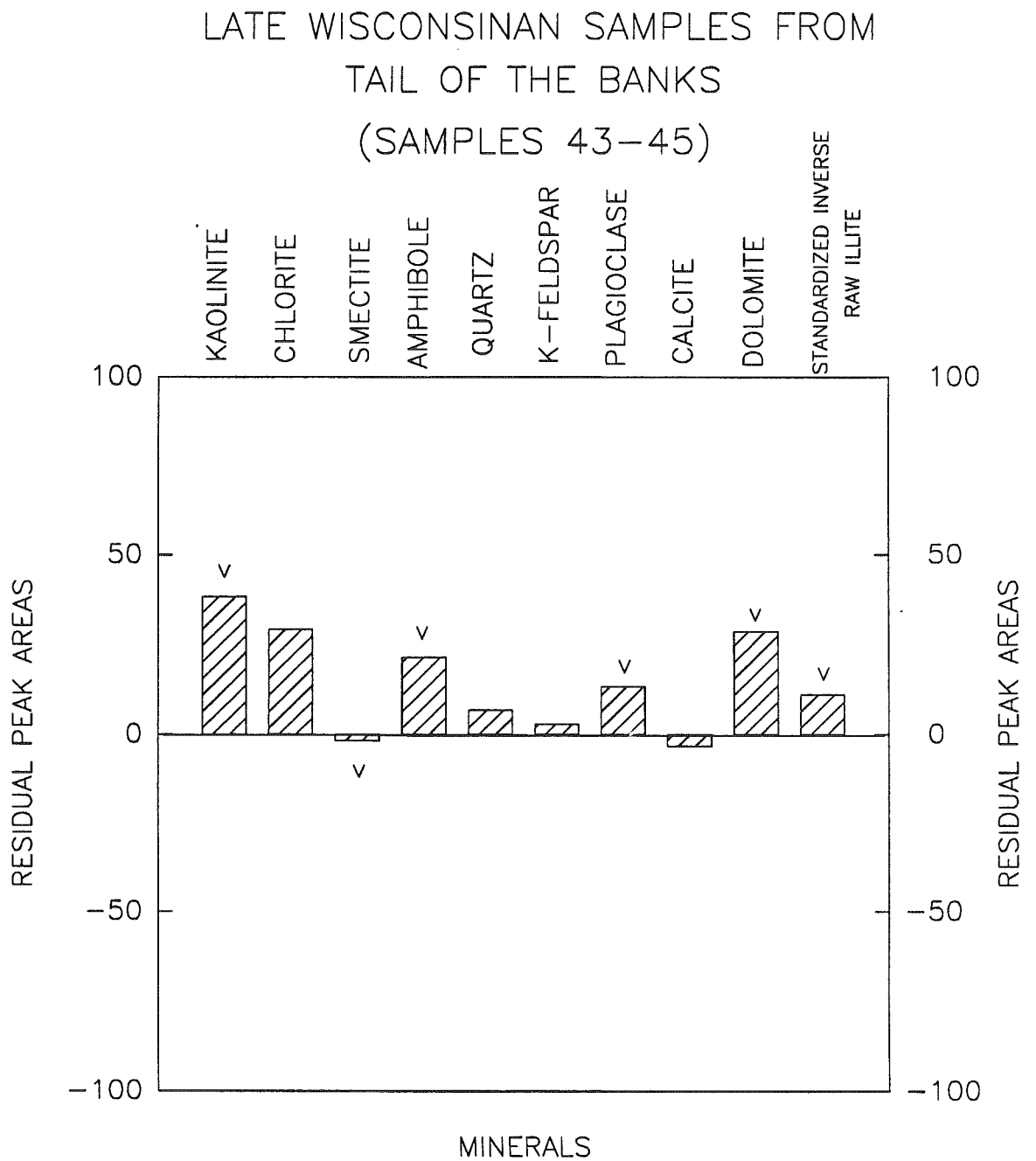

Figure 4.1j. Residual peak areas for groups of comparison samples. V = highly variable.

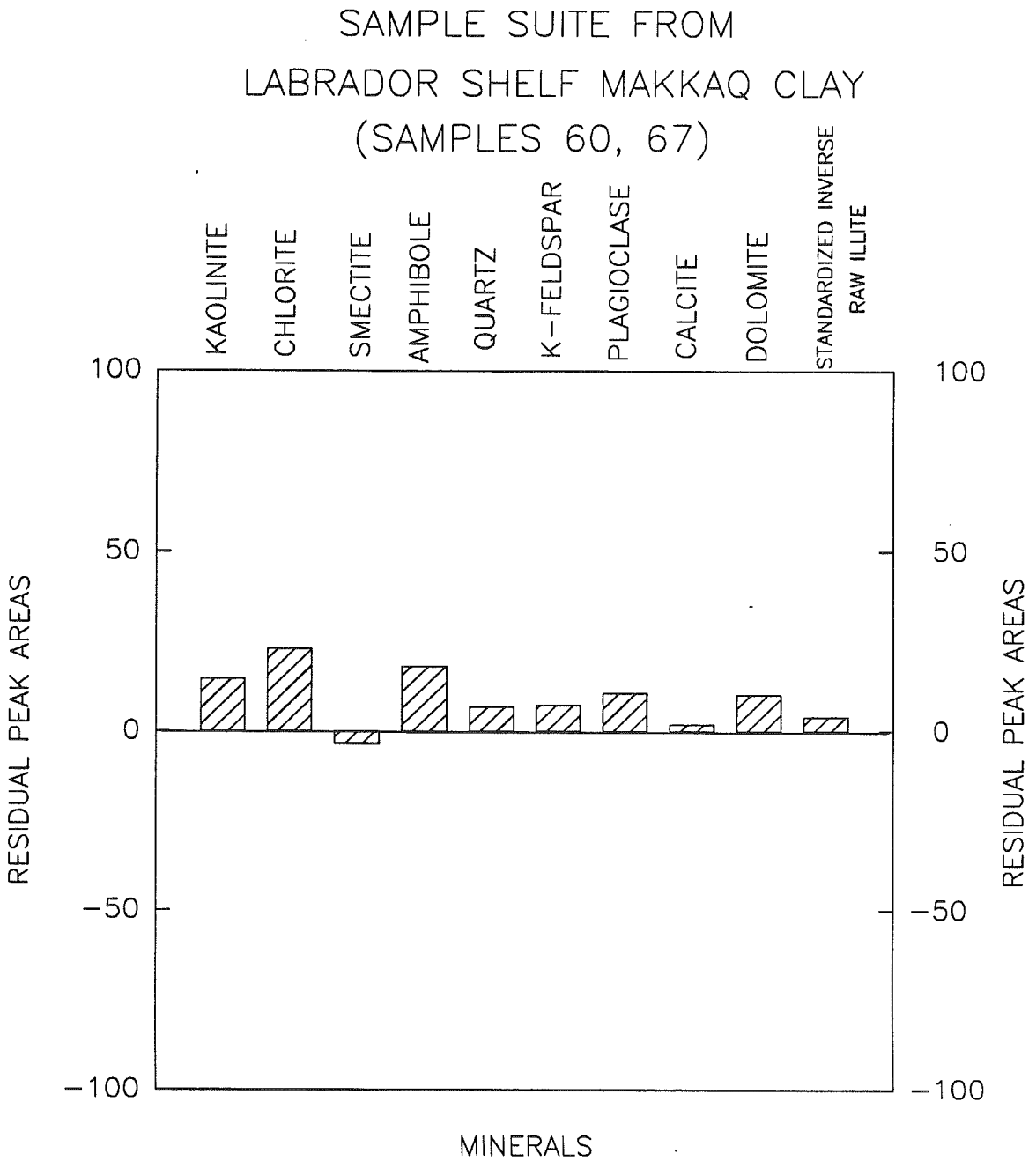

Figure 4.1k. Residual peak areas for groups of comparison samples. V = highly variable.

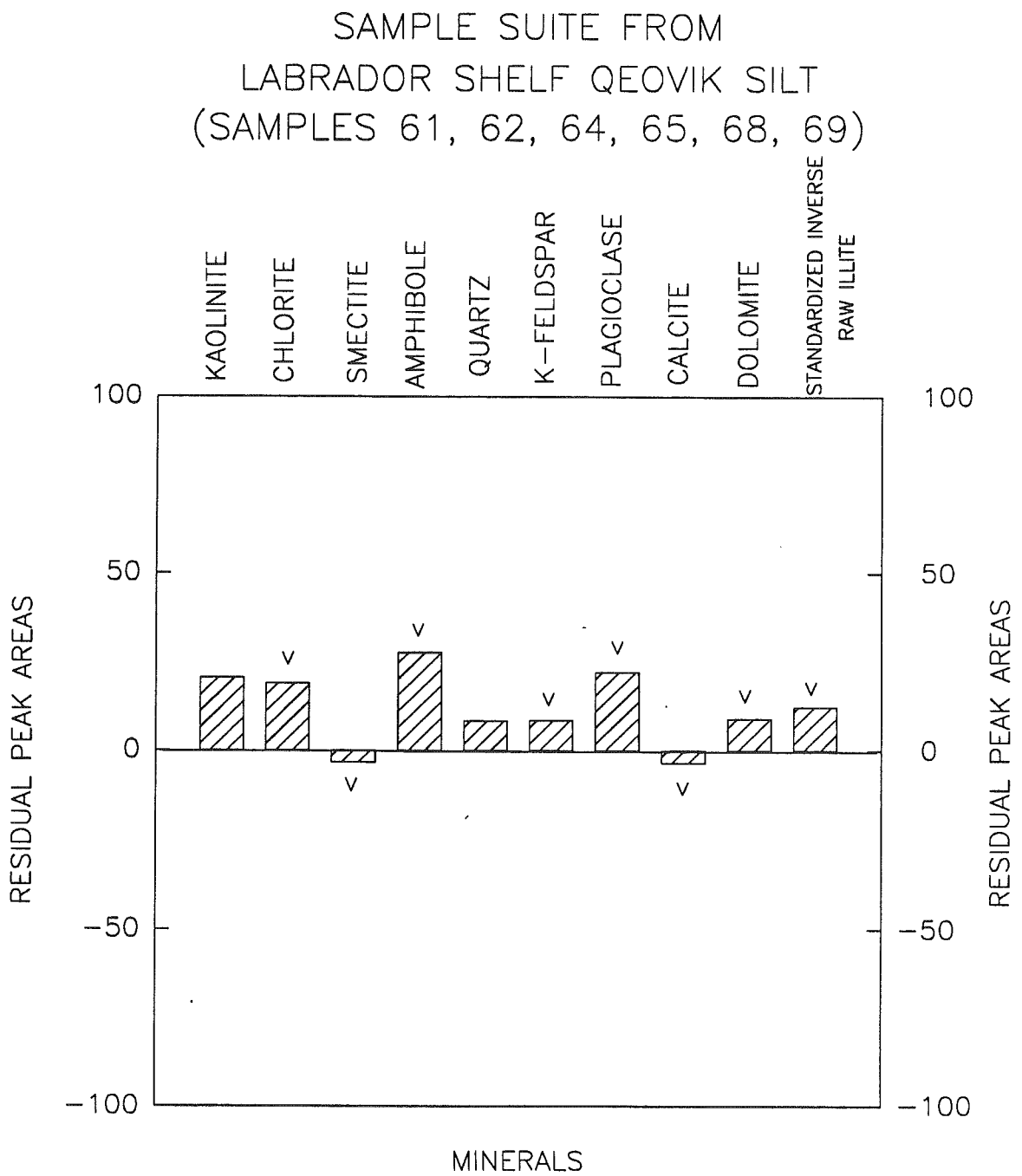

Figure 4.11. Residual peak areas for groups of comparison samples. V = highly variable.

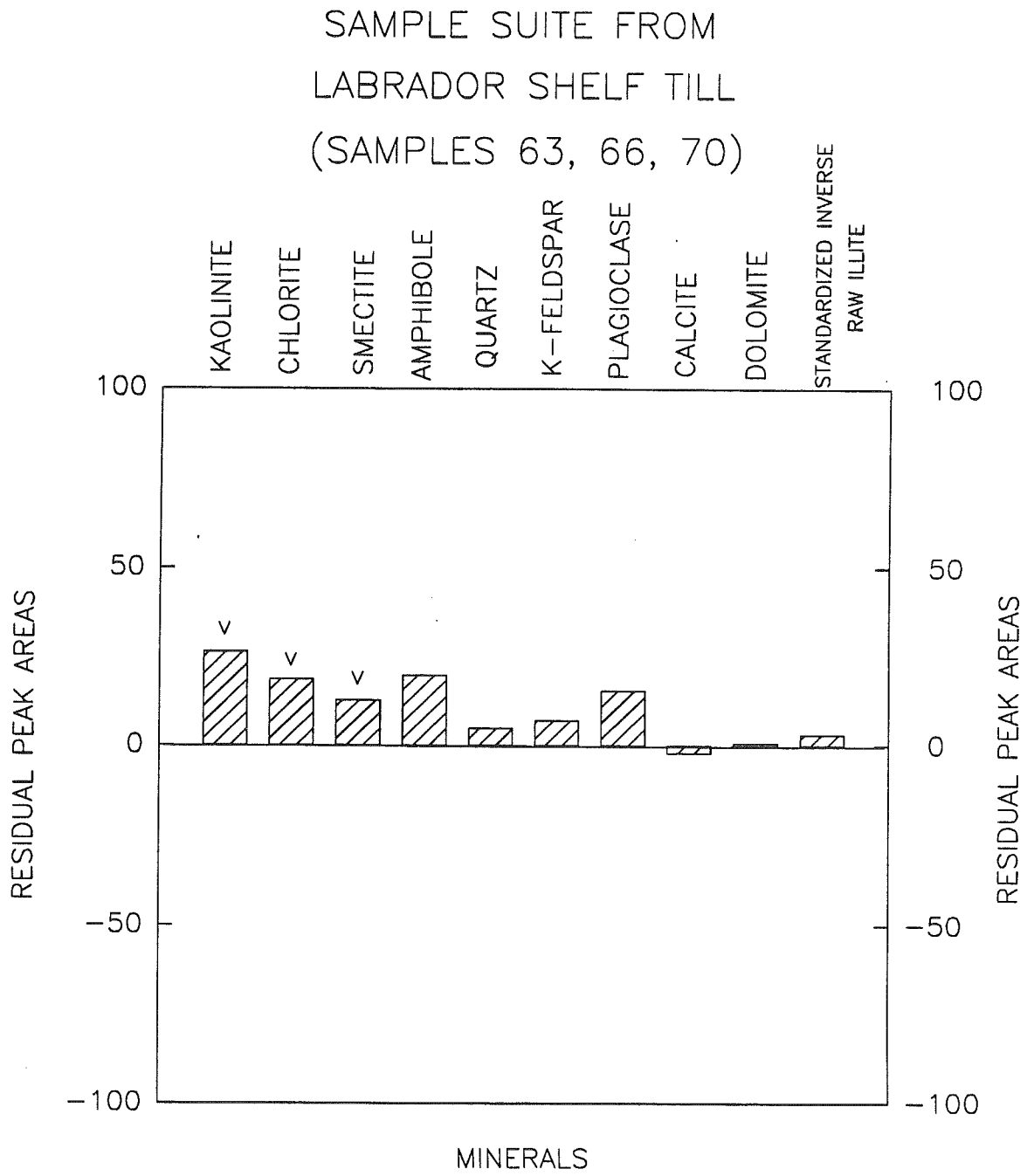

Figure 4.1m. Residual peak areas for groups of comparison samples. V = highly variable.

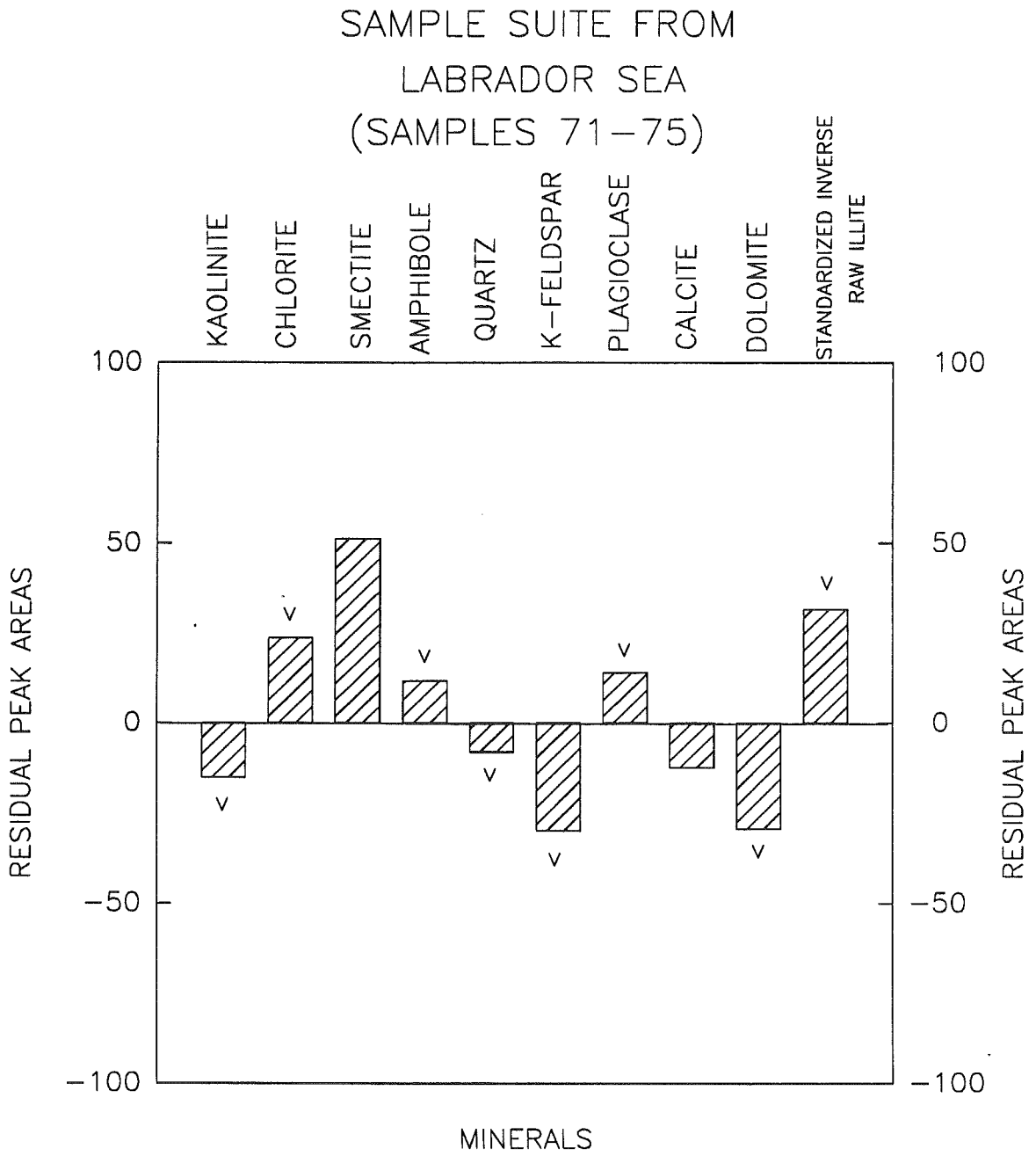

Figure 4.1n. Residual peak areas for groups of comparison samples. V = highly variable.

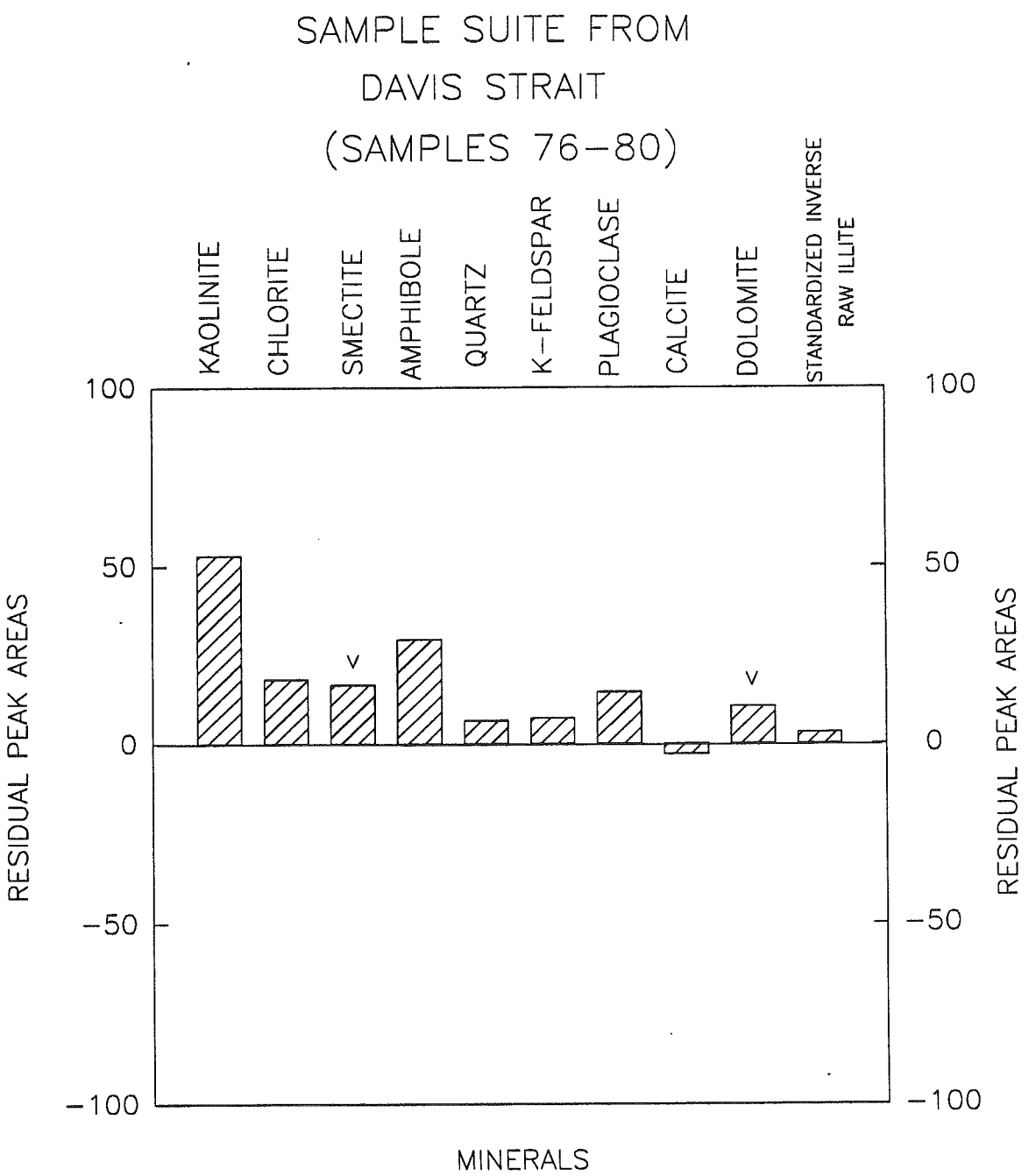

Figure 4.1o. Residual peak areas for groups of comparison samples. V = highly variable.

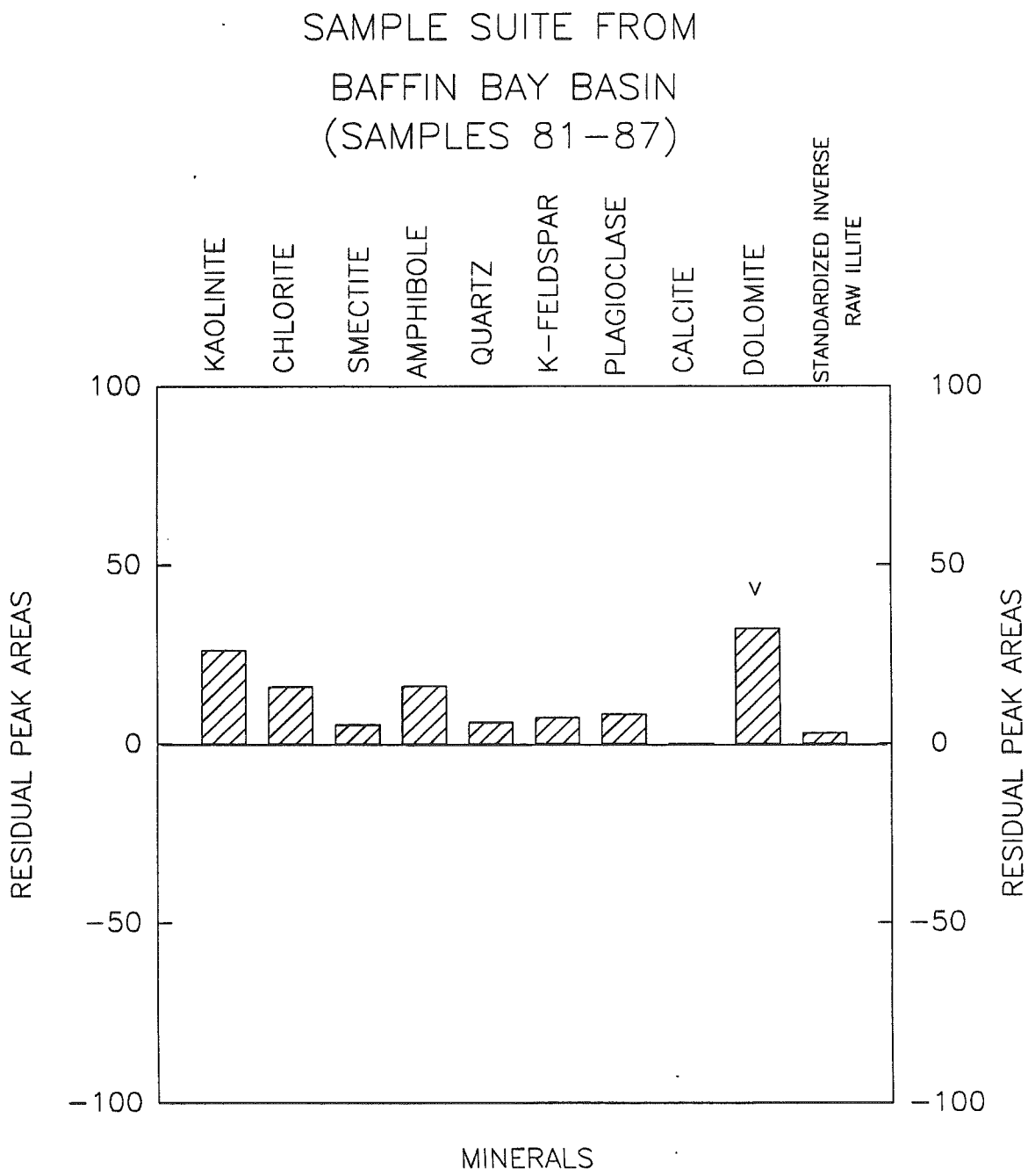

Figure 4.1p. Residual peak areas for groups of comparison samples. V = highly variable.

relatively consistent values of smectite (Fig. 4.1n).

4.4 Interpretation of source area mineralogy from comparison samples

Even the sedimentologically proximal comparison samples represent a mixture of source areas, with both marine and glacial transport. However, with a knowledge of local geology (Fader et al., 1989) and glacial history (Piper et al., 1990), in many cases a reasonably constrained interpretation of clay mineralogy can be made. Since the samples represent a complex mixing of sediment from a variety of sources, only the maximum average residual value of a given mineral over a given core interval can be used to characterize the mineralogy. These values record dominant trends regardless of variation in source input. Whether a specific mineral represents a single or multi-source provenance cannot be determined. However, consistently high values for a mineral over several samples (related to varying degrees) implies that the mineral characterizes the area, regardless of transport paths and processes. Table 4 summarizes these results. Dolomite, K-feldspar, and calcite are not included, because they do not appear to characterise particular source areas, with the possible exception of the sporadically high dolomite values in the Baffin Bay Basin.

Kaolinite appears to be a dominant mineral both in southern (late Wisconsinan Narwhal and Tantallon) and northern samples (Davis Strait). Since Cretaceous clays are known to have very high kaolinite contents, erosion of such clays is probably reponsible for high kaolinite content (Piper and Slatt, 1977). At Narwhal and Tantallon, the most likely source either is the continental shelf (or possibly in Cape Breton for Tantallon) (Fader et al., 1989). Davis Strait kaolinite appears to come from the Cretaceous strata of Cumberland sound.

Chlorite is the dominant mineral in i) Holocene and late Wisconsinan samples from Tantallon, St. Pierre Slope and Narwhal; ii) Fogo Seamounts red and brown muds; and, iii) Holocene samples from Tail of the Banks and Flemish Pass. The most obvious trend is that the greatest values for chlorite occur in southern samples as compared to chlorite values seen along the Labrador Shelf and in Baffin Bay-Davis Strait. Although chlorite may have a source either in sedimentary or low-grade metamorphic rocks, its geographic distribution would suggest a source in Applachian low-grade metamorphic rocks.

Smectite is most abundant in late Wisconsinan samples from Narwhal and, though more variable, in samples from the Labrador Sea. Alam (1979) suggested

that smectites originate from the Gulf of Mexico, being advected by the Gulf Stream. At Narwhal, smectite is abundant (along with chlorite and kaolinite), but occurs in relatively sandy sediment. This suggests that the smectite is detrital and, like the sand, is derived from the Grand Banks. The smectite is probably derived from direct erosion of Tertiary rocks outcropping on the outer part of the Grand Banks (cf. Piper and Slatt, 1977). Labrador Sea smectites may well have a more distant source, being transported by deep circulation from altered basalts on the mid-Atlantic ridge in the northern Atlantic ocean (c.f. Krissek, 1989).

Amphibole maxima are found in samples from Davis Strait, the Holocene of the Tail of the Banks, and grey muds from the Fogo Seamounts. They also occur in more variable abundance in samples from the Labrador Shelf and Wisconsinan Tail of the Banks. This geographic distribution suggests a source in the higher grade Precambrian metamorphic and plutonic rocks in Labrador, Baffin Island and Greenland, with southward transport in the Labrador Current. Sources in amphibole-rich igneous rocks of the Applachians are also possible. The origin of the grey amphibole-rich muds from the Fogo Seamounts is uncertain: Alam and Piper present evidence that they represent the most extreme glacial conditions and might therefore represent direct glacial transport across the Grand Banks from Newfoundland.

Sources of quartz are extremely variable due to its widespread abundance. Maximum values of quartz appear to be restricted to Holocene sediments. This may indicate that the source rocks for Holocene sediments are compositionally more mature than igneous and metamorphic sources eroded by glaciers in the Pleistocene. Geographically, diagnostic high quartz horizons seem to occur in samples along Grand Banks and Scotian Slope, both areas in which there are sedimentary rock sources on adjacent land.

Plagioclase tends to covary with amphibole, perhaps suggesting similar northern sources in high grade metamorphic and igneous rocks. Again, local plagioclase-rich sources in igneous rocks of the Appalachians may be responsible for some high values.

Dolomite in any appreciable quantities is usually considered to be from the erosion of lower Paleozoic dolostones in Hudson Bay and Hudson Strait and in the western parts of the Franklinian orogen (Ellesmere Island region). These dolostones are interbedded with shales rich in illite. Residual dolomite values

generally cluster about zero suggesting a strong correlation between dolomite and illite.

4.5 Type mineralogic horizons in J-anomaly ridge

Generalisations regarding downcore variability in minerals in core 87-008-003 have been made by identifying visually those core intervals that have a relatively constant residual peak area for a particular mineral. The average residual value was calculated and plotted downcore (Fig. 4.2). Where mineral abundance was very variable, the mean residual value is shown as zero. Such high frequency variability may have considerable information content, particularly if compared with high frequency variability in oxygen isotopes or sea surface temperature.

Dolomite has been treated differently from other minerals because of its strong covariance with illite. Figure 4.2 also includes the standardized dolomite values (dotted line) as an indicator of the presence or absence of dolomite.

The following discussion of variations in the type mineral horizons refers to only those minerals which are present in diagnostic amounts. Their variations and relative magnitudes can be seen in Fig. 4.2. In order that interpretations of this manipulated data be as robust as possible, emphasis is placed on the unusually high or low abundance of a mineral, rather than the relative abundance of minerals (shown in Fig. 3.4). The precision of any correlation between this generalised data and the isotopic chronology is dependant on the accuracy of the visual picks of where an interval of relatively constant residual abundances begins and ends. Care must also be taken that a "zero abundance" for a particular mineral in Fig. 4.2 does not necessarily indicate that a mineral is absent, but rather that its abundance is very variable from one sample to another.

The mineralogic horizons recognised in core 87008-003 cannot be linked to single source areas: the results of principal component analysis suggest that the sediments in the core are a result of mixing of various sources. Nevertheless, some minerals may be used as indicating that a particularly source area is important at a particular stratigraphic horizon. There are also some long-term variations in mineral abundance that deserve comment.

Stages 1-3 (partly continuing to stage 5) are characterized by high

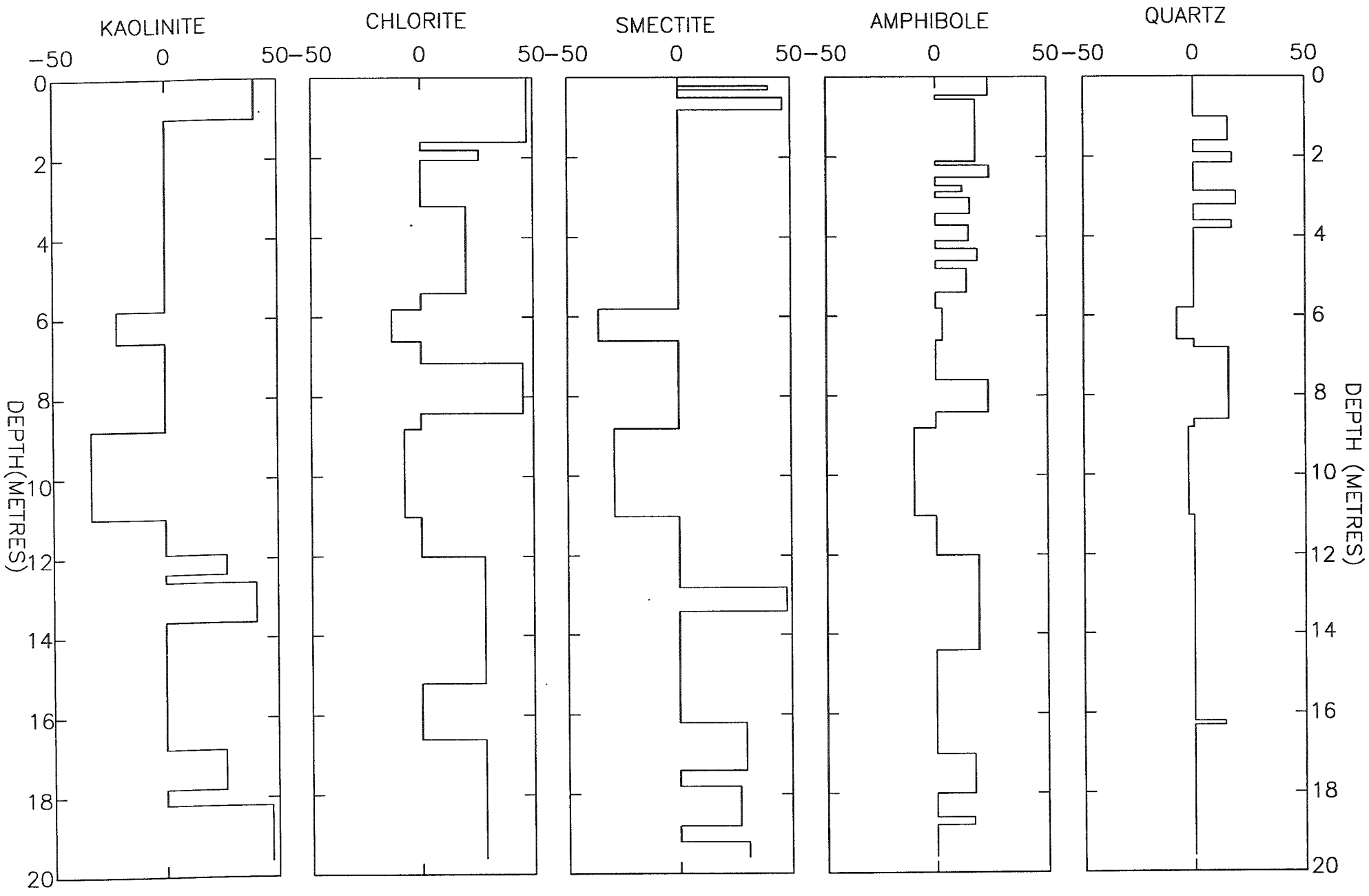

Figure 4.2a. Type mineral horizons in core 87−008−003 and their correlation with oxygen isotope stratigraphy.

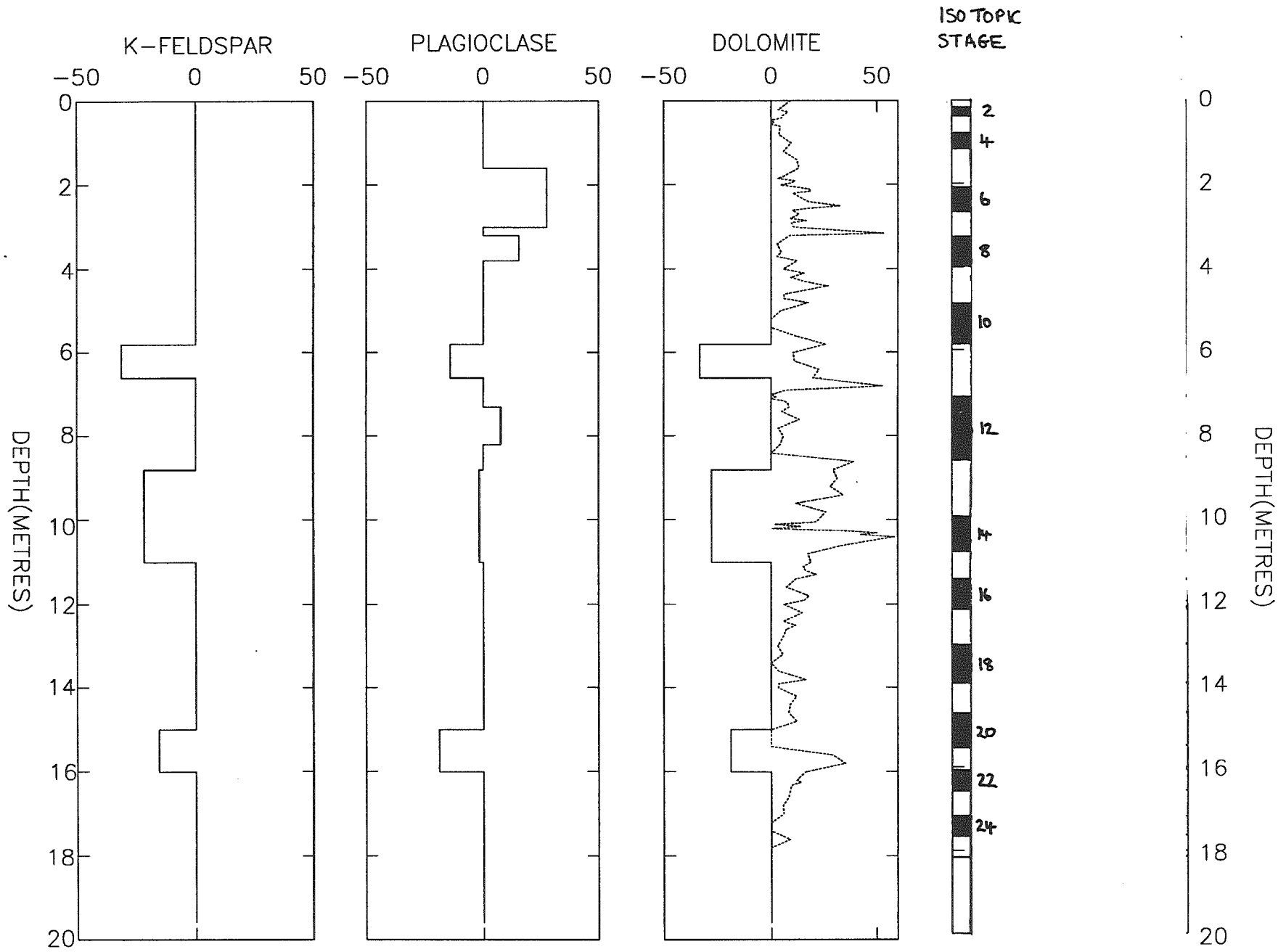

Figure 4.2b. Type mineral horizons in core 87–008–003 and their correlation with oxygen isotope stratigraphy. Standardised (dotted line) and type mineral horizons (solid line) are plotted for dolomite.

kaolinite, chlorite and smectite. Stages 4-12 have high amphibole, plagioclase, dolomite and quartz, except that dolomite is low in stage 12 and chlorite unusually high. Stages 13-15 are masked by biogenic calcite, but kaolinite, chlorite and smectite are again abundant from stage 16 to the base of the core.

4.6 Synthesis

Many of the trends in diagnostic minerals discussed above do not show a close correlation with the detailed variability of the isotopic curve, but individual stages or groups of stages commonly have a diagnostic mineral assemblage. Some diagnostic mineral assemblages persist across stage boundaries: in other cases, these stage boundaries are the site of distinct changes in the assemblage.

There is independant evidence for the extent of glacial ice on continental shelves at least during isotopic stages 1 - 4 (Piper et al., 1990) and the mineralogy of potential source areas is reasonably well defined over this time period. Thus this knowledge may be used to constrain interpretations of mineral abundances in the uppermost part of the core.

Holocene samples on the continental margin show variability similar to that in late Wisconsinan samples, which may reflect wave reworking of shallow outer shelf sediments both during and after the Holocene transgression, augemented on the Grand Banks and northwards by iceberg scouring.

The abundance of kaolinite and smectite in isotopic stages 2 and 3 at core site 87008-003 is probably related to the demonstrable extension of ice at times onto the Grand Banks. This ice presumably eroded Cretaceous and Tertiary strata on the central Grand Banks.

In isotopic stage 4, there is some evidence that ice was more extensive than in stage 2 (Piper et al., 1990, Piper and Pereira, in press). Yet the relative abundance of smectite and kaolinite (and also chlorite), potentially eroded from shales on the continental shelf is much lower than in stages 3 and 2. These minerals are not completely absent, so that their lower relative abundance may reflect dilution. In stage 4, there is a much greater proportion of terrigenous sand in the sediment (Kinney, 1990), implying much greater supply of ice-rafted detritus. The increased abundance of dolomite would suggest that this might be from a northern source. It is also possible that a change in ice sheet dynamics (e.g. cold base in stage 4, warm base in stage 3 and 2) might

have led to a reduction in erosion on the continental shelf.

At least the early part of stage 5 is characterised by a high proportion of sand (Kinney, 1990). Throughout this stage there is a "northern" mineral assemblage: dolomite, plagioclase and amphibole. Sediment supply is thus probably dominated by advection from high latitudes and melting of icebergs. The low chlorite and kaolinite reflects a lack of glacial source on the Grand Banks.

The gross mineralogical changes downcore suggest that the conditions present in stages 4 and 5 may have persisted back to stage 11 or 12, i.e. a predominance of northern sourced sediments, either because of enhanced supply from the north, or because erosion was limited in the south. The mineral assemblage in stage 12 is unique. Northern source minerals such as dolomite appear to be masked, particularly by chlorite, while plagioclase, quartz and amphibole remain dominant. Surface water temperatures were lower than at any other time in the Quaternary (Aksu and Mudie, in prep.). The abundant chlorite is empirically an indicator of a southern source, and its association with quartz, plagioclase and amphibole probably indicates an Appalachian source. The relatively low abundance of sand in stage 12, despite a relatively high sedimentation rate, suggests that much of the sediment was derived from meltwater plumes.

Mineral assemblages from stages 16 to 25 are similar to those in stages 1-4. The presence of dolomite indicates a continuing northern source. Relatively high chlorite, kaolinite and smectite is probably derived from the Grand Banks, either by glacial or by fluvial erosion. Prior to isotopic stage 25, evidence for a significant "hard-rock" source is lacking, although there is one high amphibole peak. Kaolinite is particular abundant, together with some chlorite and smectite. Again it is unclear whether these reflect glacial or fluvial erosion, although a Grand Banks source appears likely.

5.0 CONCLUSIONS

1. Modifications have been made to standard methods of analysing clay mineral abundance data based on X-ray diffraction. Data has been analysed by normalising to illite, standardising to a common scale, and subtraction of the inverse of the standardised raw illite value to yield a residual value. Principal components analysis using a correlation matrix was performed on the data set of residual values. Future work should also make use of an internal standard.

2. A set of comparison samples from the eastern Canadian continental margin have been analysed in order to identify potential sources of clay-sized minerals to the J-anomaly ridge. Variability in mineralogy there reflects changes in the relative importance of supply from (1) northern sources, principally by ice-rafting, indicated by high dolomite and plagioclase; (2) sources in the island of Newfoundland, derived through glacial erosion and dispersion in outwash plumes, indicated by high chlorite; and (3) sources on the Grand Banks, derived either by glacial or fluvial erosion, with high kaolinite and/or smectite. Although source interpretation is not possible at all levels in the core, clay-sized minerals in isotopic stages 1-3 were predominantly derived from southern sources (Newfoundland, Grand Banks); northern sources predominate in stages 4-11; and stages 16-24 have a strong indication of southern sources.

Acknowledgments

This work is part of a collaborative study of core 87008-003 with A.E. Aksu and P.J. Mudie, who provided isotopic and paleo-oceanographic control for the core. Aksu also prepared most of the clay mineral separates for the J-Anomaly ridge. Patricia Stoffyn-Egli devoted a lot of time to instructing and assisting Armstrong and Skene, and to the improvement of X-ray diffraction methods. This work was funded by the Program on Energy Research and Development, project 6.3.2.6, Stability of Continental Slopes, as part of a study to better define regional Quaternary stratigraphy.

REFERENCES

Aksu, A.E. and Mudie, P.J., in prep., Biostratigraphy, isotope stratigraphy and paleoenvironment of seamount cores, Labrador Sea. to be submitted to Canadian Journal of Earth Sciences.

Aksu, A.E. and Piper, D.J.W., 1987. Late Quaternary sedimentation in Baffin Bay. Canadian Journal of Earth Sciences, v. 24, p. 1833-1846.

Alam, M., 1979. The effect of Pleistocene climatic changes on the sediments around the Grand Banks. Unpublished Ph.D. thesis, Dalhousie University, Halifax, Nova Scotia, 222 p.

Alam, M., 1987. Late Quaternary plume, nepheloid and turbidite sedimentation and effect of the Gulf Stream near the Tail of the Grand Banks, Newfoundland. Marine Geology, v. 74, p. 277-290.

Alam, M. and Piper, D.J.W., 1977. Pre-Wisconsinan stratigraphy and paleoclimates off Atlantic Canada and its bearing on glaciation in Quebec. Geographie Physique et Quaternaire, v. 31, p. 15-22.

Alam, M. and Piper, D.J.W., 1981. Detrital mineralogy of deep-water continental margin off Newfoundland. Canadian Journal of Earth Sciences, v. 18, p. 1336-1345.

Alam, M., Piper, D.J.W. and Cooke, H.B.S., 1983. Late Quaternary stratigraphy and paleo-oceanography of the Grand Banks continental margin, eastern Canada. Boreas v. 12, p. 253-261.

Allen, V.T. and Johns, W.D., 1960. Clays and clay minerals of New England and eastern Canada. Geological Society of America Bulletin, v. 71, p. 75-86.

Armstrong, R.C., 1988. Identification and down-core quantification of clay-sized minerals using X-ray diffraction. COOP work term report for Atlantic Geoscience Centre and the University of Waterloo, 43 p.

Barnett, D.E. and Abbott, D., 1966. The evaluation of possible ceramic materials from New Brunswick. New Brunswick Research and Productivity Council, Research Note 6.

Bonifay, D. and Piper, D.J.W., 1988. Probable Late Wisconsinan ice margin on the upper continental slope off St. Pierre Bank, eastern Canada. Canadian Journal of Earth Sciences, v. 25, p. 853-865.

Boyd, R.W. and Piper, D.J.W., 1976. Baffin Bay continental shelf clay mineralogy. Maritime Sediments, v. 12, p. 17-18.

Brydon, J.E., 1958. Mineralogical analysis of the soils of the Maritime

Provinces. Canadian Journal of Soil Science, v. 38, p. 155-160.

Cremer, M., Maillet, N. and Latouche, C., 1989. Analysis of sedimentary facies and clay mineralogy of the Neogene-Quaternary sediments in ODP site 646, Labrador Sea. Proceedings of the Ocean Drilling Program, 105B, 71-82.

Drever, J.I., 1973. The preparation of oriented clay mineral specimens for X-ray diffraction analysis by a filter membrane peel technique. American Mineralogist, v. 58, p. 553-554.

Fader, G.B., Cameron, G.D.M. and Best, M.A. (comp.), 1989, Geology of the continental margin of Eastern Canada. Geological Survey of Canada map 1705A, scale 1:5 000 000.

Hill, P.R., 1981. Detailed morphology and late Quaternary sedimentation of the Nova Scotian slope, south of Halifax. unpublished Ph.D. thesis, Dalhousie University, Halifax, Nova Scotia, 331 p.

Hillaire-Marcel, C. and de Vernal, A., 1989. Isotopic and palynological records of the late Pleistocene in eastern Canada and adjacent ocean basins. Geographie Physique et Quaternaire, v. 43, p. 263-290.

Hiscott, R.N., 1984. Clay mineralogy and clay mineral provenance of Cretaceous and Paleogene strata, Labrador and Baffin shelves. Bulletin of Canadian Petroleum Geology, v. 32, p. 272-280.

Hiscott, R.N., Aksu, A.E. and Nielsen, O.B., 1989. Provenance and dispersal patterns, Plio-Pleistocene section at site 645, Baffin Bay. Proceedings of the Ocean Drilling Project, v. 105B, p. 31-52.

Jansa, L.F. and Noguera U., V.H., 1990. Geology and diagenetic history of overpressured sandsone reservoirs, Venture gas field, offshore Nova Scotia, Canada. American Association of Petroleum Geologists Bulletin, v. 74, p. 1640-1658.

Josenhans, W.H., Klassen, R.A. and Zevenhuizen, J., 1986. Quaternary geology of the Labrador Shelf. Canadian Journal of Earth Sciences, v. 23, p. 1190-1213.

Josenhans, H.W. and Zevenhuizen, J., 1989. Quaternary Geology, Labrador Sea. In Bell, J.S. (ed), East Coast Basin Atlas Series, Labrador Sea. Atlantic Geoscience Centre, Dartmouth, N.S.

Kinney, S.P., 1990. Fogo Seamount Core 87008-003, coarse sediment study. COOP work term report for the Atlantic Geoscience Centre and the University of Waterloo, 32 p.

Krissek, L.A., 1989. Bulk mineralogy of non-biogenic sediments from ODP sites 642 and 643, Norwegian Sea: implications for sediment provenance and recycling. Proceedings of the Ocean Drilling Program, v. 104B, p. 29-40.

Latouche, C. and Parra, M., 1979. La sedimentation au Quaternaire - Recent dans le "Northwest Atlantic Mid-Ocean Canyon" - apport des donnees mineralogiques et geochimiques. Marine Geology, 29, p. 137-164.

Laughton, A.S., Berggren, W.A., et al., 1972. Initial Reports of the Deep Sea Drilling Project, Volume 12; U.S. Government Printing Office, Washington, 1243 p.

Martin, R.T., Bailey, S.W., Eberl, D.D., Fanning, D.S., Guggenheim, S., Kodama, H., Pevear, D.R., Środoń, J., and Wicks, F.J., 1991. Report of the Clay Minerals Society nomenclature committee: revised classification of clay minerals. Clays and Clay Minerals, v. 39, p. 333-335.

Mudie, P.J. and Aksu, A.E., 1990. Quaternary paleoclimate of the Northwest Atlantic: planktic foraminifera, coccolith, dinocyst and pollen data. EOS, v. 71, p. 543.

Pastouret, L., Auffret, G.A., Hoffert, M., Melguen, M., Needham, H.D. and Latouche, C., 1975: Sedimentation sur la Ride de Terre-Neuve: Canadian Journal of Earth Sciences, 12, p. 1019-1035.

Piper, D.J.W., 1991. Seabed geology of the Canadian eastern continental shelf. Continental Shelf Research, v. (in press)

Piper, D.J.W., Mudie, P.J., Fader, G.B., Josenhans, H.W., MacLEan, B. and Vilks, G., 1990. Quaternary Geology. Chapter 10 in Geology of the continental margin off eastern Canada, ed. M.J.Keen and G.L.Williams. Geological Survey of Canada, Geology of Canada, no. 2, (also Geological Society of America, The Geology of North America, v. I-1), p. 475-607.

Piper, D.J.W. and Pereira, C.G.P., 1991. Late Quaternary sedimentation in Flemish Pass. Canadian Journal of Earth Sciences (in press).

Piper, D.J.W. and Slatt, R.M. 1977. Late Quaternary clay mineral distribution on the eastern continental margin of Canada. Geological Society of America Bulletin, 88, 267-272.

Segall, M.P., Barrie, J.V., Lewis, C.F.M., and Maher, M.L.J. 1985. Clay minerals across the Tertiary-Quaternary boundary, northeastern Grand Banks of Newfoundland: preliminary results. In Current research, part B, Geological Survey of Canada, Paper 85-1B, pp. 63-68.

Segall, M.P., Buckley, D.E., and Lewis, C.F.M. 1987. Clay mineral indicators of geological and geochemical subaerial modification of near-surface Tertiary sediments on the northeastern Grand Banks of Newfoundland. Canadian Journal of Earth Sciences, 24: 2172-2187.

Skene, K.I., 1991. Analysis and preliminary interpretation of selected transects on the continental shelf off Eastern Canada: morphologic constraints of Late Quaternary sedimentation. Geological Survey of Canada Open File *****.

Slatt, R.M. and Lew, A., 1973. Provenance of Quaternary sediments on the Labrador continental shelf and slope. Journal of Sedimentary Petrology, v. 43, p. 1054-1960.

Slatt, R.M., 1977: Late Quaternary terrigenous and carbonate sedimentation on the Grand Bank of Newfoundland: Geological Society of America Bulletin, v. 88, p. 1357-1367.

Stow, D.A.V., 1977: Late Quaternary stratigraphy and sedimentation on the Nova Scotian outer continental margin: unpublished Ph.D. thesis, Dalhousie University, Halifax, Nova Scotia, 360 p.

Stow, D.A.V., 1978. Regional review of the Nova Scotian outer margin: Maritime Sediments, v. 14, p. 17-32.

Thiébault, F., Cremer, M., Debrabant, P., Foulon, J., Nielsen, O.B. and Zimmerman, H., 1989. Analysis of sedimentary facies, clay mineralogy and geochemistry of the Neogene-Quaternary sediments in ODP site 645, Baffin Bay. Proceedings of the Ocean Drilling Program, v. 105B, p. 83-100.

Tucholke, B.E., Vogt, P.R. et al., 1979: Initial Reports of the Deep Sea Drilling Project, Leg 43: U.S. Government Printing Office, Washington, 1115 p.

Umpleby, D.C., Stevens, G.R. and Colwell, J.A., 1978. Clay minerals analysis of Mesozoic-Cenozoic sequences, Labrador Shelf - a preliminary report. Geological Survey of Canada Paper 78-1B, p. 111-114.

Table 1: Measurement Parameters for X-ray Diffraction

Range	Parameter	Scan Type Long	Short	Glycol
1	start angle	2°	24°	2°
	stop angle	15°	26°	15°
	step	0.02°	0.01°	0.02°
	time step (seconds)	2	4	3
2	start angle	15°		
	stop angle	52°	n/a	n/a
	step	0.02°		
	time step (seconds)	1		

All scans are step scan, use sample rotation, and use the theta/two-theta coupled goniometer configuration. The long and glycol scans use 0.3/0.15° slits; whereas the short scan uses 1.0/0.05° slits. Incident beam slits and detection slit were respectively 0.39° and 0.15° for the long and glycol scans and 1.0° and 0.05° for the short scan.

Table 2: Minerals and the 2θ values of their major peak for CuKα radiation

Mineral	° 2θ
smectite	5.2
illite	8.8
chlorite	12.3
kaolinite	12.3
amphibole	10.5
*quartz	20.85
K-feldspar	27.35-27.79
plagioclase	27.80-28.15
calcite	29.4
dolomite	30.9

*The major peak of quartz is overlain by an illite peak and separation of the two is difficult. As a result, this secondary quartz peak is used.

Table 3. Geologic setting of the comparison samples.
Stratigraphic columns are shown in Appendix 4.

1-5 **Tantallon**, 86-034-017, 43° 51.1'N 58° 21.9'W, 1518 m. 86-034-019, 43° 51.2'N 58° 23.1'W, 1536 m. Samples 1-2 are Holocene, 3-5 are from a proglacial red mud radiocarbon dated at about 16 ka.

6-11 **St Pierre Slope**, various cores. 86-034-005, 44° 49.1'N 56° 9.3'W, 499 m, samples the top of a ?till on the upper slope dated at about 12 ka. 84-003-10 44° 50.2'N 55° 58.7'W, 719 m, and 84-003-11 44° 50.1'N 55° 54.1'W 586 m sample the latest Pleistocene - Holocene stratigraphic section above the till (Bonifay and Piper, 1988). Samples 6 and 9 are late Holocene; all other samples are latest Pleistocene.

12-15 **Narwhal well site**, 86-003-001, 44° 18.2'N 53° 44.9'W, 1614 m. (Unpublished data of Piper and Bonifay). Sample 12 is late Holocene; 13-15 are late Pleistocene.

16-39 **Fogo Seamounts** Cores 85-001-11 and 13: 42° 06'N 52° 45'W, 3320 m and 85-001-14: 42° 18'N 53° 01'W, 3189 m. (unpublished data, projected in to stratigraphy of Alam et al., 1983). Samples that represent "end-member" lithologies are as follows:

Red mud	16, 25, 26, 33
Grey mud	21, 22, 28
Brown mud	?17, 24, 34
Foram ooze	19, 23, 32, 35, 37

40-45 **Tail of the Banks**, 87-008-007, 42° 42.0'N 50° 5.7'W, 1262 m. Stratigraphy in Skene (1991). Continental slope experiencing considerable reworking (and advection) by Western Boundary Undercurrent.

46-48 **East Flemish Pass**, 87-008-013, 47° 00.7'N 46° 42.1'W, 1080 m. Stratigraphy in Piper and Pereira (in press). 46-47 are early Holocene sandy muds; 48 a late Pleistocene hemipelagic mud with abundant ice rafted detritus.

49 **Flemish Cap**, 87-008-21, 47° 23.3'N 46° 24.5'W, 820 m, grab sample of surficial sediment unconformably overlying Tertiary strata.

50-59 **Orphan Knoll**, DSDP 111A (Laughton, Berggren et al., 1979), 50° 25.6'N, 46° 22.1'W, 1797 m. Hemipelagic muds with some ice rafted detritus, ranging from Early Pleistocene to Late Pliocene age.

60-63 **Cartwright Saddle, Labrador Shelf**, 87-033-18, 54° 44.7'N, 56° 3.05'W, 460 m (from Josenhans and Zevenhuizen, 1989). 60 at base of postglacial Makkak Clay; 61 and 62 are from Qeovik Silt (proglacial outwash, strongly influenced by carbonates though Hudson Strait), 63 from Upper Till (Labrador provenance).

64-66 **Hopedale Saddle, Labrador Shelf**, 83-030-36, 56° 4.1'N 58° 54.8'W, 420 m., from Josenhans et al. (1986). 64, 65 from Qeovik Silt, 66 from Upper Till (c.f. Cartwright Saddle).

67-70 **Karlsefni Trough, Labrador Shelf**, 87-033-15, 58° 45.8'N 62° 15.4'W, 188 m. (from Josenhans and Zevenhuizen, 1989). 67 from Makkak Clay, 68, 69 from Qeovik Silt, 70 from Upper Till (c.f. Cartwright Saddle).

71-75 **Labrador Sea**, core HU75-037, 59° 09'N, 48° 23.1'W, 3208 m. (from Hillaire Marcel and de Vernal, 1989). Samples range from late Holocene to isotopic stage 4.

76-80 **Davis Strait**, 77029-17 66° 54.1'W, 58 17.7'W, 935 m. (from Aksu and Piper, 1987). Stratigraphic sequence of late Pleistocene samples in order to have a comparison with the detailed data set of Aksu (1981: see also Aksu and Piper, 1987).

81-87 **Central Baffin Bay basin**, 76-029-33 (plus one sample from -34), 71° 20'N, 64° 16'W, 2207 m. (from Aksu and Piper, 1987). Sequence of samples in various lithofacies defined by Aksu (1981) in order to have a comparison with the detailed data set of Aksu (1981: see also Aksu and Piper, 1987).

Table 4. Comparison sites with high average residual values of mineral abundances

MINERAL	LOCATION	RESIDUAL VALUE
kaolinite	Wisconsinan Tantallon	45.9
	Wisconsinan Narwhal	44.0
	Davis Strait	52.9
chlorite	Holocene Tantallon, St. Pierre Slope, and Narwhal	59.6
	Holocene Tail of the Banks	39.5
	Holocene Flemish Pass	52.8
	Wisconsinan Tantallon	53.0
	Wisconsinan St. Pierre Slope	64.1
	Wisconsinan Narwhal	58.4
	Fogo Seamounts red muds	51.1
	Fogo Seamounts brown muds	59.8
smectite	Wisconsinan Narwhal	41.8
	Labrador Sea	51.2
amphibole	Fogo Seamounts grey mud	27.3
	Davis Strait	29.6
	Holocene Tail of the Banks	20.1
quartz	Holocene Tail of the Banks	14.1
	Holocene Flemish Pass	17.2
	Holocene Tantallon, St. Pierre Slope, and Narwhal	9.8
plagioclase	Holocene Tail of the Banks	36.4
	Labrador Shelf till	15.4
	Fogo Seamounts grey muds	12.4
	Davis Strait	14.7

Table 5. Raw peak areas normalised to illite for core 87008-003

Depth in cm	Kaol.	Chlor.	Smectite	Amphibole	Quartz	K-Feldspar	Plag.	Calcite	Dolomite
1	59.41	82.96	378.41	18.32	16.32	29.53	68.51	32.18	12.47
21	55.98	121.92	805.57	27.61	16.01	12.26	52.11	0.08	4.75
26	70.77	74.84	840.39	20.46	18.45	6.69	45.12	0.05	11.10
31	64.59	98.00	864.35	18.02	15.49	9.84	35.79	0.06	9.76
36	71.80	113.65	442.05	16.82	28.97	12.01	78.65	0.08	7.35
41	80.55	123.06	717.61	19.77	20.53	11.09	48.19	0.07	7.07
46	62.27	90.17	520.42	14.95	25.83	17.07	71.31	0.08	0.08
51	68.10	96.34	1017.69	2.18	15.32	7.52	49.64	0.05	2.12
56	52.20	103.47	1023.73	13.80	14.62	4.73	36.03	3.42	0.04
61	58.49	85.91	798.58	11.19	11.08	9.40	30.32	0.04	6.08
81	70.73	102.77	615.04	16.61	14.72	4.65	25.65	0.04	5.31
101	56.55	87.61	304.66	13.20	19.03	8.17	27.39	7.55	13.27
121	35.66	107.17	294.22	15.21	24.09	21.86	43.74	3.30	8.26
141	41.71	104.38	369.75	15.03	21.77	8.06	38.19	0.07	16.94
161	52.20	140.94	388.57	20.93	27.85	17.12	70.79	48.71	18.33
181	37.82	67.28	287.38	12.60	16.01	22.63	62.61	0.05	8.03
186	23.18	71.53	172.17	10.77	14.83	9.84	50.32	0.04	4.46
191	33.86	72.23	301.84	22.58	30.32	21.61	153.80	0.08	15.88
196	46.16	61.45	209.33	16.41	29.92	16.51	101.58	9.62	13.44
201	40.54	79.35	254.61	14.42	27.04	19.65	86.35	114.13	6.45
206	65.18	58.63	255.08	13.12	20.32	8.48	70.22	10.39	16.67
211	44.85	70.04	281.08	22.71	38.65	24.16	100.47	16.20	24.82
216	96.78	70.17	167.40	10.70	26.74	17.62	82.36	71.44	26.27
221	50.19	65.78	415.98	18.18	21.36	11.89	70.27	38.12	14.17
241	49.65	78.49	327.17	22.31	29.99	15.14	104.86	0.11	24.53
246	220.51	153.08	239.58	11.58	27.69	14.26	93.98	54.35	32.67
251	60.78	43.58	428.17	37.10	47.82	54.16	173.06	195.01	45.66
256	63.11	84.76	159.27	13.92	31.20	26.68	110.27	187.47	27.13
261	39.00	72.19	182.17	17.27	25.20	25.74	96.72	272.46	14.06
271	31.52	53.98	335.44	17.09	32.97	13.15	69.75	340.80	18.30
281	40.89	47.49	141.03	12.72	16.94	10.15	57.69	152.19	12.95
286	48.91	54.00	354.02	15.04	31.63	18.62	70.62	18.01	23.08
291	46.07	43.90	318.60	12.29	21.75	7.90	65.48	172.94	13.40
296	288.46	312.64	306.94	21.45	44.76	16.29	117.07	24.37	50.49
301	56.10	61.92	192.16	14.48	21.67	16.38	67.75	0.06	14.65
306	93.12	98.39	162.96	11.69	28.70	17.99	64.86	0.06	39.82
311	310.89	268.75	263.58	16.79	34.76	15.46	101.89	166.66	55.99
316	44.78	80.86	702.48	34.60	68.57	0.22	101.62	98.71	74.41
321	60.97	73.34	390.59	14.78	25.62	12.72	63.23	49.24	12.27
341	10.02	49.95	125.96	10.30	8.59	12.60	34.74	0.02	3.98
361	14.45	69.30	318.95	14.67	29.85	11.28	60.88	40.24	6.62
371	21.62	51.95	211.01	8.64	15.33	8.70	34.09	0.03	3.92
381	37.59	71.89	502.48	15.36	27.95	14.66	70.91	146.83	17.22
401	26.77	44.78	217.11	13.01	13.76	7.32	21.89	9.26	8.07
411	36.81	30.91	402.42	9.89	17.53	8.92	40.59	43.05	21.59
421	35.94	49.28	482.57	14.17	21.48	19.12	60.69	93.35	12.81
431	22.76	34.92	422.49	12.18	13.88	5.57	48.32	36.73	22.53
441	26.98	43.60	359.57	15.47	25.69	9.80	76.35	98.55	37.37
461	65.31	60.38	588.25	17.68	13.77	5.44	24.94	95.08	8.60
471	2.41	65.48	370.92	7.46	20.43	7.93	64.90	0.06	8.48
481	30.68	84.52	490.16	24.98	27.32	18.34	66.85	158.73	24.41
501	25.60	76.39	277.97	11.77	15.95	6.28	30.79	59.35	6.27
521	9.31	54.04	98.29	12.43	12.36	17.62	40.37	0.03	0.03
541	32.94	82.25	239.08	11.20	14.65	12.53	27.76	0.05	0.05
561	28.16	44.28	538.57	11.37	17.41	13.30	42.18	309.44	15.53
581	40.77	87.07	99.17	51.27	45.14	46.11	129.99	3127.60	35.86
601	28.09	43.52	131.15	16.77	21.31	8.70	38.48	649.09	14.53
621	30.22	82.30	391.32	15.95	28.91	10.78	33.79	110.98	15.19
641	25.15	58.76	276.42	21.50	29.96	10.38	59.73	966.95	31.62
661	60.98	67.06	444.22	32.92	49.88	0.32	98.79	1994.70	27.63
681	65.95	45.90	578.84	26.42	35.81	0.15	54.75	659.10	74.03
691	63.39	80.14	280.04	8.18	36.35	11.59	39.48	102.95	9.49
701	37.08	94.64	494.76	2.23	14.59	4.18	20.80	0.04	0.04

706	42.20	86.53	402.64	11.29	21.05	6.88	29.18	0.04	3.12
711	5.94	14.04	414.54	0.11	36.96	0.11	42.44	0.11	0.11
716	40.84	90.96	440.41	18.68	35.76	14.16	38.51	371.01	8.33
721	69.19	96.10	501.33	16.82	26.71	26.37	43.51	152.30	10.95
731	13.78	82.47	412.74	16.84	30.98	9.10	47.77	353.40	11.90
741	26.19	111.33	357.98	1.95	15.87	19.98	30.79	0.04	7.07
761	19.43	108.85	235.41	14.36	15.84	6.52	32.00	0.04	18.62
781	22.00	111.36	172.23	12.31	12.36	10.96	24.88	9.44	4.79
801	19.88	88.70	214.93	13.38	22.87	6.35	29.62	0.04	8.12
821	35.53	96.83	156.09	18.49	20.96	15.89	39.16	0.06	5.92
841	18.26	89.65	666.14	20.25	15.09	12.37	28.77	0.05	0.05
861	58.84	53.51	233.85	13.56	25.50	11.51	36.95	230.86	55.10
881	25.34	69.19	375.95	32.30	35.28	28.07	145.84	1815.80	40.98
901	15.23	94.48	381.83	28.59	77.03	0.36	74.74	1900.03	43.82
921	17.73	90.52	196.58	22.56	64.17	57.47	186.33	1670.68	39.22
941	29.60	97.51	130.43	31.14	51.05	21.82	78.72	967.65	47.77
961	26.92	68.48	378.04	19.74	21.32	24.60	39.00	0.07	16.02
981	20.85	67.58	222.20	15.28	29.99	20.81	72.51	569.85	36.15
1001	32.80	73.37	500.97	28.82	41.73	0.25	59.77	1335.60	31.22
1006	3.78	115.36	580.50	20.32	45.18	30.07	133.72	1565.67	29.09
1011	2.15	7.04	31.66	1.75	2.73	0.02	8.82	102.58	2.52
1016	9.96	85.20	500.72	15.43	25.73	0.13	65.97	800.41	19.70
1021	25.89	98.12	500.92	29.10	39.11	0.31	137.55	1757.62	0.31
1026	20.71	124.01	1110.24	27.45	38.62	27.08	110.09	1209.51	48.67
1031	48.10	60.84	729.35	23.64	70.31	77.45	107.67	1712.69	70.62
1036	48.66	67.97	388.96	24.22	59.52	47.67	170.86	1576.10	58.73
1041	39.59	133.79	344.90	36.78	59.35	26.24	164.40	1719.70	81.84
1061	44.55	87.23	718.85	18.78	32.70	23.31	110.28	893.08	46.84
1081	33.01	82.78	335.97	17.96	20.80	37.43	90.19	976.34	24.16
1101	31.73	44.40	164.72	13.89	22.51	28.88	46.63	406.72	26.38
1111	35.32	54.78	554.23	15.99	22.22	14.40	65.23	239.36	21.37
1121	23.39	56.69	370.21	15.15	20.33	20.73	41.83	217.53	22.51
1131	45.21	59.58	731.01	16.95	35.08	0.12	98.89	545.92	29.98
1141	41.22	99.61	361.90	21.44	25.30	22.87	80.61	63.26	16.31
1161	30.45	48.12	287.58	12.11	11.58	8.26	23.18	181.84	10.09
1181	40.60	63.36	291.72	13.28	24.99	0.14	60.78	467.24	25.07
1191	54.03	31.67	474.20	12.50	22.71	17.31	70.60	314.69	21.97
1201	42.55	69.01	575.31	21.40	15.27	25.85	60.59	0.07	8.41
1221	65.40	67.20	446.17	17.43	25.77	19.73	32.37	0.08	20.43
1241	43.30	45.77	426.88	12.79	10.90	10.29	29.90	0.05	7.96
1251	25.42	71.27	593.46	15.07	29.48	0.07	100.55	27.82	16.15
1261	47.38	58.52	428.50	14.34	14.40	8.23	33.48	0.06	9.91
1281	52.11	56.82	694.80	17.41	12.13	5.50	33.72	24.78	7.68
1301	62.98	73.28	865.62	14.49	8.42	7.65	16.96	3.85	4.38
1321	83.08	88.23	1126.93	11.78	20.06	5.00	30.36	17.86	7.79
1341	84.09	85.07	929.55	14.35	10.09	7.03	20.01	0.05	0.05
1361	46.96	108.34	532.41	16.62	16.29	2.59	25.61	10.59	4.98
1381	36.83	104.29	372.74	16.71	28.33	16.33	59.85	146.78	23.09
1391	22.30	76.46	464.06	14.01	18.61	7.78	36.61	55.32	5.03
1401	29.93	66.57	247.74	11.69	12.61	5.43	22.82	7.75	4.83
1421	39.79	54.95	305.19	16.15	13.52	9.21	32.01	94.20	16.74
1441	32.19	67.20	540.20	20.93	18.24	20.61	57.76	160.01	12.65
1461	27.58	72.80	498.78	13.37	19.31	17.64	70.73	327.34	11.67
1481	44.12	76.43	801.26	19.38	23.00	11.79	44.10	202.59	17.05
1501	49.44	83.35	547.62	0.11	26.72	0.11	30.06	494.51	0.11
1521	43.99	83.03	489.49	10.12	23.99	17.04	39.00	223.38	0.09
1541	25.35	55.10	507.67	10.90	20.09	12.43	40.40	452.49	0.11
1561	47.08	68.22	633.06	17.04	30.14	12.79	57.07	780.36	40.73
1581	58.42	62.98	464.94	21.65	28.69	35.30	74.95	1253.33	49.04
1601	47.58	71.67	638.45	0.14	30.20	0.14	38.44	637.47	22.59
1621	49.92	58.06	555.87	17.95	20.50	9.96	49.00	143.24	16.79
1626	31.94	29.62	491.05	13.41	25.21	10.20	54.49	340.56	19.96
1631	37.49	40.74	630.87	16.62	20.33	18.14	52.24	78.52	14.30
1636	29.72	43.38	557.88	12.45	27.75	0.11	53.23	238.09	13.00
1641	41.12	43.95	689.04	11.90	15.53	0.06	28.45	8.03	12.77
1661	29.33	66.02	771.50	12.51	20.13	17.01	30.17	110.31	11.47
1681	38.20	54.02	1197.39	9.11	12.42	16.29	41.08	50.09	7.76
1701	33.83	42.01	471.43	11.62	9.25	0.04	17.42	0.04	8.21
1721	53.24	62.43	548.29	10.43	11.83	11.58	22.15	0.06	0.06

1741	40.82	47.92	933.02	13.97	11.16	5.06	17.72	0.05	0.05
1761	48.58	62.76	375.95	15.33	21.24	12.67	23.81	57.29	12.43
1781	59.02	71.78	620.23	16.79	9.44	6.69	20.47	0.05	0.05
1801	0.12	148.36	731.95	14.69	15.16	10.74	33.77	0.05	0.05
1821	61.88	68.87	760.88	0.04	11.30	18.84	21.57	0.04	0.04
1841	44.18	82.80	232.46	0.02	6.07	0.02	6.41	0.02	0.02
1861	66.89	59.55	516.75	10.49	7.22	0.04	9.88	0.04	0.04
1881	49.73	84.49	387.81	11.90	9.44	4.43	10.61	0.03	0.03
1901	61.13	72.82	103.58	0.02	5.39	12.88	5.76	0.02	0.02
1921	94.40	63.51	884.60	5.90	11.09	6.93	10.18	0.05	0.05
1941	76.86	63.47	442.70	0.05	9.44	0.05	10.47	0.05	0.05
1961	81.77	59.30	643.40	3.84	17.61	5.95	15.02	0.06	0.06

Table 6 Location of comparison samples
Sample code corresponds to the codes used in Table 7 and in the text.

Location	Cruise	Core	depth in core (cm)	approx. age ka	Sample Code
ORPHAN KNOLL	DSDP 111A	1/4	25-50	1600	51
ORPHAN KNOLL	DSDP 111A	1/2	50-75	1600	50
ORPHAN KNOLL	DSDP 111A	1/5	100-125	1600	52
ORPHAN KNOLL	DSDP 111A	2/1	78-100	1700	53
ORPHAN KNOLL	DSDP 111A	2/3	25-50	1800	54
ORPHAN KNOLL	DSDP 111A	2/4	100-125	1800	55
ORPHAN KNOLL	DSDP 111A	3/4	75-100	1800	56
ORPHAN KNOLL	DSDP 111A	4/2	75-95	2000	57
ORPHAN KNOLL	DSDP 111A	4/3	105-120	2200	58
ORPHAN KNOLL	DSDP 111A	5/5	12-40	2800	59
TAIL OF BANKS	87-008	007	17-20	1	40
TAIL OF BANKS	87-008	007	41-44	1.5	41
TAIL OF BANKS	87-008	007	63-66	2	42
TAIL OF BANKS	87-008	007	709-712	20	43
TAIL OF BANKS	87-008	007	770-773	20	44
TAIL OF BANKS	87-008	007	831-834	20	45
TANTALLON	86-034	019	52-55	16	4
TANTALLON	86-034	019	844-847	16.5	5
EAST FLEMISH PASS	87-008	013	6-9	1	46
EAST FLEMISH PASS	87-008	013	25-28	2	47
ST. PIERRE SLOPE	86-034	005	3-6	2	9
ST. PIERRE SLOPE	86-034	005	20-23	11.5	10
ST. PIERRE SLOPE	86-034	005	40-43	12	11
ST. PIERRE SLOPE	84-003	010	68-71	2	6
ST. PIERRE SLOPE	84-003	011	77-80	11	7
ST. PIERRE SLOPE	84-003	011	770-773	11.5	8
EAST FLEMISH PASS	87-008	013	986-989	22	48
NARWHAL	86-013	001	85-88	5	12
NARWHAL	86-013	001	993-996	18	13
NARWHAL	86-013	001	1014-1017	18	14
NARWHAL	86-013	001	1057-1060	18	15
TANTALLON	86-034	017	18-21	1	1
TANTALLON	86-034	017	60-63	6	2
TANTALLON	86-034	017	818-821	16	3
FLEMISH CAP	87-008	021	GRAB	4000	49
LABRADOR SEA	75-009	037	55-57	1	71
LABRADOR SEA	75-009	037	192-194	9	72
LABRADOR SEA	75-009	037	296-298	18	73
LABRADOR SEA	75-009	037	447-450	30	74
LABRADOR SEA	75-009	037	800-802	70	75
L SHELF HOPEDALE	83-030	036	49-52	8.5	64
L SHELF HOPEDALE	83-030	036	258-260	9.5	65
L SHELF HOPEDALE	83-030	036	349-352	10.5	66
L SHELF KARLSEFINI	87-033	015	150-153	4	67
L SHELF KARLSEFINI	87-033	015	297-300	8.5	68
L SHELF KARLSEFINI	87-033	015	500-503	9.5	69
L SHELF KARLSEFINI	87-033	015	700-703	10.5	70
L SHELF CARTWRIGHT	87-033	018	300-303	7	60
L SHELF CARTWRIGHT	87-033	018	500-503	8.5	61
L SHELF CARTWRIGHT	87-033	018	995-998	9.5	62
L SHELF CARTWRIGHT	87-033	018	1475-1478	10.5	63
FOGO SEAMOUNTS	85-001	013 TWC	50-52	15.4	16
FOGO SEAMOUNTS	85-001	013 TWC	70-72	15.4	17
FOGO SEAMOUNTS	85-001	013 TWC	90-93	15.4	18
FOGO SEAMOUNTS	85-001	013 TWC	132-135	30.8	19
FOGO SEAMOUNTS	85-001	013	70-72	65.5	20
FOGO SEAMOUNTS	85-001	013	130-133	77	21
FOGO SEAMOUNTS	85-001	013	150-153	125	22
FOGO SEAMOUNTS	85-001	013	190-200	154	23

FOGO SEAMOUNTS	85-001	013	280-282	154	24
FOGO SEAMOUNTS	85-001	013	310-312	154	25
FOGO SEAMOUNTS	85-001	013	335-338	154	26
FOGO SEAMOUNTS	85-001	013	370-372	154	27
FOGO SEAMOUNTS	85-001	013	1370-1372	346.5	28
FOGO SEAMOUNTS	85-001	013	1390-1395	385	29
FOGO SEAMOUNTS	85-001	013	1403-1408	385	30
FOGO SEAMOUNTS	85-001	013	1435-1437	446	31
FOGO SEAMOUNTS	85-001	014	1-2		32
FOGO SEAMOUNTS	85-001	014	61-62		33
FOGO SEAMOUNTS	85-001	014	69-71		34
FOGO SEAMOUNTS	85-001	014	115-116		35
FOGO SEAMOUNTS	87-008	004	237-238	3000	36
BAFFIN BASIN	76-029	034	8-10	4	81
BAFFIN BASIN	76-029	033	19-21	3	82
BAFFIN BASIN	76-029	033	97-100	18	83
BAFFIN BASIN	76-029	033	240-243	30	84
BAFFIN BASIN	76-029	033	288-290	30	85
BAFFIN BASIN	76-029	033	290-292	30	86
BAFFIN BASIN	76-029	033	398-400	30	87
FOGO SEAMOUNTS	85-001	011D	7-10	3	37
FOGO SEAMOUNTS	85-001	011D	25-27	15.4	38
FOGO SEAMOUNTS	85-001	011D	37-38	15.4	39
BAFFIN BASIN	77-027	017	40-43	8	76
BAFFIN BASIN	77-027	017	132-134	18	77
BAFFIN BASIN	77-027	017	262-264	70	78
BAFFIN BASIN	77-027	017	390-391	110	79
BAFFIN BASIN	77-027	017	422-423	125	80

Table 7. Peak areas normalised to illite for comparison samples
Sample code is related to sample location in Table 6.

SAMPLE	PEAK AREAS NORMALIZED TO ILLITE								
CODE	Kaol.	Chlor.	Smectite	Amph.	Quartz	K Feld.	Plag.	Calcite	Dolomite
51	169.32	73.39	2499.88	13.29	15.14	0.00	14.63	13.93	4.65
50	142.45	71.85	2145.24	10.42	9.96	5.61	8.73	7.83	6.36
52	166.88	75.58	2337.80	6.43	14.73	0.00	12.96	17.83	4.58
53	122.18	70.21	1932.51	7.19	13.26	0.00	11.20	20.78	6.19
54	151.67	90.92	2639.29	6.91	16.55	12.52	15.31	7.12	4.52
55	155.54	85.95	3442.24	8.07	28.01	10.99	14.01	0.00	0.00
56	132.87	61.19	4144.74	0.00	17.54	0.00	9.11	0.00	6.91
57	129.38	84.51	2721.76	0.00	18.96	11.50	12.44	0.00	1.47
58	164.08	115.18	3691.39	0.00	16.86	11.07	16.80	0.00	0.00
59	166.27	80.86	2672.39	9.78	22.38	5.08	26.91	0.00	0.00
40	0.00	90.26	79.38	13.87	13.65	16.27	70.13	0.00	5.38
41	0.00	99.41	142.68	18.96	29.92	34.00	120.74	0.00	28.81
42	0.00	77.71	92.32	16.11	22.06	14.12	86.96	12.80	9.83
43	125.30	76.54	139.98	16.01	22.17	15.39	59.07	392.61	139.96
44	31.24	61.99	182.33	13.16	11.55	4.72	36.17	9.60	10.60
45	29.35	76.53	213.88	20.98	14.40	12.36	54.26	7.37	16.14
4	61.47	95.61	85.45	9.71	10.01	5.86	12.54	18.95	0.00
5	70.84	117.16	163.28	9.65	13.56	6.70	19.02	17.56	7.96
46	53.72	115.32	215.54	11.57	12.28	4.88	27.46	11.31	3.37
47	19.79	111.82	0.11	11.22	39.10	18.47	60.78	372.91	0.00
9	48.76	150.05	202.55	0.00	17.24	6.85	24.92	31.89	0.00
10	33.88	113.34	81.27	12.97	15.91	3.60	24.78	34.63	9.33
11	41.83	131.57	139.77	0.00	17.13	9.72	22.16	25.65	14.43
6	35.08	99.11	226.30	12.90	12.11	6.10	29.92	137.34	22.64
7	48.65	133.98	202.38	0.00	19.44	6.77	15.64	56.27	0.00
8	43.66	132.55	194.44	0.00	17.69	12.68	18.89	43.24	0.00
48	33.93	69.62	141.61	11.32	15.77	6.35	24.90	173.58	24.97
12	71.70	126.17	991.36	0.00	25.72	0.00	21.89	49.57	0.00
13	59.19	125.88	862.78	19.61	18.04	8.96	26.91	21.49	0.00
14	73.56	117.88	689.12	0.00	18.53	0.00	15.67	30.31	5.91
15	80.93	120.37	1059.99	0.00	14.41	9.13	13.93	39.73	0.00
1	25.62	106.54	346.85	18.27	24.32	8.92	61.68	32.71	0.00
2	52.17	116.16	350.49	8.68	10.13	7.82	19.44	7.01	3.93
3	52.24	78.71	82.06	3.88	8.31	3.64	9.00	10.60	0.00
49	0.00	56.27	116.32	10.62	18.41	9.77	53.41	268.61	9.38
71	0.00	167.33	1539.97	21.00	46.22	0.00	109.82	1394.68	0.00
72	36.99	82.93	1368.28	22.83	23.39	0.00	81.36	170.06	0.00
73	42.96	72.04	1173.49	26.86	11.53	6.62	85.39	13.95	15.61
74	23.06	52.87	862.76	26.72	8.96	0.00	63.36	0.00	0.00
75	0.00	103.73	1563.29	14.06	10.81	0.00	101.02	112.08	0.00
64	33.43	78.57	88.53	19.68	16.85	12.87	68.33	247.19	35.46
65	62.12	66.06	620.84	39.83	27.06	30.41	154.47	8.29	12.58
66	68.72	66.94	695.63	11.46	11.26	11.30	57.22	8.70	4.73
67	27.65	54.32	39.64	11.19	14.06	10.76	36.06	191.99	28.25
68	70.13	64.04	83.64	17.69	22.89	18.13	53.61	334.56	58.37
69	32.81	60.42	79.56	14.10	16.80	12.21	50.97	253.20	38.11
70	23.86	32.45	91.10	12.85	6.94	3.59	32.83	37.71	8.65
60	18.76	46.22	45.82	11.39	7.40	6.57	28.20	13.67	11.25
61	27.04	45.15	61.16	15.44	9.93	12.68	36.93	64.72	22.70
62	20.02	27.94	89.89	15.66	13.91	9.83	41.70	13.63	9.79
63	17.59	25.77	42.74	10.67	7.45	8.35	27.21	0.00	1.98
16	29.62	80.11	142.17	14.14	14.18	7.93	26.61	19.31	12.16
17	24.76	95.83	146.71	12.35	16.27	12.38	29.24	28.79	4.77
18	23.28	109.65	35.33	2.20	10.40	4.19	18.20	27.84	7.35
19	34.96	75.77	336.35	2.61	9.53	5.17	20.10	64.30	11.12
20	20.88	73.99	162.33	14.85	8.19	8.79	30.71	14.08	2.14
21	18.88	47.77	125.15	13.25	7.78	4.61	29.87	7.50	0.00
22	16.97	52.69	152.18	17.53	9.68	6.87	34.52	12.79	3.86
23	18.99	76.62	497.64	17.78	38.55	21.14	64.91	1762.66	43.73
24	50.44	94.32	114.91	6.78	5.71	6.07	11.14	5.91	0.00
25	52.66	100.93	350.27	3.35	11.49	8.19	16.05	69.80	5.36
26	45.00	95.40	87.66	7.53	8.85	3.68	18.38	25.27	4.20

27	51.93	114.04	122.32	1.71	8.03	5.82	14.91	17.51	3.12
28	17.33	52.88	103.23	13.98	7.11	6.23	29.60	14.06	4.98
29	42.41	48.95	657.52	13.70	11.04	5.31	28.32	131.80	20.55
30	31.56	74.56	365.44	9.91	8.42	5.30	19.69	39.72	3.42
31	24.05	72.31	95.86	12.22	7.14	5.53	22.04	11.75	4.41
32	33.73	60.77	406.84	13.05	11.33	6.55	32.16	140.93	5.71
33	32.18	102.91	83.90	8.06	10.72	3.21	20.22	24.73	4.80
34	0.00	127.44	76.11	2.88	7.36	4.91	12.35	15.76	4.24
35	28.32	98.07	249.96	11.68	14.64	6.73	28.55	71.59	12.48
36	0.00	0.00	0.00	0.00	0.00	0.00	0.00	0.00	0.00
81	21.85	45.21	80.04	5.32	8.94	7.83	26.38	47.78	56.93
82	60.86	33.60	199.51	13.80	7.33	5.32	36.24	0.00	5.80
83	42.82	32.79	316.54	10.05	7.51	4.12	22.97	0.00	4.30
84	42.24	37.40	146.69	7.55	8.32	6.95	12.21	51.46	48.79
85	17.71	43.28	73.84	8.87	11.08	13.36	26.41	66.00	82.13
86	44.55	34.63	216.88	11.02	6.92	6.18	28.35	7.02	10.16
87	28.09	38.35	126.82	13.00	16.55	13.03	32.22	180.67	139.00
37	32.11	65.11	0.00	13.41	14.64	9.98	46.17	183.49	14.11
38	53.94	95.37	0.00	6.41	12.72	3.59	17.31	19.56	8.84
39	52.55	107.55	0.00	11.14	11.79	3.55	21.25	11.94	2.11
76	77.76	16.00	0.00	13.44	4.27	2.83	17.19	0.00	0.00
77	63.69	42.20	0.00	12.28	7.58	4.32	27.25	0.00	8.76
78	78.05	20.24	0.00	17.79	9.36	7.30	44.34	0.00	5.05
79	67.83	68.93	0.00	15.23	13.41	14.38	51.61	11.95	51.82
80	63.98	60.03	0.00	25.09	15.16	11.48	49.34	4.80	30.58

Table 8. Peak areas normalised to 20% corundum for samples from Flemish Pass

Core/depth	Illite	Kaol.	Chlor.	Smect.	Amph.	Qtz.	K-feld.	Plag.	Calcite	Dolomite
87-015										
TWC 5-7	152.5	72.2	79.7	149.8	21.9	37.1	22.5	145.3	10.2	52.2
TWC 45-47	57.9	54.1	70.5	55.8	8.3	28.0	26.6	62.5	559.0	118.5
TWC 52-54	107.0	108.7	151.6	236.8	17.2	43.2	35.1	83.8	56.4	32.3
126-128	112.7	109.2	162.9	278.2	17.0	41.4	28.0	99.7	95.8	61.1
239-241	85.4	69.1	151.3	144.7	11.1	37.7	10.2	72.5	0.0	20.3
285-287	70.7	50.6	81.0	64.0	11.1	24.0	15.1	66.0	293.5	69.9
568-570	145.4	68.2	89.4	225.6	20.8	32.8	31.7	109.9	45.9	78.9
648-650	194.5	168.6	323.7	264.8	17.2	40.3	15.6	85.2	0.0	17.2
753-755	141.5	87.1	171.2	148.5	17.3	40.2	59.0	135.7	45.2	48.0
766-768	173.0	116.7	230.7	186.3	21.3	37.7	22.0	107.5	42.2	32.9
795-797	133.2	73.1	160.1	137.8	17.0	36.4	18.9	99.6	35.4	38.6
884-886	150.9	92.8	182.8	228.6	18.8	38.9	15.5	112.2	34.4	24.7
87-013										
TWC 4-6	144.7	30.7	88.6	151.7	18.2	36.1	31.5	133.5	211.7	77.8
12-15	117.5	61.5	95.3	237.0	20.7	46.2	40.1	150.4	162.8	103.3
414-416	97.3	76.8	106.4	228.1	16.0	27.6	11.9	72.7	90.8	52.6
519-521	112.3	99.5	102.5	294.4	19.9	46.5	30.2	129.7	131.5	78.1
644-646	47.1	42.1	37.3	0.0	6.1	19.6	15.0	46.4	493.1	106.4
738-740	119.2	157.7	129.6	169.5	12.7	30.8	16.8	66.6	18.0	15.3
86-012										
TWC 67-70	123.1	88.6	232.6	159.0	19.2	40.3	12.3	68.3	0.0	22.4
TWC115-117	147.0	122.3	215.1	283.4	18.4	36.8	13.4	83.7	17.4	20.8
169-171	205.5	80.5	102.6	291.3	29.4	32.9	25.2	146.1	0.0	25.6
276-278	167.9	63.6	96.5	267.1	20.5	28.7	29.7	139.6	10.8	49.4
334-336	153.5	79.8	104.3	245.9	21.4	34.2	23.7	135.9	15.9	59.6
514-516	159.5	99.0	209.0	117.9	13.2	36.3	16.6	84.5	19.7	19.8

APPENDIX 1: CONTAMINATION IN 87-008-003 SAMPLES

Apparently due to the storage of the samples in $MgCl_2$ and Na metaphosphate, the initial set of samples analysed by Armstrong in 1988 were contaminated by the formation of Mg-phosphate precipitates. When doing the comparison of A31661 (done by Armstrong in 1988) and A31661B (done by Skene in 1990) the presence of a foreign substance was so obvious on the diffractogram that further investigation was warranted. This sample was mounted for SEM analysis and with the discovery of at least two different crystal forms of Mg-phosphate. These were taken to be contaminants for two reasons. First, because of the lack of these compounds in the original diffractogram. Second, the size of the crystals was on average >10 μms in a sample that was prepared to consist solely of the <2 μm fraction.

There were two effects that the contamination had on the diffractogram. On one hand, there was the splitting of the 14 Å peak into a 14 Å and 13.2 Å peak. This is seen on the majority of the samples processed. More importantly, there is considerable worry that the kaolinite/chlorite peak at 7.0 Å was being overlapped with a peak produced by the contaminant(s). This would then lead to an overestimation of the kaolinite/chlorite peak area obtained in the new data. However, there does appear to be a correlation between the appearance of a peak at 8 Å and the possible overlapping of the 7 Å peak. In samples A30246, A30296 and A30311 there is a relatively strong 8 Å peak and concurrently an obvious splitting of the 7 Å peak. In all samples with the 8 Å peak, there appears to be deformation of the 7 Å kaolinite/chlorite peak. In those samples that have only the 13.2 Å peak, the effect of the contamination is not as clear.

Consequently, though most of the samples from 88008-003 worked on by Skene were contaminated, not all reflect the same degree of error in the final peak areas. The following parameters should be used when evaluting the accuracy of the data:

1) An 8 Å peak identified - chlorite and kaolinite estimate may be wrong
2) A 13 Å peak identified - contaminated sample, unknown error.

APPENDIX 2: DATA STANDARDIZATION -- METHODS

Purpose

Clay-sized mineralogical studies employ X-ray diffraction (XRD) techniques. Using these methods to study any significant amount of samples (normally several hundred) produces a large numerical data set for analysis. Each mineral analysed has a characteristic range of values which is related to the regional abundance of that mineral. Standardization combats both the size and unrelated nature of the data set.

Background

X-ray diffraction data are first studied to identify the minerals present given their respective peak positions. Following mineral identification, the peak areas are calculated for one particular peak for each mineral. Because the area enclosed under the peak is proportional to the mineral's relative concentration in the sample, peak areas are used as a semi-quantitative measure of these abundances. However, the areas cannot be used in their raw form because they also depend upon such variables as sample preparation, sample iron content, and mount quality. These experimental influences are not readily quantifiable. To compensate for this variability, the data has been normalised with respect to illite. The data is reported as a percentage of the illite peak area according to the equation:

$$\text{normalized area} = \frac{\text{peak area of mineral}}{\text{peak area of illite}} * 100$$

Illite is an abundant mineral, easily recognized in X-ray diffraction investigations; hence, it is most useful as a standard of comparison.

Implications of Standardization

After normalization in this fashion, the data set is prepared for investigation of the sample to sample variations in the relative abundance of a mineral (i.e. the minerals can only be studied as separate variables). This report attempts to outline and evaluate a ranking procedure which would standardize all the data to the same scale. This standardization would allow for inter-mineral relationships to be studied; subsequent determination of such relationships would enable geologists to propose characteristic mineral assemblages. These mineral assemblages would then lead to a more rigorous definition of depositional setting and provenance.

In addition to illustrating both the standardization method and the improved ability to interpret the scaled data, the retention of statistical validity through the data transformation will be investigated. Mean, standard deviation, and Pearson's correlation coefficient are the most useful statistics calculated for X-ray diffraction data; thus, the investigation will be restricted to these parameters.

METHOD OF DATA STANDARDIZATION

Algorithm Development

The premise behind data standardization is a simple scaling of the data with respect to 100. The transformation was developed using a finite sequence

approximation to relate varying data ranges to a common 0-100 range. The formula is as follows:

$r = 100*(n - n_{min})/R$ if $n>n_{min}$ (Equation 1)
$r = 0$ if $n=n_{min}$ (Equation 2)
$r = 0$ if $n=0$ (Equation 3)

where r = standardized datum point
R = range of normalized data (maxima - nonzero minima)
n = normalized datum point
n_{min} = nonzero minima of normalized data

Boundary Conditions

Equation 1 forms the bulk of the standardization algorithm, whereas Equation 2 and Equation 3 act as boundary conditions. Equation 2 sets the minima of the normalized data to 0; and Equation 3 sets zero values of the normalized data to zero. This minima-zero distinction is explictly stated to reinforce the effect of detection limits when dealing with XRD data. Minimae reflect low mineralogical values most probably due to dilution of this mineral by other minerals in the sample. In this sense, dilution refers to the presence of a mineral being suppressed because so much more of another mineral is present. For example, calcite, in large amounts, will suppress the peak areas of all other minerals present, making these minerals appear, on the whole, as only minor constituents. However, if one were to remove calcite from the sample this suppression would not be seen. Consequently, low mineralogical values are circumspect during geological interpretation. Those minerals which possess non-zero peak areas from the sample suite are illite, chlorite, quartz, and plagioclase.

In contrast, zero values reflect mineral abundances which are below the detection limit. Therefore, zero values do not neccessarily mean the absence of a mineral from the assemblage. There appears to be no satisfactory criteria for distinguishing i) the importance of determining trace amounts of a mineral, and ii) the definition of what values below the detection limit renders a mineral as "absent". Minerals which have zero values in some samples in this study are kaolinite, K-feldspar, amphibole, calcite, and dolomite. (Calcite and dolomite are not considered in the interpretative examples but have the same properties as values for kaolinite, K-feldspar, and amphibole.)

EFFECT ON DATA COMPARISON

Problems of Comparison Using Unranked Data

Though this fitting procedure appears overly simple and lacking in rigour, its application to geologic data sets allows for a greater ability to visually interpret data. With unranked data, the interpreter must scan large amounts of numerically unrelated data. What is a high value for one mineral is not necessarily a high value for another mineral. One, therefore, has to shift back and forth between definitions of magnitude when trying to investigate inter-mineral relationships. In so doing, the tendency is to redefine one's initial premises to fit into expected trends, thereby, possibly overlooking unexpected and/or diagnostic anomalies in the mineralogy.

Comparison Using Standardized Data

The data set, fitted to a common scale by the standardization algorithm, is in a more useable form. Each nonzero value is reported as a percentage of the maximum value for that mineral. Therefore, a smectite value of 50 and a kaolinite value of 50 both represent the same percentage (half) of their respective maximae. Consequently, one can assume that the relative importance of these two minerals in the sedimentation regime is equal.

The standardization also relieves the interpreter from distinguishing actual variations from normal regional abundances. For example, chlorite is an abundant clay-sized mineral while amphibole is not. A chlorite-amphibole comparison using unranked data would always show this trend (i.e. chlorite>amphibole). Utilizing standardized data, one would be able to see if anomalously high amphibole values occur regardless of the regional abundances.

Examples Taken From Core 87-008-003

The original and standardized data sets are reproduced in Table 1 and Table 3, respectively. The data were taken from Core 87-008-003, a deep sea core retrieved from the J-anomaly Ridge. Table A2.1 represents a small portion of the X-ray diffraction data. In total, 19.8 m of core and 148 samples were analysed. These 148 samples were used to determine the parameters n_{min} and R employed in the algorithm and applied to the Table A2.1 data. The algorithm parameters by mineral are presented in Table A2.2. The transformation results are reproduced in Table A2.3.

Table A2.1: Normalized data versus depth in cm (from core 87-008-003)

DEP	KAO	CHL	SMEC	AMPH	QTZ	KFE	PLAG
1301	62.981	73.275	865.619	14.492	8.418	7.647	16.964
1321	83.084	88.227	1126.931	11.776	20.057	4.996	30.359
1341	84.091	85.071	929.554	14.348	10.091	7.032	20.009
1361	46.961	108.342	532.414	16.622	16.292	2.589	25.605
1381	36.831	104.29	372.738	16.714	28.329	16.327	59.846

*NOTE: dep = depth, kao = kaolinite, chl = chlorite, smec = smectite, amph = amphibole, qtz = quartz, kfe = K-feldspar, and plag = plagioclase.

Table A2.2: Algorithm Parameters by Mineral (data taken from 148 samples of core 87-008-003)

MINERAL	n_{min}	R
KAOLINITE	2	95
CHLORITE	7	142
SMECTITE	31	1167
AMPHIBOLE	2	36
QUARTZ	6	72
K-FELDSPAR	2	36
PLAGIOCLASE	5	92

Table A2.3: Standardized data versus depth in cm (taken from core 87-008-003)

DEP	RKAO	RCHL	RSMEC	RAMPH	RQTZ	RKFE	RPLAG
1301	64.191	46.672	71.518	34.7	3.3583	15.686	13.004
1321	85.351	57.202	93.910	27.155	19.523	8.322	27.564
1341	86.411	54.979	76.996	34.3	5.681	13.977	16.314
1361	47.327	71.367	42.966	40.61	14.294	1.636	22.396
1381	36.664	68.514	29.283	40.872	31.012	39.797	59.615

*NOTE: The prefix R- refers to standardized minerals.

Even by briefly scanning the two data sets, one can see the difficulties involved in interpreting the normal data. The values in Table A2.1 are obviously unrelated between minerals as is seen in the difference between the smectite and kaolinite values, for example. Smectite-kaolinite comparison using the data in Table A2.3 shows that these minerals have approximately the same magnitude and trend downcore. The subsequent interpretation is that smectite and kaolinite sources, at depths 1301-1381 cm, are of equal activity or strength and decrease in strength downcore. Whereas the decrease can be seen in both Table A2.1 and Table A2.3, the equality is only apparent in the standardized data.

The advantage of standardization over normalization is more readily seen in graphical examples. Figure A2.1 illustrates the chlorite-amphibole comparison discussed earlier. The natural abundance of chlorite over amphibole is easily seen in Figure A2.1. This same data is again presented in Figure A2.2 after applying the standardization algorithm. The relationship between chlorite and amphibole is now readily apparent. By visual inspection one can see the pattern of convergence and divergence between the two minerals; and, that this pattern is less noticeable when graphing the unranked data. Consequently, the standardization procedure greatly aides the visual interpretation of the data.

EFFECT ON STATISTICAL ANALYSIS

Statistics Calculated for X-ray Diffraction Data

Three statistics are normally calculated to assist in the interpretation of X-ray diffraction data: mean, standard deviation, and Pearson's correlation coefficient. Mean and standard deviation aid in reporting the trend present in a group of data; whereas, correlation coefficients quantitatively assess the degree of inter-relationship between two minerals.

Effect on Mean and Standard Deviation

In general, mean and standard deviation are slightly altered through the data transformation. The mean and standard deviation calculated for the normalized data reflect the average value and variation, respectively, for data from differing scales of measurement. These same statistics calculated for standardized data, like the individual standardized data, reflect descriptions of the data set when measured on the same scale. The resulting statistics can be directly related between different minerals producing comparable summaries of the mineralogy. For example, standard deviation of the standardized data, represents the degree of variation within a set of samples with respect to some

mineral. Comparison of the standard deviation of one mineral with another allows for the determination of which mineral shows the greater variance. Such determinations are important when determining long-term mineralogical trends.

Table A2.4 contains the means and standard deviations calculated for the minerals both before and after standardization. The standardized means can be compared just as the individual minerals are compared. The standardized standard deviations show the relative variance between the minerals.

Table A2.4: Elementary statistics for normal and ranked data
core 87-008-003 depth = 1301-1681 cm

	NORMALIZED DATA		STANDARDIZED DATA	
MINERAL	MEAN	STANDARD DEVIATION	MEAN	STANDARD DEVIATION
KAOLINITE	45.9	16.235	46.21	17.089
CHLORITE	72.178	16.438	45.9	11.576
SMECTITE	635.773	250.601	51.823	21.474
AMPHIBOLE	13.332	5.751	32.034	14.565
QUARTZ	19.914	6.671	19.325	9.265
K-FELDSPAR	11.205	8.563	26.403	22.702
PLAGIOCLASE	40.44	16.517	38.522	17.953

Interpretive Examples Taken From Core 87-008-003

The effect of standardization on statistical analysis is much like its effect on the individual data points; the data becomes more comparable. Consequently, it is easier to interpret.

Interpretation of the normalized data in Table 4 is hampered by its unrelated nature. Obviously, smectite=635.773 is the highest value, but is that a high value for smectite? Does smectite represent the most abundant mineral in this section of core? Does smectite show the greatest variance as predicted by its high standard deviation?

These questions arise because smectite values range from 30-1197, whereas kaolinite values range from 2-95, amphibole values from 2-36 etc. Standardization, by applying a common 0-100 scale, provides answers to these questions. The smectite value is moderate, 51.823 (about half of the maximum value for smectite), and is the highest of the minerals present. K-feldspar and not smectite shows the highest variance, but the smectite variance is high, suggesting variable data without downcore stability over these depths.

Effect on Pearson's Correlation Coefficient

Pearson's correlation coefficient is not altered by the data standardization. The correlation coefficient, by nature of its calculation, uses only the relative magnitudes of the values being correlated. Because the data transformation retains the relative magnitude between values, the statistical validity of the correlation coefficient is unaffected.

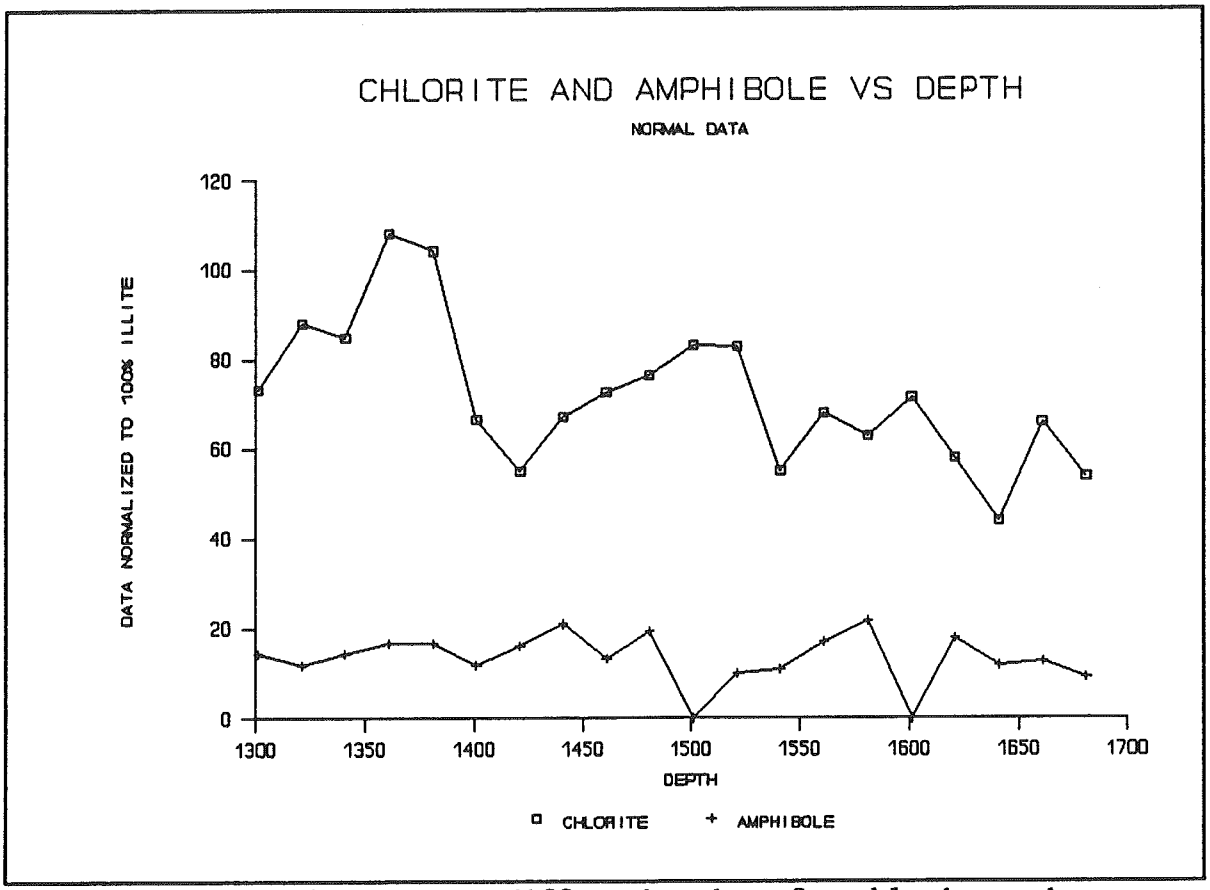

Figure A2.1 Normalized X-ray diffraction data for chlorite and amphibole taken from core 87-008-003.

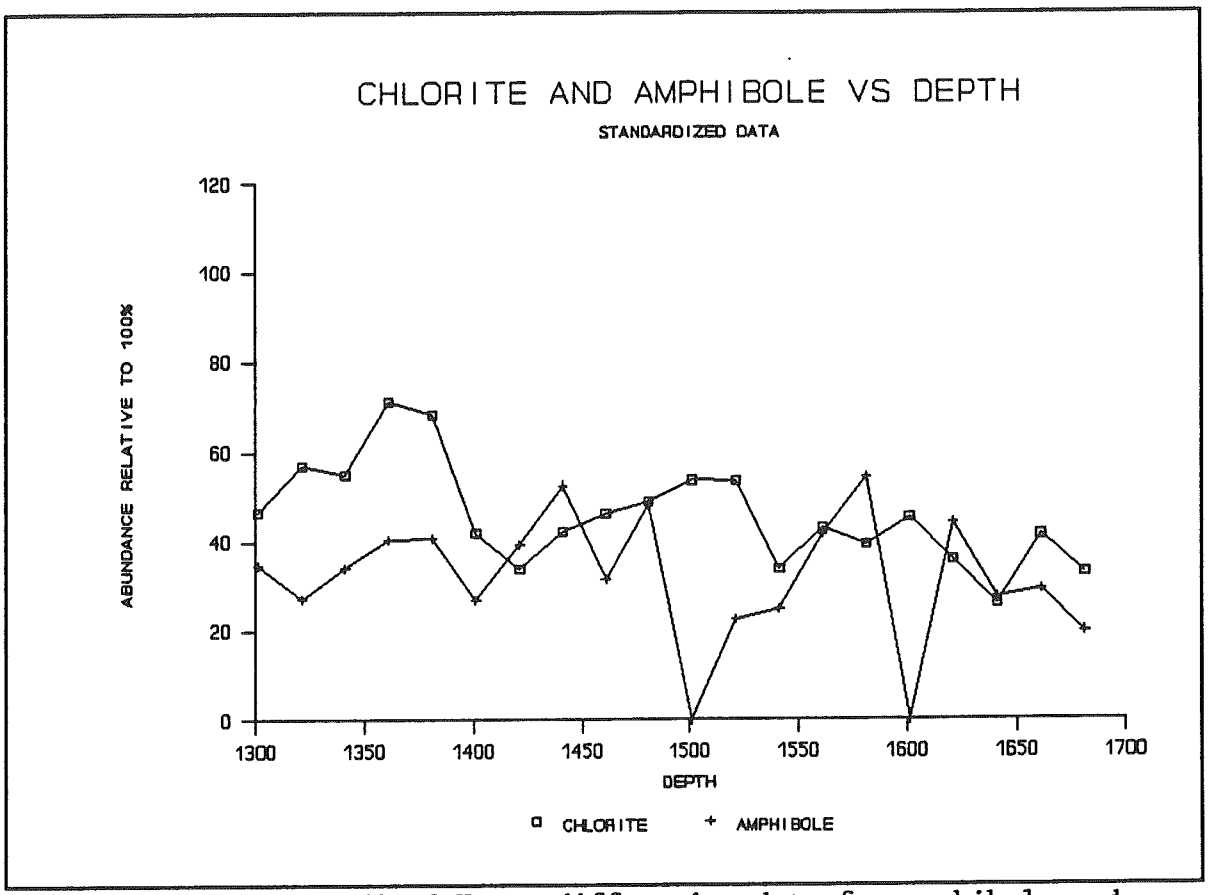

Figure A2.2 Standardized X-ray diffraction data for amphibole and chlorite taken from core 87-008-003.

CONCLUSIONS

Standardization produces data that are on comparable scales of measurement. This greatly facilitates interpretation of XRD analyses. The procedure also removes normal regional abundances in the data set by equally weighting the magnitudes reported for each mineral. Such a transformation creates data which are readily comparable both downcore (as in the case of numerous equally spaced analyses in the same core) and between cores.

Statistics calculated from the standardized data reflect the common scale of measurement and are thus modified. Pearson's correlation coefficient is unaffected allowing for more powerful statistical analyses to be used (i.e. principal components analysis on correlation matrices).

REFERENCES

Aitchison, J. (1986). "The Statistical Analysis of Geochemical Compositions," Mathematical Geology, vol. 16, no. 5-8, pp. 531-564.

Davis, J.C. (1986). Statistics and Data Analysis in Geology 2nd ed., John Wiley & Sons, Inc., New York, 386 pages.

Fraleigh, J.B. (1984). Calculus with Analytical Geometry 2nd ed., Addison-Wesley Publishing Co., Reading, Mass., 1182 pages.

APPENDIX 3: PROCEDURES FOR FLEMISH PASS SAMPLES WITH AN INTERNAL STANDARD CLAY-SIZED MINERALOGY OF FLEMISH PASS

Introduction

Twenty-four samples from selected Flemish Pass cores (87-008-013 and 015, 86-018-012 -- both trigger weight and piston cores) were analysed for clay-sized mineralogy by X-ray diffraction. No difficulties were experienced in data collection after the initial determination of corundum as an internal standard. The samples were normalized to corundum, corrected to 20% by weight, after applying Biscaye's factors. The subsequent presentation of the data is in semiquantitative percentages following the form outlined in Segall et al. (1987).

Sample Preparation

Preparation techniques, in general, followed those outlined in this paper. However, there were the following exceptions: 1) 6 mg corundum (<10 μm, 6mg/mL) was added to each sample before filtration, which was then mounted on to a pre-weighed glass slide; 2) slurry volume used was 0.5 mL; 3) the count time per step for the long scan was doubled to achieve a smoother, more reproducible diffractogram; 4) slit size was increased for the long scan to 1/0.15 degrees from 0.3/0.15 to increase peak intensity; 5) the surface area of the sample was increased by 30% by the use of square 2.5 x 2.5 cm slides, rather than disks 2.5 cm in diameter.

Data Normalization

Corundum, instead of illite was used as the basis for normalization (i.e. corrundum = 100). The concentration of corundum in each sample was back calculated by adding a known amount of standard and pre-weighing each slide. Since the 0.5 mL of slurry used for mounting is never the same concentration, the percent corundum in each sample also varies. Graphical analysis of percent corrundum versus peak area corundum suggests a linear relationship. Consequently, peak areas of corundum were corrected back to 20% making this value the common reference from which a mineral's presence could be expressed as a percentage of the bulk mineralogy -- i.e. bulk mineralogy = 100 (Segall et al., 1987).

Summary of Clay-sized Mineralogy: External Comparison

To compare the data with other analyses from the Eastern Canadian continental margin, the data was first normalized to illite. A general summary of each core's mineralogy, as related to values taken from previous analyses, was then completed and is as follows.

Core 87-015

With the exception of the top sample from the trigger weight core, kaolinite (101-54) and plagioclase (107-62) start from high values but decrease downcore. Chlorite (120-177) is variable but strong present. Amphibole (12-16) is moderate and consisently present downcore, showing little fluctuation. Calcite and dolomite peak together in two samples (45-47 cm TWC and 245-247 cm PC). On the whole calcite (0-84) is variable and dolomite (16-54) is variable but strongly present. The sample from 568-570 cm stands out by not following the aforementioned trends having low values for all minerals except dolomite

(50, extremely high).

Core 87-013

The trigger weight core sample (4-6 cm) again is characterized by depressed kaolinite (21) and chlorite (61) values. The piston core's kaolinite values (52-132) show an overall increase from moderately low to high values downcore. Chlorite (61-108) is variable and less than 87-015. Amphibole, quartz, and K-feldspar values are more or less the same when comparing 87-013 to 87-015. Calcite and dolomite have one peak (644-646 cm) and are strongly present in most of the core, becoming depressed in the bottom sample along with plagioclase. Plagioclase (74-128) is otherwise elevated but variable.

Core 86-012

Amphibole (12-15) remains moderate and consistently present in this core as it did in 87-013 and 87-015. The only contradictions to this generalization are amphibole values of 8 found in 87-015 648-650 cm and 86-012 514-516 cm. Calcite (0-12) and dolomite (12-39) are significantly lower in comparison to the 87008 cores. Dolomite, however, remains moderately high to high. Plagioclase (52-88) also appears lower. The top three samples of the piston core have markedly lower kaolinite (39-52) and chlorite (49-67). Otherwise kaolinite (62-83) moderate and chlorite (131-188) is variable but elevated.

General Summary of Illite Normalized Data

Regionally, the samples analysed from Flemish Pass are characterized by high chlorite and dolomite with consistent amphibole of moderate strength. Smectite (0-262) is variable but low even for these near-shelf samples. K-feldspar (8-45) is variable though it does reach some of its highest values yet seen. Kaolinite and quartz are variable and unless otherwise stated do not appear to show any diagnostic trend.

APPENDIX 4: STRATIGRAPHIC COLUMNS SHOWING LOCATION OF COMPARISON SAMPLES

A: Orphan Knoll (from Laughton, Berggren et al., 1979)

B: Tail of the Banks (from Skene, 1991)

C: Tantallon (unpublished data)

D: East Flemish Pass (from Piper and Pereira, in press)

E: St Pierre Slope (from Piper and Bonifay, 1988)

F: Narwhal (unpublished data of Piper and Bonifay)

G: Labrador Sea (from Hillaire Marcel and de Vernal, 1989)

H: Labrador Shelf - Karlsefni, Hopedale and Cartwright (from Josenhans and Zevenhuizen, 1989)

I: Fogo Seamounts (unpublished data, projected in to stratigraphy of Alam et al., 1983)

J: Baffin Bay basin (from Aksu and Piper, 1987).

APPENDIX 4: STRATIGRAPHIC COLUMNS SHOWING LOCATION OF COMPARISON SAMPLES

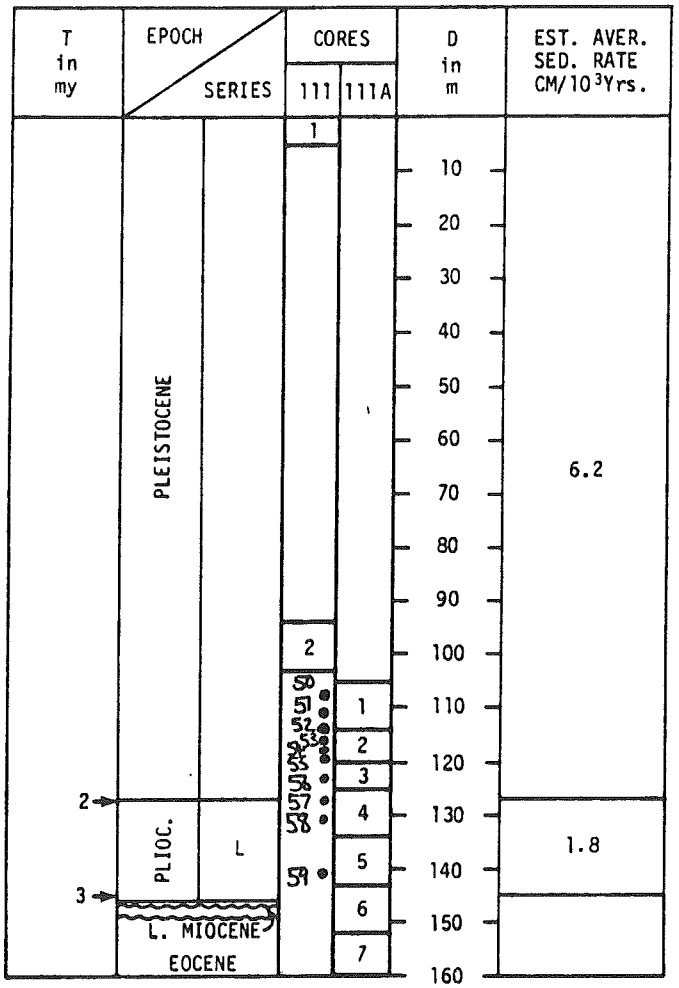

Figure 20. *Estimated average rates of sedimentation for the Late Pliocene and Pleistocene at Site 111 (Orphan Knoll).*

A: Orphan Knoll (from Laughton, Berggren et al., 1979)

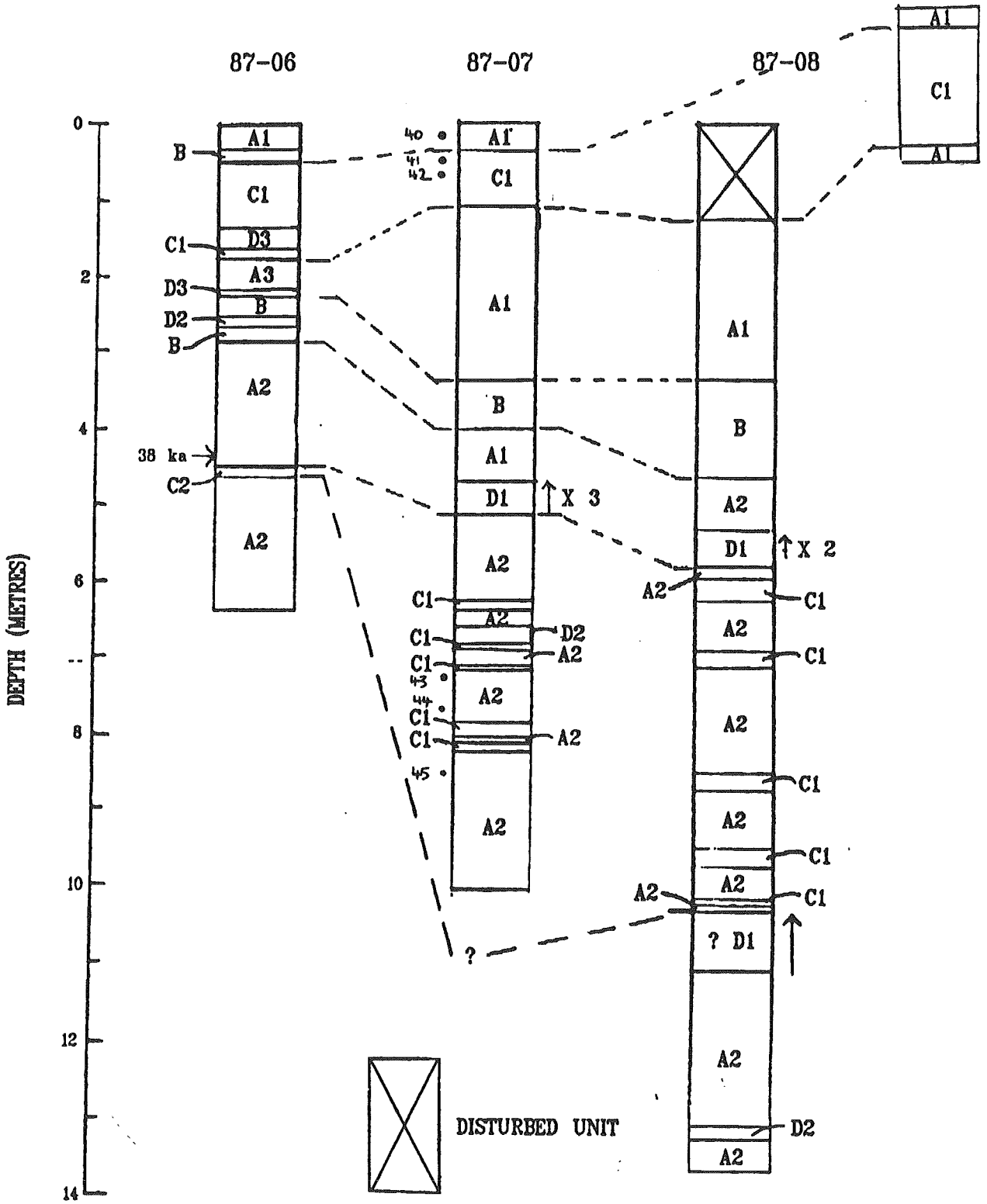

B: Tail of the Banks (from Skene, 1991)

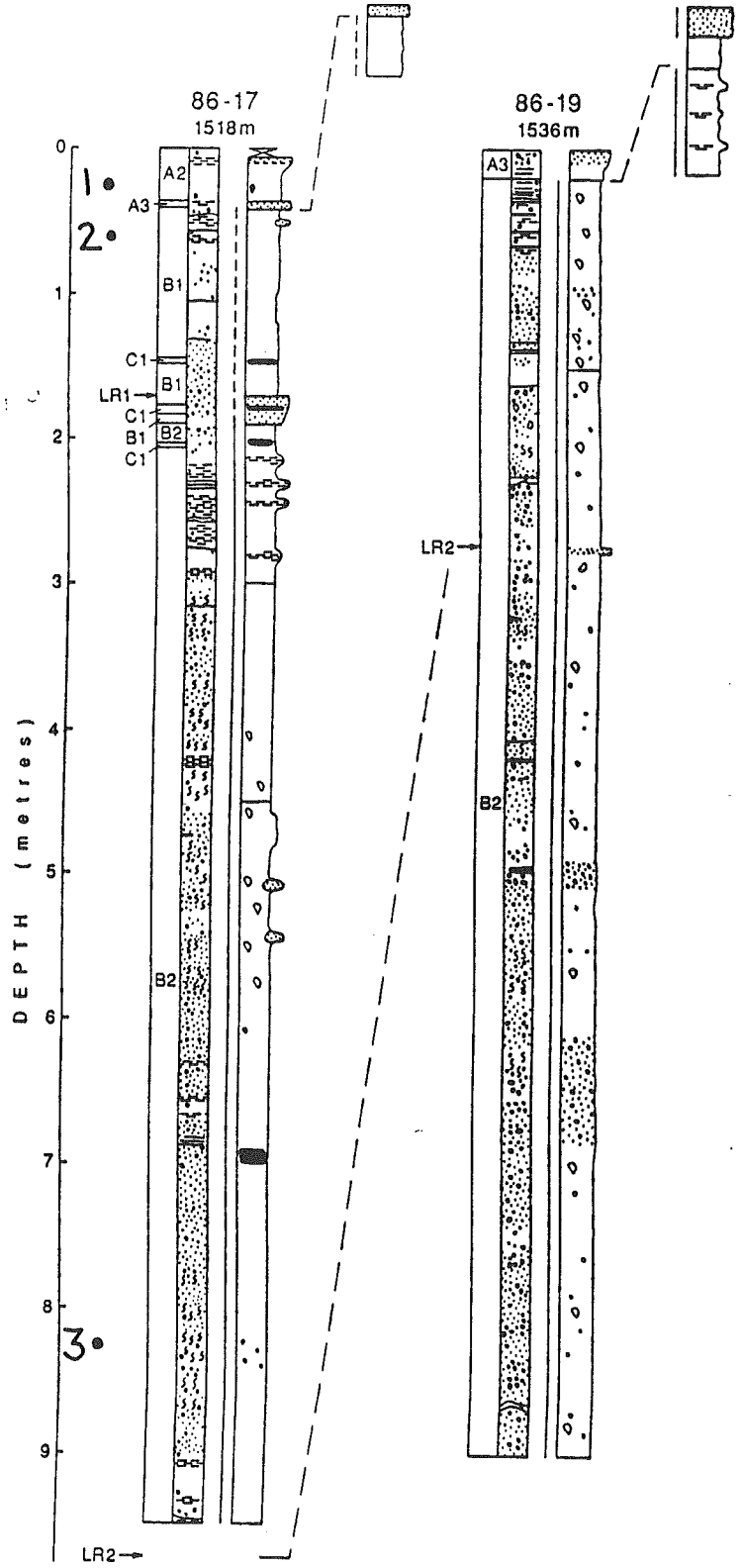

C: Tantallon (unpublished data)

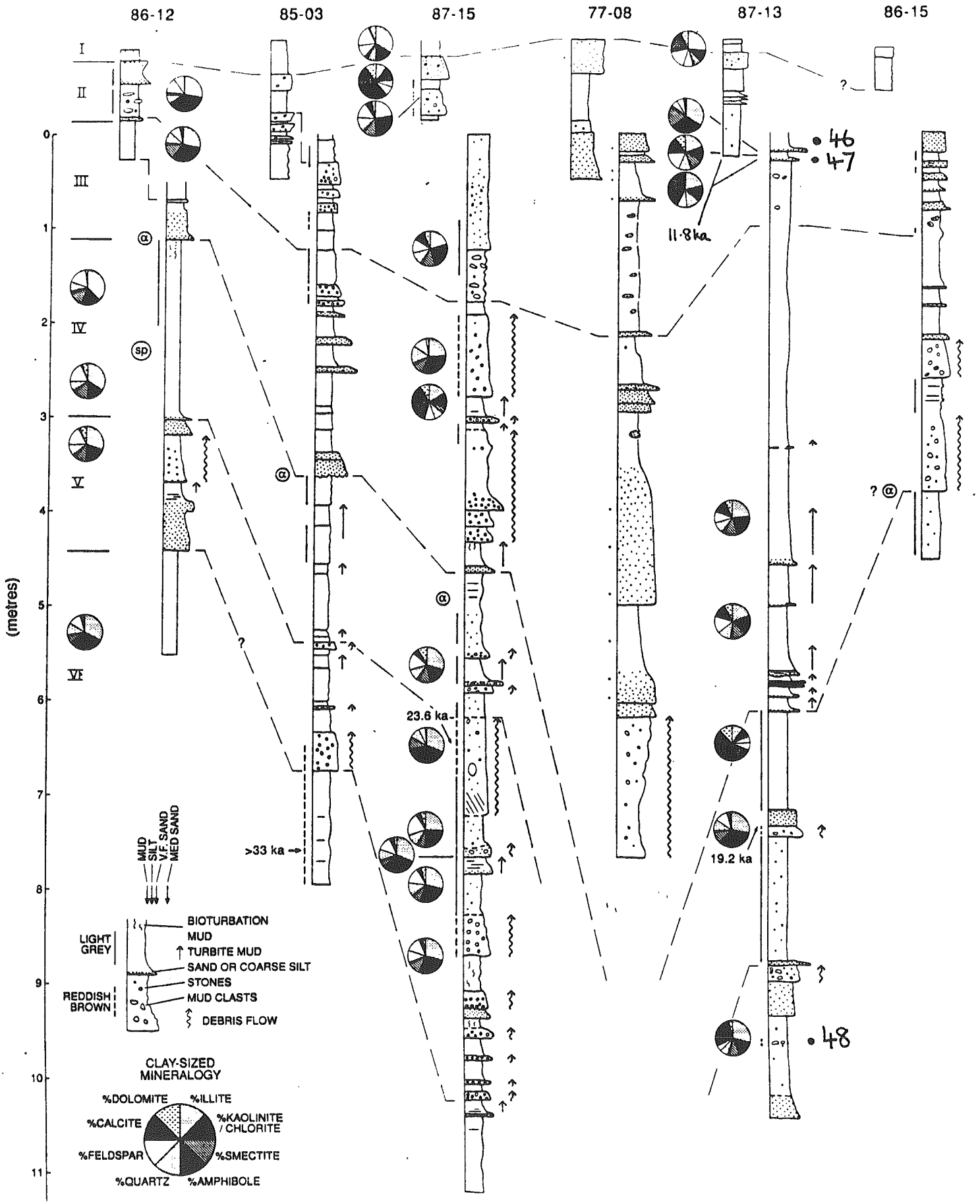

D: East Flemish Pass (from Piper and Pereira, in press)

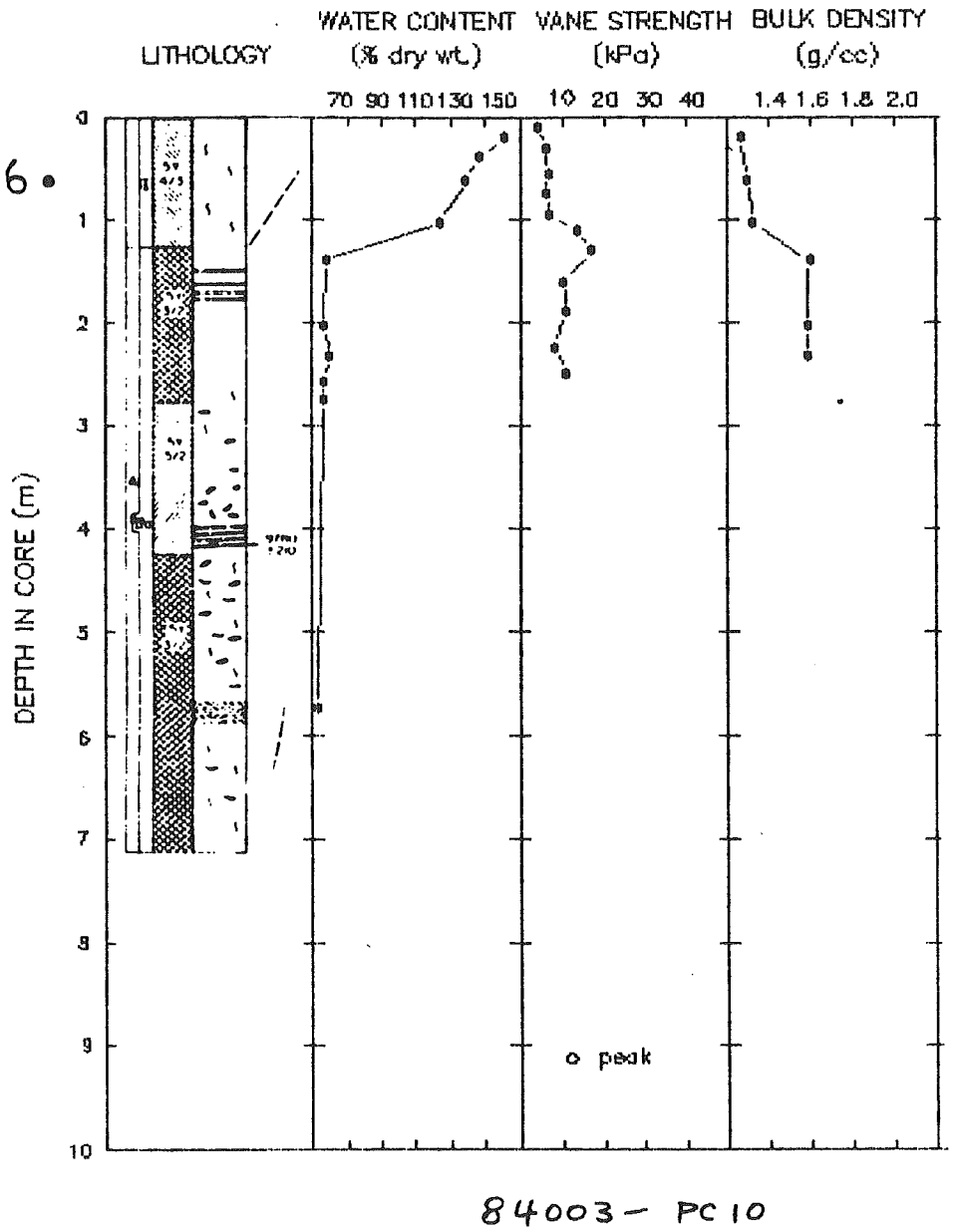

6.

84003 – PC 10

E: St Pierre Slope (from Piper and Bonifay, 1988)

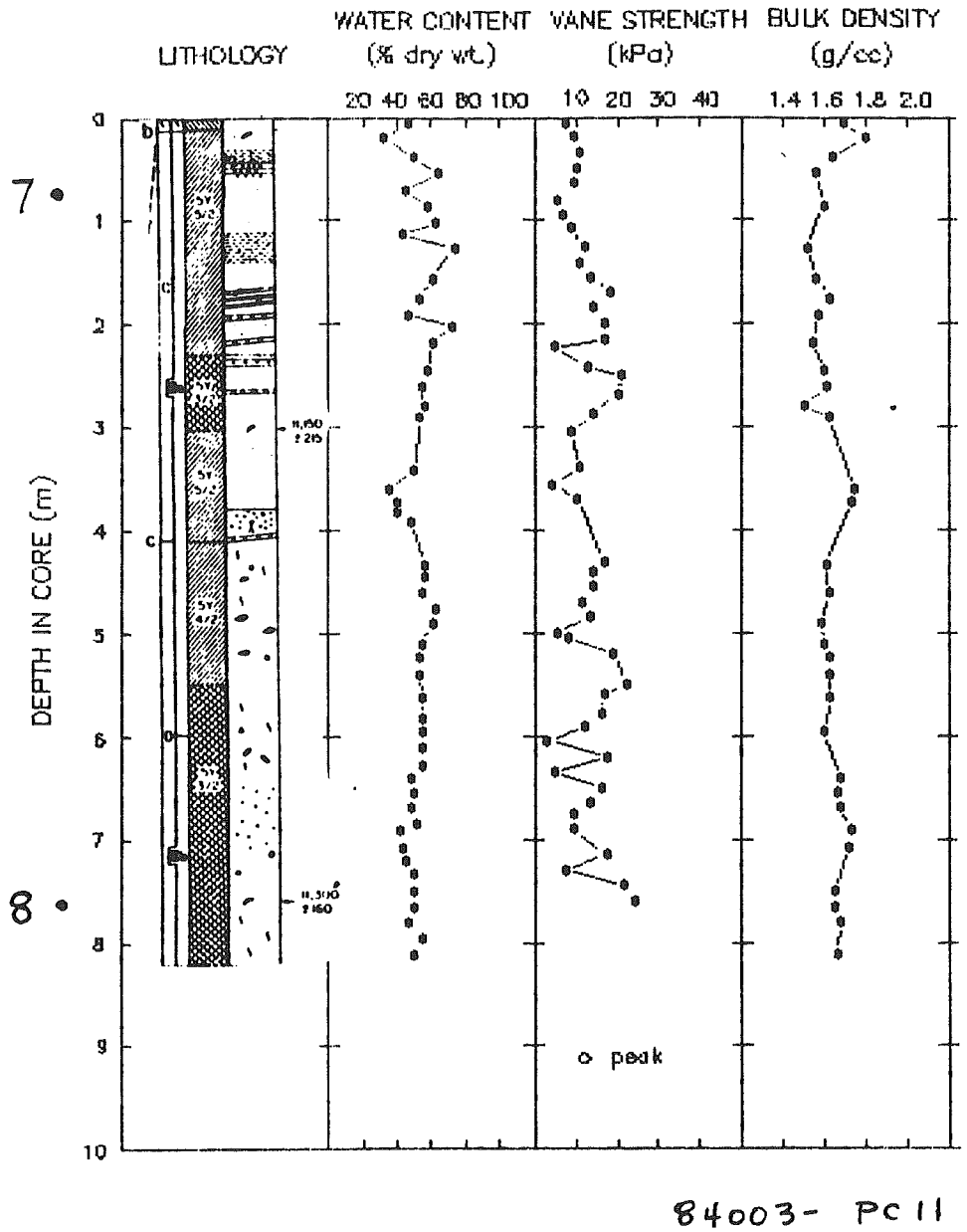

7 •

8 •

84003- PC 11

CORE 5

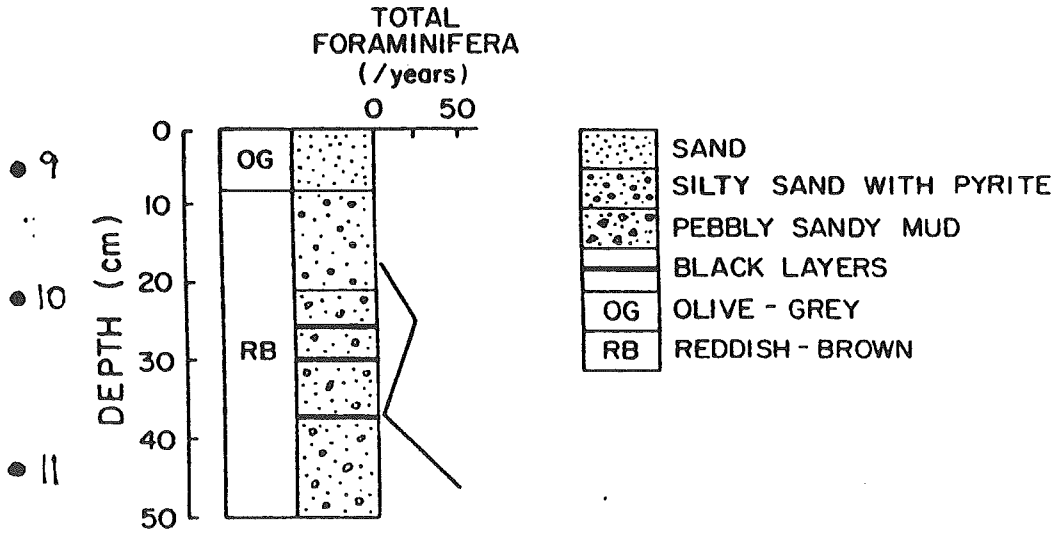

• 9

• 10

• 11

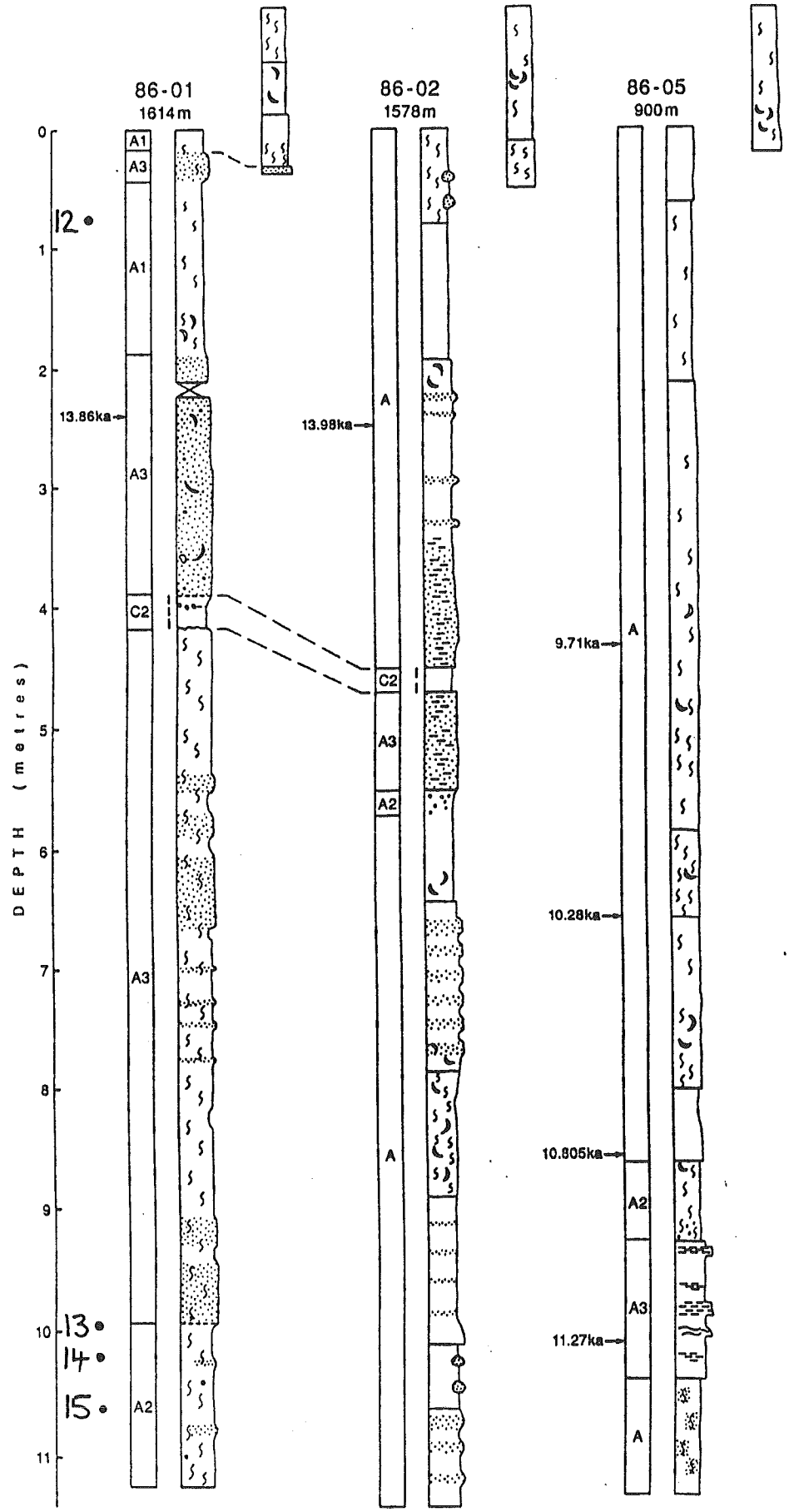

F: Narwhal (unpublished data of Piper and Bonifay)

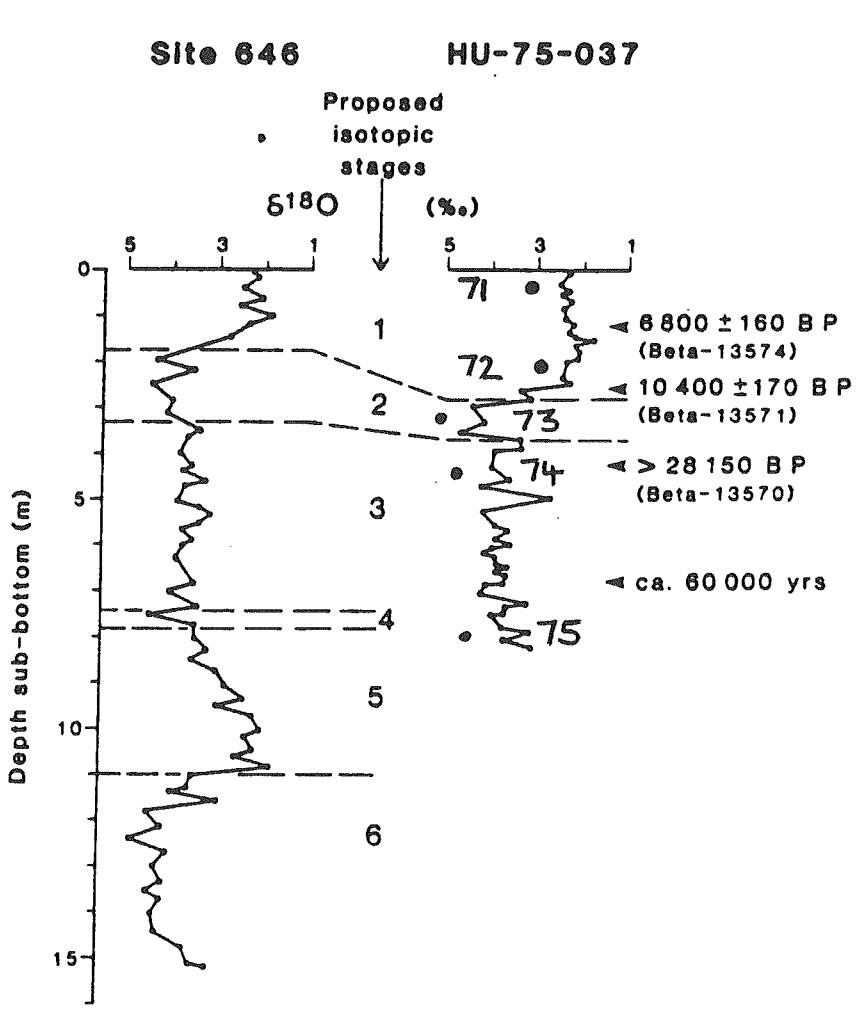

FIGURE 2C. The ^{18}O-records off southwest Greenland (the composite record of site 646 is from Aksu *et al.*, 1989; the core HU-75-37 data are first published in this paper).

G: Labrador Sea (from Hillaire Marcel and de Vernal, 1989)

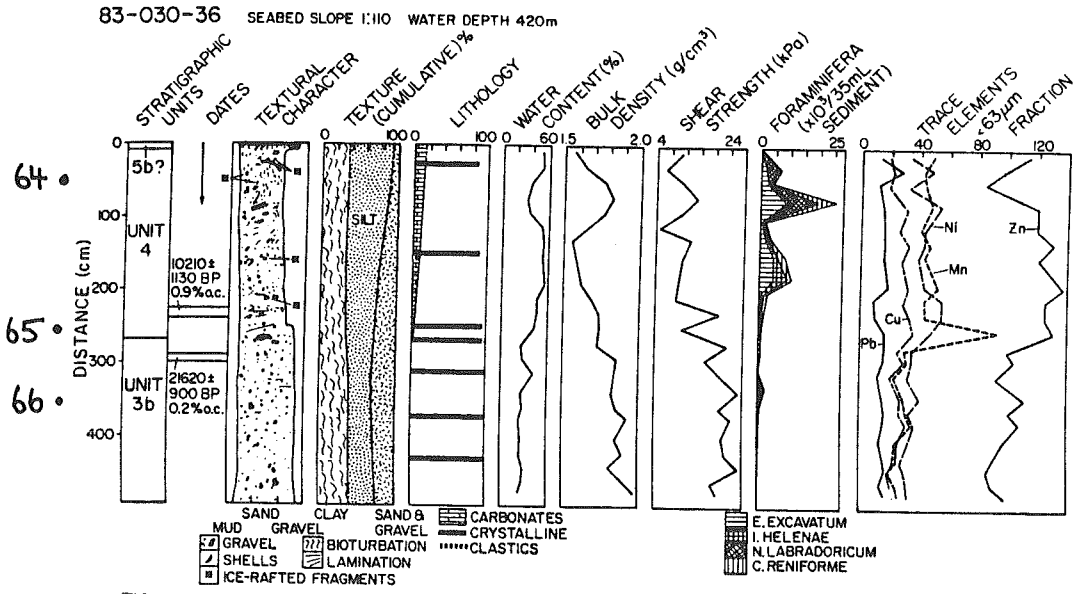

H: Labrador Shelf - Karlsefni, Hopedale and Cartwright (from Josenhans and Zevenhuizen, 1989)

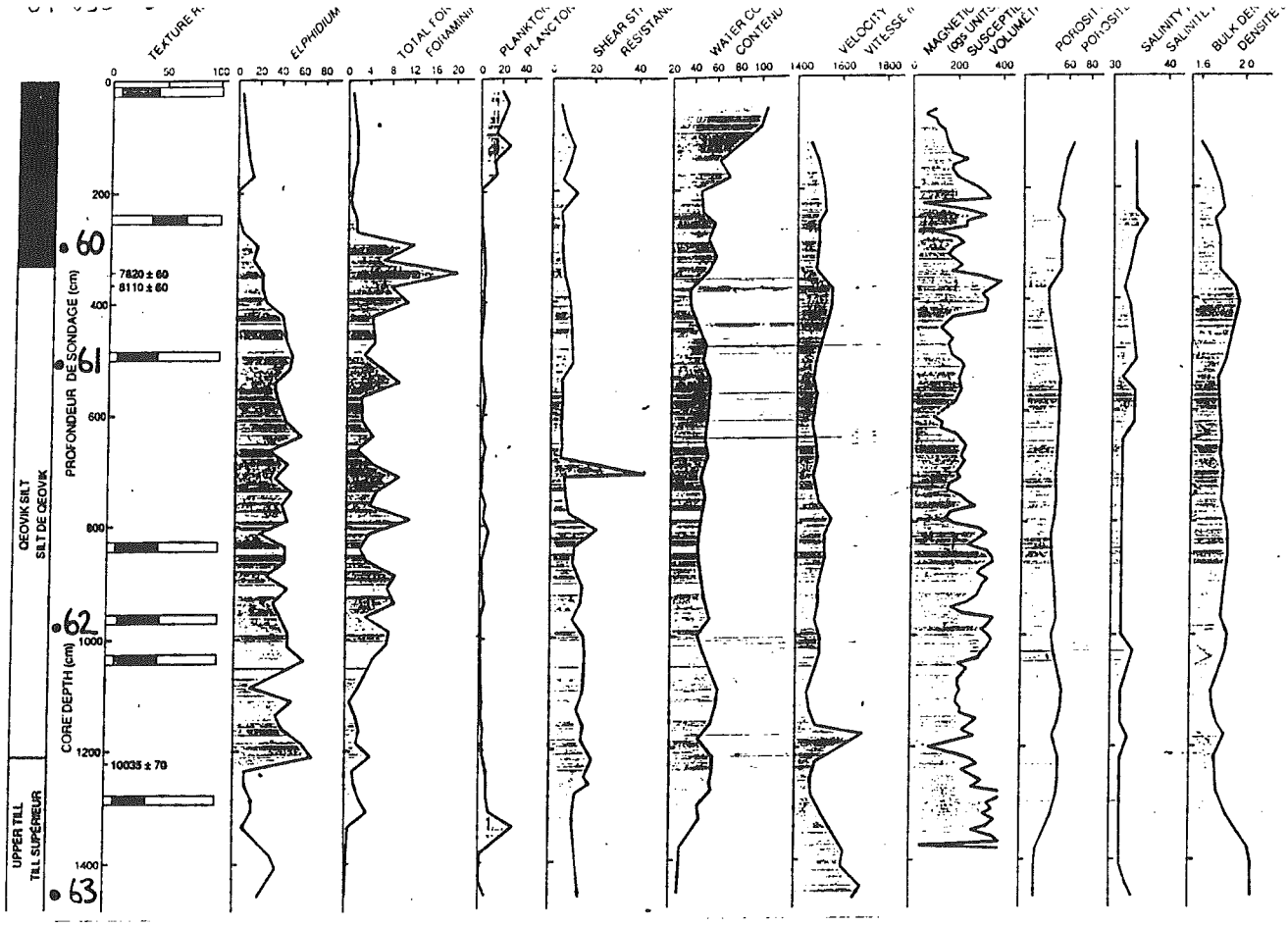
TEXTURE R.
ELPHIDIUM
TOTAL FO
FORAMINI
PLANKTO
PLANCTO
SHEAR ST
RESISTAN
WATER CO
CONTENU
VELOCITY
VITESSE
MAGNETI
(SI UNIT
SUSCEPTI
VOLUME
POROSI
POROSITE
SALINITY
SALINITE
BULK DE
DENSITE
0 50 100
0 20 40 60 80
0 4 8 12 16 20
0 20 40
20 40
20 40 60 80 100
1400 1600 1800
200 400
60 80
30 40
1.6 2.0
PROFONDEUR DE SONDAGE (cm)
CORE DEPTH (cm)
7820 ± 60
8110 ± 60
10035 ± 70
60
61
62
63
QEOVIK SILT
SILT DE QEOVIK
UPPER TILL
TILL SUPÉRIEUR

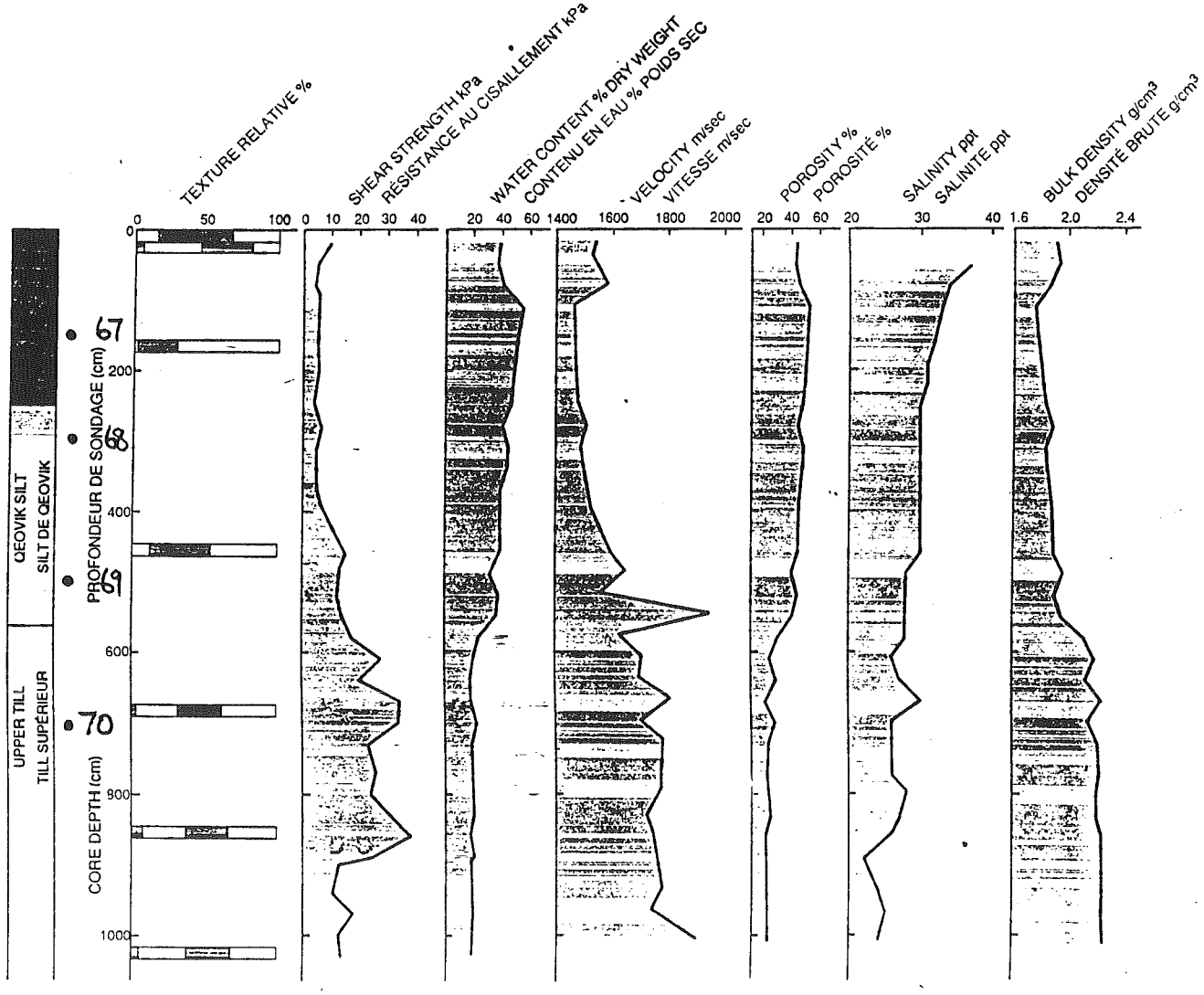
TEXTURE RELATIVE %
SHEAR STRENGTH kPa
RÉSISTANCE AU CISAILLEMENT kPa
WATER CONTENT % DRY WEIGHT
CONTENU EN EAU % POIDS SEC
VELOCITY m/sec
VITESSE m/sec
POROSITY %
POROSITÉ %
SALINITY ppt
SALINITÉ ppt
BULK DENSITY g/cm3
DENSITÉ BRUTE g/cm3
0 50 100
0 10 20 30 40
20 40 60
1400 1600 1800 2000
20 40 60
20 30 40
1.6 2.0 2.4
PROFONDEUR DE SONDAGE (cm)
CORE DEPTH (cm)
67
68
69
70
QEOVIK SILT
SILT DE QEOVIK
UPPER TILL
TILL SUPÉRIEUR

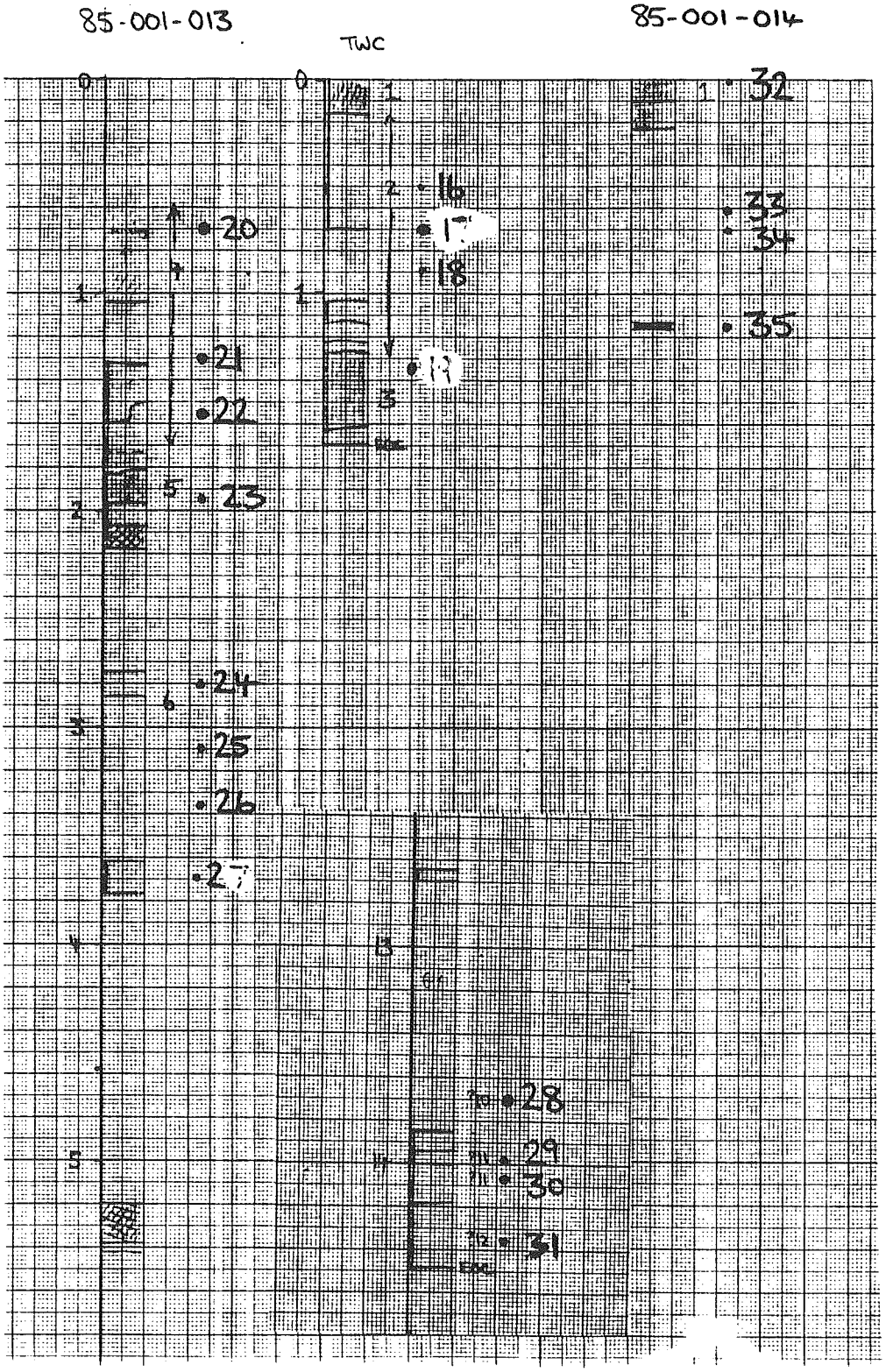

I: Fogo Seamounts (unpublished data, projected in to stratigraphy of Alam et al., 1983)

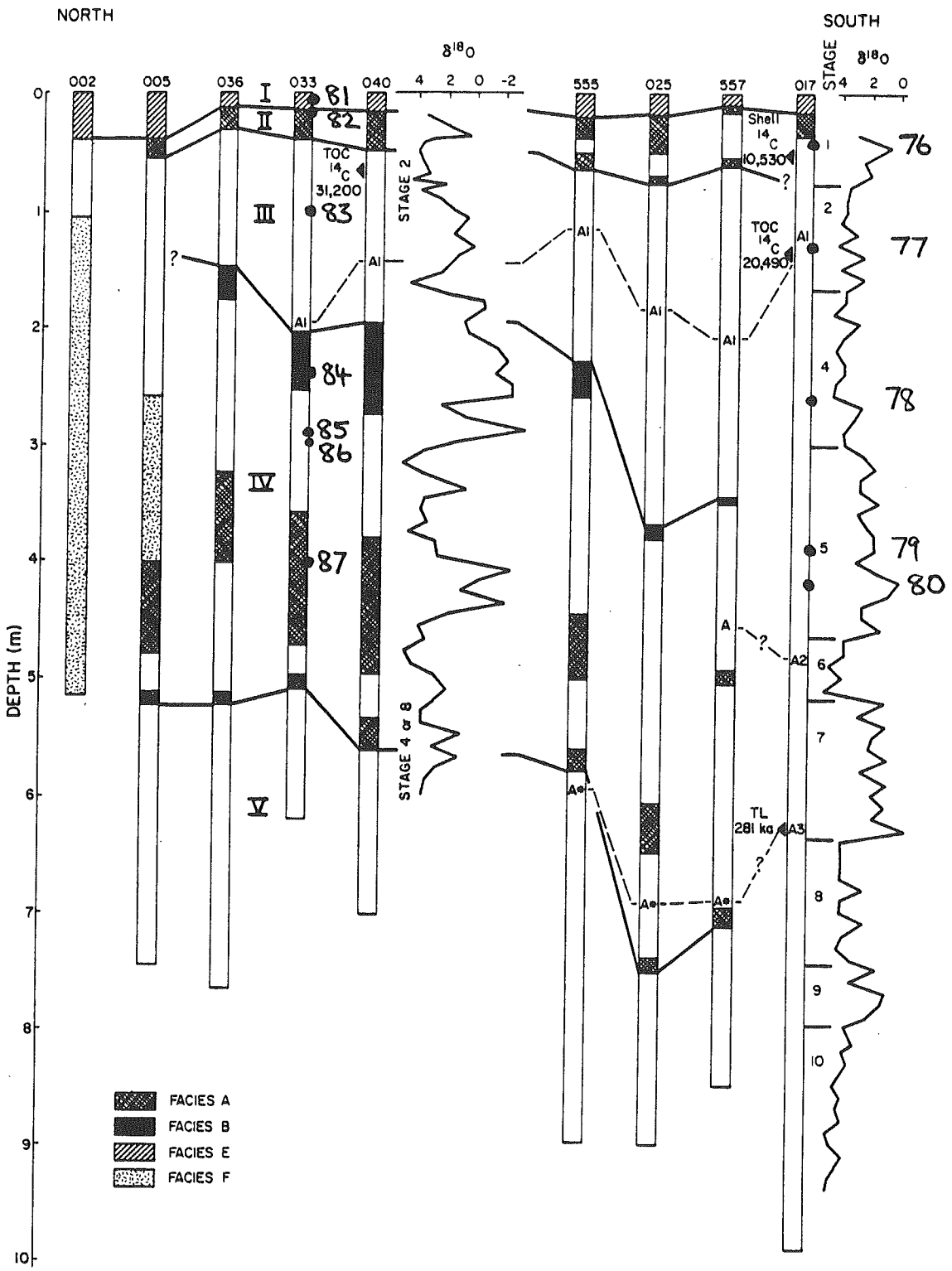

FIG. 8. Summary of stratigraphic correlation of piston cores. Isotopic data and ash horizons from Aksu (1981). For explanation of zones I–V, see text. TL = thermoluminescence date (±20%) cited in Mudie and Aksu (1984). TOC = total organic carbon radiocarbon date. Isotopic stages in core 017 from Mudie and Aksu (1984); stages for core 040 are discussed in text.

J: Baffin Bay basin (from Aksu and Piper, 1987).